



University of
Nebraska
Lincoln

Department of Electrical Engineering
209N Walter Scott Engineering Center
P.O. Box 880511
Lincoln, NE 68588-0511
Phone (402) 472-3771
FAX (402) 472-4732

December 2, 2000

U.S. Army Research Office
4300 South Miami Boulevard
P.O. Box 12211
Research Triangle Park, NC 27709-2211
ATTN: AMSRL-RO-RI (Sylvia Hall)

Dear Sylvia,

Enclosed are the Final Progress Report for DAAG55-98-0462. This report has been granted a 60 extension to submitted before December 15, 2000.

If you have questions regarding the report, please contact me at the following address:

Dr. H. Walter Yao
AMD
915 Deguigne St. Room 270 D
P.O. Box 3453, MS 143
Sunnyvale, CA 94088-3453

Phone: (408) 749-3544
FAX: (408) 749-5585
Email: walter.yao@amd.com

Best Regards,

H. Walter Yao
Professor of Electrical Engineering

DTIC QUALITY ASSURED

20010116 134

REPORT DOCUMENTATION PAGE			Form Approved OMB NO. 0704-0188	
Public Reporting burden for this collection of information is estimated to average 1 hour per response, including the time for reviewing instructions, searching existing data sources, gathering and maintaining the data needed, and completing and reviewing the collection of information. Send comment regarding this burden estimate or any other aspect of this collection of information, including suggestions for reducing this burden, to Washington Headquarters Services, Directorate for Information Operations and Reports, 1215 Jefferson Davis Highway, Suite 1204, Arlington, VA 22202-4302, and to the Office of Management and Budget, Paperwork Reduction Project (0704-0188), Washington, DC 20503.				
1. AGENCY USE ONLY (Leave Blank)		2. REPORT DATE December 2, 2000		3. REPORT TYPE AND DATES COVERED Final: 15 July 1998 – 14 July, 2000
4. TITLE AND SUBTITLE Optical Properties of GaN and Other III-Nitride Semiconductor Materials Studied by Variable Angle Spectroscopic Ellipsometry			5. FUNDING NUMBERS DAAG55-98-1-0462	
6. AUTHOR(S) Huade Walter Yao				
7. PERFORMING ORGANIZATION NAME(S) AND ADDRESS(ES) University of Nebraska-Lincoln Research Grants and Contracts Office 303 Administration Building Lincoln, NE 68588-0430			8. PERFORMING ORGANIZATION REPORT NUMBER	
9. SPONSORING / MONITORING AGENCY NAME(S) AND ADDRESS(ES) U. S. Army Research Office P.O. Box 12211 Research Triangle Park, NC 27709-2211			10. SPONSORING / MONITORING AGENCY REPORT NUMBER ARO38864.11-EL	
11. SUPPLEMENTARY NOTES The views, opinions and/or findings contained in this report are those of the author(s) and should not be construed as an official Department of the Army position, policy or decision, unless so designated by the documentation.				
12 a. DISTRIBUTION / AVAILABILITY STATEMENT Approved for public release; distribution unlimited.			12 b. DISTRIBUTION CODE	
1. ABSTRACT (Maximum 200 words) In this 2-year project, we have determined anisotropic optical dielectric functions of GaN, AlN and Sapphire. It is for the first time, the ordinary and extraordinary optical constants of the important III-Nitride materials, GaN, AlN and sapphire, have been determined by variable angle spectroscopic ellipsometry (VASE), in the energy range of 0.75 eV to 6.5 eV. Our results indicate that anisotropic optical properties are important feature of the GaN and other hexagonal structured III-nitride materials. The extraordinary optical properties of those materials, which were omitted before, influence in many ways the optoelectronic devices properties made from GaN, AlN etc. We have also discovered a method to characterize the ordinary and extraordinary dielectric optical functions by VASE under c-plane direction. Our method indicates that the ordinary optical dielectric functions ($E \perp \langle c \rangle$) can be precisely determined by the isotropic mode VASE measurements at small angles of incidence, e.g., between 20 and 40 degrees, while the anisotropic dielectric functions ($E \parallel \langle c \rangle$) can be detected most-sensitively at large angles of incidence (near the pseudo-Brewster angle).				
14. SUBJECT TERMS Optical Properties; GaN; AlN; Sapphire; Anisotropic optical response; Ordinary and extraordinary dielectric functions; Variable angle spectroscopic ellipsometry (VASE).			15. NUMBER OF PAGES 6	
			16. PRICE CODE	
17. SECURITY CLASSIFICATION OR REPORT UNCLASSIFIED	18. SECURITY CLASSIFICATION ON THIS PAGE UNCLASSIFIED	19. SECURITY CLASSIFICATION OF ABSTRACT UNCLASSIFIED	20. LIMITATION OF ABSTRACT UL	

MASTER COPY: PLEASE KEEP THIS "MEMORANDUM OF TRANSMITTAL" BLANK FOR REPRODUCTION PURPOSES. WHEN REPORTS ARE GENERATED UNDER THE ARO SPONSORSHIP, FORWARD A COMPLETED COPY OF THIS FORM WITH EACH REPORT SHIPMENT TO THE ARO. THIS WILL ASSURE PROPER IDENTIFICATION. NOT TO BE USED FOR INTERIM PROGRESS REPORTS; SEE PAGE 1 FOR INTERIM PROGRESS REPORT INSTRUCTIONS.

MEMORANDUM OF TRANSMITTAL

U.S. Army Research Office
ATTN: AMXRO-ICA (Hall)
P.O. Box 12211
Research Triangle Park, NC 27709-2211

- | | |
|---|---|
| <input checked="" type="checkbox"/> Reprint (Orig + 2 copies) | <input type="checkbox"/> Technical Report (Orig + 2 copies) |
| <input checked="" type="checkbox"/> Manuscript (1 copy) | <input checked="" type="checkbox"/> Final Progress Report (Orig + 2 copies) |
| | <input type="checkbox"/> Related Materials, Abstracts, Theses (1 copy) |

CONTRACT/GRANT NUMBER: DAAG55-98-1-0462

REPORT TITLE:

Optical Properties of GaN and Other III-Nitride Semiconductor Materials Studied by Variable Angle Spectroscopic Ellipsometry

is forwarded for your information.

SUBMITTED FOR PUBLICATION TO (applicable only if report is manuscript):

Sincerely,

OPTICAL PROPERTIES OF GaN AND OTHER III-NITRIDE
SEMICONDUCTOR MATERIALS STUDIED BY VARIABLE ANGLE
SPECTROSCOPIC ELLIPSOMETRY

FINAL PREGRESS REPORT

Huade Walter Yao

November 26, 2000

U.S. AMRY RESEARCH OFFICE

DAAG55-98-1-0462

University of Nebraska

Department of Electrical Engineering

APPROVED FOR PUBLIC RELEASE:

DISTRIBUTION UNLIMITED

THE VIEWS, OPINIONS, AND/OR FINDINGS CONTAINED IN THIS REPORT ARE
THOSE OF THE AUTHOR(S) AND SHOULD NOT BE CONSTRUED AS AN OFFICIAL
DEPARTMENT OF THE ARMY POSITION, POLICY, OR DECISION, UNLESS SO
DESIGNATED BY OTHER DOCUMENTATION.

1. List of Appendixes

1. Reprints of publication in Material Research Society Symposium Proceeding:

Optical Anisotropy of GaN/sapphire Studied by Generalized Ellipsometry and Raman Scattering C.H. Yan, H.W. Yao, J.M. Van Hove, A.M. Wowchak, P.P. Chow, J.M. Zavada, SPIE Proceeding, **3621**, 73-84 (1999).

2. Reprints of publication in Journal of Applied Physics:

Anisotropic Optical Responses of Sapphire (α -Al₂O₃) Single Crystals H. Yao, and C.H. Yan, J. Appl. Phys. **85**, 6717-6722 (1999),

3. Reprints of publication in Material Research Society Symposium Proceeding:

Nondestructive Characterizations of Gan Films Grown at Low and High Temperatures C. H. Yan, H.W. Yao, J. M. Van Hove, A. M. Wowchak, P. P. Chow, J. Han, J. M. Zavada, Mat. Res. Soc. Symp. Proc. **591**, (2000).

4. Reprints of publication in SPIE Symposium Proceeding:

Optical properties of AlN/sapphire grown at high and low temperatures studied by variable angle spectroscopic ellipsometry and micro Raman scattering C. H. Yan, H. Yao, A. C. Abare, S. P. Denbaars, J. J. Klaassen, M. F. Rosamond, P. P. Chow, J. M. Zavada, SPIE Proceedings **3938**, 113-123 (2000).

5. Reprints of publication in Journal of Applied Physics:

Ordinary Optical Dielectric Functions of Anisotropic Hexagonal GaN Film Determined by Variable Angle Spectroscopic Ellipsometry C. H. Yan, H. Yao, J. M. Van Hove, A. M. Wowchak, P. P. Chow, J. M. Zavada, J. Appl. Phys **3463-3469** (2000).

6. Preprints of manuscript submitting to Journal of Applied Physics:

Extraordinary optical dielectric functions of anisotropic hexagonal GaN film determined by variable angle spectroscopic ellipsometry C. H. Yan, H. Yao, J. M. Van Hove, A. M. Wowchak, P. P. Chow, J. M. Zavada, J. Appl. Phys, submitted, (2000).

7. Copy of cover page of the Ph.D. Dissertation:

Optical Characterization of Anisotropic III-Nitride Wide Band-Gap Semiconductors and Related Materials by C.H. Yan, supervised by Prof. H. Walter Yao

2. Statement of problems studied

In this two year research project, we have investigated an important issue: anisotropic optical properties of III-Nitride and related semiconductor materials. Those materials are

GaN, AlN and Sapphire substrate. In this report we will summarize the most important results of this study.

A. Ordinary and extraordinary optical dielectric functions of GaN

The wide band gap semiconductor GaN is an important material for light emitting device applications in the green, blue and UV regions. GaN films grown on sapphire substrates usually have hexagonal structure, which is optically anisotropic. The ordinary optical dielectric functions of GaN have been studied intensively since 1960's.. But the extraordinary dielectric functions of GaN, on the other hand, are not well documented. Polarized reflectance spectroscopy is a straightforward technique to measure the extraordinary response of GaN. However it may be lack of accuracy because not only reflectance is an intensity sensitive method, but also it is lack of sensitivity on surface roughness.

In this work, variable angle spectroscopic ellipsometry (VASE) has been employed to study the ordinary and extraordinary optical dielectric response of hexagonal gallium nitride (GaN) thin film grown on c-plane sapphire substrates ($\alpha\text{-Al}_2\text{O}_3$) by molecular beam epitaxy (MBE). Room temperature VASE measurements were made, in the range of 0.75 to 6.5 eV, at the angle of incidence in between of 20 and 80 degree. VASE data simulations by isotropic and anisotropic models indicate that the ordinary optical dielectric functions ($E \perp \langle c \rangle$) can be precisely determined by the isotropic mode VASE measurements at angles of incidence between 20 and 40 degrees while the anisotropic dielectric functions ($E \parallel \langle c \rangle$) can be detected most-sensitively at large angles of incidence (near the pseudo-Brewster angle). Thus the ordinary and extraordinary optical dielectric functions are precisely determined by standard VASE measurements in the range of 0.75 to 6.5 eV. The surface roughness was also considered in the VASE data analysis in order to separate it from the anisotropic effect. The VASE data is analyzed by a model dielectric function based on the GaN critical point structure, which allows for a non-zero extinction coefficient k below the band gap. The thicknesses of these GaN films are accurately determined via the analysis as well.

B. Anisotropic optical response of AlN

Variable angle spectroscopic ellipsometry (VASE) and micro Raman scattering have been employed to study the optical anisotropy and optical constants of AlN films grown at high and low temperatures (HT and LT). The AlN films were grown by metalorganic vapor phase epitaxy (MOVPE) and molecular beam epitaxy (MBE) on c-plane sapphire ($\alpha\text{-Al}_2\text{O}_3$) substrates, respectively. Anisotropic optical phonon spectra of AlN have been measured along two directions so that the optical axis $\langle c \rangle$ of AlN is either perpendicular or parallel to the polarization of the incident beam. Nonzero off-diagonal elements A_{ps} and A_{sp} of Jones matrix in the reflection VASE (RVASE) measurements indicate that the $\langle c \rangle$ of AlN is slightly away from surface normal due to substrate miscut. The ordinary optical constants of both HT AlN have been determined spectroscopic ellipsometry at small angles of incidence so that

the extraordinary response is greatly reduced. The film thickness along with the surface overlayer was determined via the VASE data analysis as well.

C. Anisotropic optical properties of Sapphire (α -Al₂O₃)

Sapphire crystals have many attractive properties that make them widely applied in solid-state device fabrications. More recently, due to the dramatic progress in the GaN related blue LEDs and lasers field, sapphire as a good substrate candidate becomes even more important than the past since its crystal structure is similar to GaN and allows to realize a small lattice mismatch growth.

Anisotropic dielectric functions of sapphire have been determined by both reflection and transmission variable angle spectroscopic ellipsometry. The measurements were made on a-plane ($2\bar{1}\bar{1}0$) sapphire substrates in the energy range of 0.75 eV to 6.5 eV at room temperature. The orientation of the optic axis of the a-plane sapphire sample was determined by polarized Raman scattering based on which the Euler angles are set for the fitting model. Two pairs of Cauchy user-defined functions were constructed to describe the optical constants of both ordinary $n_o(\omega)$ and extraordinary $n_e(\omega)$ rays, respectively. The resulted optical constants from the generalized ellipsometry analysis are in good agreement with the reported data. The Kramers-Kronig (KK) relation between the real part and the imaginary part have been carefully checked for both ordinary and extraordinary rays. The perfect fitting between the calculated and experimental $\epsilon_1(\omega)$ function indicates that both functions of ordinary and extraordinary are KK consistent. The refractive index difference between the ordinary and extraordinary rays is close to a constant (+0.008), which is mainly determined by the off-diagonal signal of the transmission ellipsometry data. The extinction coefficients are zero below 6 eV, and increase rapidly above 6 eV.

3. Summary of most important results

There are two most important results from this two-year studies:

1. Anisotropic dielectric optical constants of GaN, AlN and Sapphire

It is for the first time, the ordinary and extraordinary optical constants of the important III-Nitride materials, GaN, AlN and sapphire, have been determined by VASE. Our results indicate that anisotropic optical properties are important feature of the GaN and other hexagonal structured III-nitride materials. The extraordinary optical properties of those materials, which were omitted before, influence in many ways the optoelectronic devices properties made from GaN, AlN etc.

2. Nondestructive method of characterize optical properties of uniaxial structured semiconductor materials

It has been well known a difficult task to precisely determine the optical properties of uniaxial structured semiconductor materials, especially when the c/a ratio is small. We have

discovered a method to characterize the ordinary and extraordinary dielectric optical functions by VASE under c-plane direction. Our method indicates that the ordinary optical dielectric functions ($E \perp \langle c \rangle$) can be precisely determined by the isotropic mode VASE measurements at small angles of incidence, e.g., between 20 and 40 degrees, while the anisotropic dielectric functions ($E \parallel \langle c \rangle$) can be detected most-sensitively at large angles of incidence (near the pseudo-Brewster angle).

4. List of publications and technical reports

A. Refereed Journal Publications:

1. *Anisotropic Optical Responses of Sapphire ($\alpha\text{-Al}_2\text{O}_3$) Single Crystals* H. Yao, and C.H. Yan, J. Appl. Phys. **85**, 6717-6722 (1999).
2. *Optical Anisotropy of GaN/sapphire Studied by Generalized Ellipsometry and Raman Scattering* C.H. Yan, H.W. Yao, J.M. Van Hove, A.M. Wowchak, P.P. Chow, J.M. Zavada, SPIE Proceeding, **3621**, 73-84 (1999).
3. *Nondestructive Characterizations of GaN Films Grown at Low and High Temperatures* C. H. Yan, H.W. Yao, J. M. Van Hove, A. M. Wowchak, P. P. Chow, J. Han, J. M. Zavada, Mat. Res. Soc. Symp. Proc. **591**, (2000).
4. *Optical properties of AlN/sapphire grown at high and low temperatures studied by variable angle spectroscopic ellipsometry and micro Raman scattering* C. H. Yan, H. Yao, A. C. Abare, S. P. Denbaars, J. J. Klaassen, M. F. Rosamond, P. P. Chow, J. M. Zavada, SPIE Proceedings **3938**, 113-123 (2000).
5. *Ordinary Optical Dielectric Functions of Anisotropic Hexagonal GaN Film Determined by Variable Angle Spectroscopic Ellipsometry* C. H. Yan, H. Yao, J. M. Van Hove, A. M. Wowchak, P. P. Chow, J. M. Zavada, J. Appl. Phys **3463-3469** (2000).

B. Refereed Conference Presentations:

1. *Anisotropic Optical Properties of GaN Studied by Generalized Variable Angle Spectroscopic Ellipsometry*, C.H. Yan, H. Yao, J.M. Van Hove, A.M. Wowchak, P.P. Chow, S.P. DenBaars, J.M. Zavada, Mater. Res. Soc. Fall Meeting, Boston, Nov. 30 - Dec. 4, 1998.
2. *Optical Anisotropy of GaN/sapphire Studied by Generalized Ellipsometry and Raman Scattering*. C.H. Yan, H.W. Yao, J.M. Van Hove, A.M. Wowchak, P.P. Chow, J.M. Zavada, SPIE PhotonicsWest '99, San Jose, CA, 23-29 January, 1999.
3. *Optical Characterization of AlN Films Grown on Sapphire Substrate*, C.H. Yan, H.W. Yao, J.J. Klassen, M.F. Rosamond, P.P. Chow, Mat. Res. Soc. Spring Meeting, San Francisco, April 5-9, 1999.
4. *Optical Anisotropic Dielectric Functions of Hexagonal GaN Film Determined by Variable Angle Spectroscopic Ellipsometry*, C. H. Yan, H.W. Yao, J. M. Van Hove, A. M. Wowchak, P. P. Chow, J. M. Zavada, Mater. Res. Soc. Fall Meeting, Boston, Nov. 29 - Dec. 3, 1999.

5. *Anisotropic optical dielectric functions of AlN studied by polarized reflection and variable angle spectroscopic ellipsometry*, C. H. Yan, H. W. Yao; J.J. Klaassen, M.F. Rosamond, P.P. Chow, SPIE Photonics West '2000, San Jose, CA, 22-28 January, 2000.

- C. Dissertation for Ph.D. degree in Electrical Engineering:

Optical Characterization of Anisotropic III-Nitride Wide Band-Gap Semiconductors and Related Materials by C.H. Yan, supervised by Prof. H. Walter Yao

- D. Manuscript submitted to Journal of Applied Physics:

Extraordinary optical dielectric functions of anisotropic hexagonal GaN film determined by variable angle spectroscopic ellipsometry C. H. Yan, H. Yao, , J. M. Van Hove, A. M. Wowchak, P. P. Chow, J. M. Zavada, J. Appl. Phys, submitted, (2000).

- E. Technical Reports:

1. Interim Report 1998;

2. Accomplishment Report 1998; Interim Report 1999;

3. Interim Report 1999.

5. **List of participating personel (including a Ph.D. degree of Electrical Engineering earned while employed on the project)**

Professor Huade Walter Yao (PI)

C.H. Yan (Graduate Student for Ph.D. degree)

6. **Appendixes**

Optical anisotropy of GaN/sapphire studied by generalized ellipsometry and Raman scattering

Chunhui Yan^a, H. Walter Yao^{*a}, James M. Van Hove^b, Andrew M. Wowchak^b, Peter P. Chow^b,
John M. Zavada^c

^aUniversity of Nebraska, Center for Microelectronic and Optical Material Research,
and Department of Electrical Engineering, Lincoln, NE 68588

^bSVT Associates, Eden Prairie, MN

^cEuropean Research Office, London, UK

ABSTRACT

Generalized variable angle spectroscopic ellipsometry (VASE) and Raman scattering have been employed to study the optical anisotropy of GaN/Sapphire structures. The GaN films were grown by hydride vapor phase epitaxy (HVPE) and molecular beam epitaxy (MBE) on both m-plane and c-plane sapphire (α -Al₂O₃) substrates, respectively. Anisotropic optical phonon structure of sapphire have been measured, based on which the optical axis of sapphire substrate has been determined. A 541 cm⁻¹ TO phonon of GaN grown on m-plane sapphire substrate has been discovered experimentally which is due the coupling of A₁ and E₁ TOs. Optical axis orientation of GaN film on m-sapphire has been fully determined by the anisotropic angular dependence of the coupled TO phonon. Off-diagonal elements A_{pst} and A_{spt} of transmission VASE (TVASE) are very sensitive parameters related to the optical anisotropy. The optical axis orientation of GaN on m-sapphire has also been accurately determined by TVASE at two special sample positions. The optical anisotropy due to GaN film and sapphire substrate has been successfully separated at 90° sample position allowing to study the optical anisotropy of GaN film only.

Keywords: GaN, sapphire, Raman scattering, generalized ellipsometry, optical anisotropy

1. INTRODUCTION

The wide band gap semiconductor GaN and related materials, with their excellent thermal conductivity, large breakdown field, and resistance to chemical attack, have a very promising application potential for both high temperature electronic devices and short wave-length optical emitters.^{1,2} The recent development of high-brightness, blue and green light emitting diodes (LEDs),³ room temperature pulsed⁴ and continuous-wave (CW)⁵ quantum well lasers has greatly encourage researchers to continue the work on these materials. Most of the GaN films were grown on c-plane sapphire substrates, and they usually have wurtzite crystal structure (α -GaN), which is anisotropic (uniaxial). Several valuable optical property studies have been carried out on the GaN/c-sapphire structure by both Raman⁶ and ellipsometry⁷. However, there are not much data available about the optical anisotropy of GaN possibly due to the shortage of GaN samples grown on sapphire substrates other than c-plane orientations. For GaN/c-sapphire case, it is difficult to study the optical anisotropy of GaN film since the polarization of most of the probe light-wave is perpendicular to the optical axis $\langle c \rangle$. For GaN grown on m-plane sapphire, on the other hand, its optical axis $\langle c \rangle$ is certain degree away from the surface normal as pointing out by Matsuoka *et al*⁸, which provides the possibilities for the optical anisotropy study. It was found that the crystal orientation relation between GaN and m-plane sapphire is (01 $\bar{1}$ 3)/(01 $\bar{1}$ 0) as the interface plane, and [03 $\bar{3}$ 2]/[2 $\bar{1}$ 10] as the in-plane orientation preference. Most importantly, it was concluded that GaN grown on m-plane sapphire has a smoother surface, lower background carrier concentration and stronger PL intensity which indicate that GaN grown on m-plane is superior than on c-plane sapphire substrates. In this work, based on our previous optical anisotropy study of sapphire⁹, a GaN/m-sapphire

* Correspondence: H. Walter Yao, Email: wyao@Sandia.gov, or hyao1@unl.edu; telephone: 925-294-2169; Fax: 925-294-1489

sample grown by HVPE has been studied by Raman scattering and generalized ellipsometry. The optical axis orientation of GaN film grown on m-plane sapphire has been fully determined by both anisotropic coupled TO phonon and the off-diagonal elements of transmission Jones matrix.

2. Theory

2.1 Raman Scattering

It is well known that sapphire and GaN are all optically anisotropic (uniaxial) materials due to their rhombohedral and wurtzite crystal structures. Group theoretical analysis shows that the irreducible representation for the optical modes of sapphire is¹⁰.

$$\Gamma = A_{1g} + 2A_{1u} + 3A_{2g} + 5E_g + 4E_u, \quad (1)$$

and the irreducible representation for the acoustical modes is $A_{2u} + E_u$. Since the unit cell has center-of-inversion symmetry, all vibrations that are Raman allowed are infrared forbidden and vice versa. More specifically, two A_{1g} modes and five E_g modes are Raman active only, while two A_{2u} modes and four E_u modes are infrared active only. The A_{1u} and A_{2g} vibrations are neither infrared nor Raman active.

The irreducible representation of Wurtzite GaN optical phonons is:¹¹

$$\Gamma = A_1(z) + 2B_1 + E_1(x, y) + 2E_2, \quad (2)$$

for phonon propagating along or perpendicular to the optical axis $\langle c \rangle$. Where x, y, z in parentheses repent the directions of phonon polarization. The A_1 and E_1 modes are both Raman and infrared active, two E_2 modes are only Raman active, and B_1 modes are both Raman and IR silent. Using selection rules of the anisotropic phonon structures of sapphire and GaN, the optical orientation can be quickly determined.

2.2 Generalized Ellipsometry

The variable angle spectroscopic ellipsometry is designed to accurately determine the values of two standard ellipsometry parameters ψ and Δ , which are related to the complex ratio of reflection (or transmission) coefficients for light polarized parallel (p) and perpendicular (s) to the plane of incidence.¹² For isotropic material systems,

$$\rho = \frac{R_p}{R_s} = \tan(\psi)e^{i\Delta}. \quad (3)$$

The electric-field reflection coefficient at an incident angle of ϕ is defined as r_p (r_s) for p (s)- polarized light. They are the diagonal elements of Jones matrix,

$$[J]_{\text{sample}} = \begin{bmatrix} r_p & 0 \\ 0 & r_s \end{bmatrix}. \quad (4)$$

The ψ and Δ are not only dependent on material dielectric responses, also on the surface condition, sample structure, and other properties such as the optical anisotropy.

For the anisotropic material system, the non-diagonal elements of Jones matrix are not necessary to be zero. In the transmission VASE configuration,

$$[J]_{\text{sample}} = \begin{bmatrix} t_{pp} & t_{sp} \\ t_{ps} & t_{ss} \end{bmatrix}. \quad (5)$$

By using the same approach with considerably more algebra involved, we can still predict the ψ and Δ values, but the Fourier coefficients related to ψ and Δ become more complicated.¹³ The generalized ellipsometric parameters are defined as below:

$$A_{nEt} = \frac{t_{pp}}{t_{ss}} = \tan \psi_{nE} e^{i\Delta_{nE}}, \quad (6)$$

$$A_{pst} = \frac{t_{ps}}{t_{pp}} = \tan \psi_{ps} e^{i\Delta_{ps}}, \quad (7)$$

$$A_{\text{spt}} = \frac{t_{\text{sp}}}{t_{\text{ss}}} = \tan \psi_{\text{sp}} e^{i\Delta_{\text{sp}}}, \quad (8)$$

where the A_{pst} and A_{spt} describe how much amount p- or s-polarized light becomes s- or p-polarized light after the transmission, respectively. If the optical axis is strictly either perpendicular (perfect c-plane situation) or parallel to the electric field of the incident beam, the Jones matrix is diagonal. While it may not true for GaN films grown on non c-plane sapphire substrates, such as m-plane sapphire substrates since the optical axis of both GaN and sapphire may form an angle respect to the incident polarization so that the off-diagonal elements of Jones matrix may not vanish. The off-diagonal elements A_{pst} and A_{spt} are dependent on sample position, angle of incidence, which can be used to determine the optical axis orientation of crystals. Generalized ellipsometry was first introduced by Azzam and Bashara.¹⁴ The recent developments makes this technique more complete and powerful.^{15, 16} In a word, the Generalized ellipsometry is a technique which can be used to determined all the elements of Jones matrix of arbitrarily anisotropic and homogeneous layered systems with nonscalar dielectric susceptibilities.

3. Experiments

The Raman spectra were taken at room temperature with a SPEX 1877E triple spectrometer equipped with a liquid-nitrogen cooled CCD camera. The excitation light source was an Ar⁺ laser operating at 488 nm with the output power kept at 150 mW. A back scattering geometry was employed for all the Raman measurements.

The GaN films used in this work were grown by both HVPE and MBE on m-plane and c-plane sapphire substrates. The backside of the substrate was polished so that the transmission type VASE measurements could be made. The TVASE optical measurements of anisotropic mode were performed in the energy range of 0.75eV to 4eV with a 0.03eV increment at room temperature since the sample is opaque above the GaN band gap 3.4eV. A rotational sample stage allowed us to take the data from different sample positions marked by the angle between the optical axis $\langle c \rangle$ and the x-axis of the lab coordinates. Multiple angles of incidence from -30° to $+30^\circ$ were used in order to see the angular dependence of the optical anisotropy of the GaN/m-sapphire sample.

4. Results and discussion

4.1. Optical phonons of sapphire and GaN

Raman scattering is a nondestructive technique used to detect the lattice vibration modes related with crystal orientation and symmetry. A series of Raman scattering measurements have been carried out on c-plane and a-plane sapphire samples. The spectrum of Raman scattering on a c-plane sapphire at back-scattering geometry $Z(Y, Y+X)\bar{Z}$ are shown in Fig. 1(a). A similar Raman phonon spectrum shown in Fig. 1(b) was obtained from an a-plane sapphire with its optical axis perpendicular to the polarization of the incident laser beam. While a different spectrum shown in Fig. 1(c) was obtained from the same a-plane sapphire with the optical axis parallel to the polarization. Only two TOs appeared for this configuration, and the 645 cm^{-1} (LO, A_{1g}) is a new phonon which is forbidden in both Fig 1(a) and Fig 1(b) configurations. This indicates that the 645 cm^{-1} (LO) mode is allowed or forbidden when the optical axis of the a-plane sample is parallel or perpendicular to the polarization of the Raman probe, respectively.

Optical phonons of GaN films grown on c- and m-plane sapphire substrates are shown in Fig. 2. The dash line refers to the GaN on c-plane sapphire, a E_2 and a A_1 LO phonon are observed at 569 cm^{-1} and 734 cm^{-1} , respectively. They are consistent with reported values.¹⁷ The solid line represents GaN grown on m-plane sapphire substrate. Except the E_2 and E_1 TOs, a new 541 cm^{-1} appeared in the spectrum, which was never reported as the experimental result. Notice that this phonon is not any of the standard zone center phonons propagating along or perpendicular to the optical axis $\langle c \rangle$.¹¹ According to Loudon's theory,¹⁸ this one belongs to a coupled mode of two TO phonons (A_1 TO and E_1 TO) when the angle θ between phonon propagation direction $\langle q \rangle$ and the optical axis $\langle c \rangle$ is in between of 0° and 90° . For non-zero θ values, the coupled modes satisfy the followings:

$$\omega^2(\text{TO}_1) = \omega^2(A_1(\text{TO}))\sin^2 \theta + \omega^2(E_1(\text{TO}))\cos^2 \theta \quad (9)$$

$$\omega^2(\text{TO}_2) = \omega^2(E_1(\text{TO})) \quad (10)$$

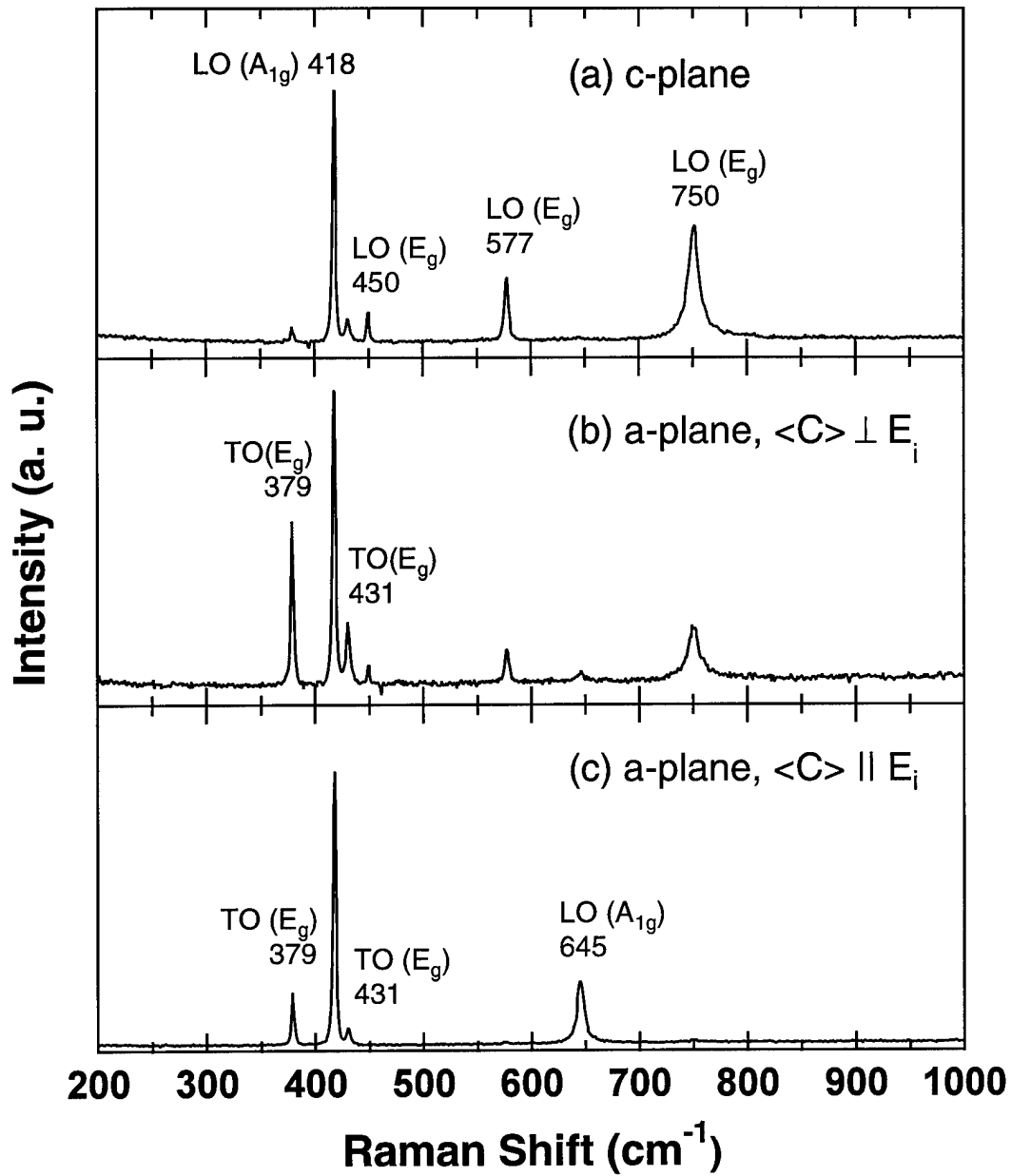


Fig. 1. Optical phonons of sapphire. (a) c-plane; (b) a-plane, $\langle c \rangle_s \perp E_i$; (c) a-plane, $\langle c \rangle_s \parallel E_i$.

where the TO_1 is the new coupled TO phonon with a strong θ angular dependence, and the $\omega(TO_2)$ is same as $\omega(E_1 TO)$. Applying equation (9) to the measured 541 cm^{-1} coupled TO phonon mode, the related angle θ is about 58° .

In the back scattering geometry, the phonon wave vector $\langle q \rangle$ is perpendicular to the sample surface. In order to located the orientation of $\langle c \rangle$ of GaN ($\langle c \rangle_g$), the reference direction $\langle c \rangle$ of sapphire ($\langle c \rangle_s$) has to be determined first. Based on the analysis of Fig. 1, we can use the 645 cm^{-1} LO phonon of sapphire to find the $\langle c \rangle_s$ position. As shown in Fig. 3, The 645

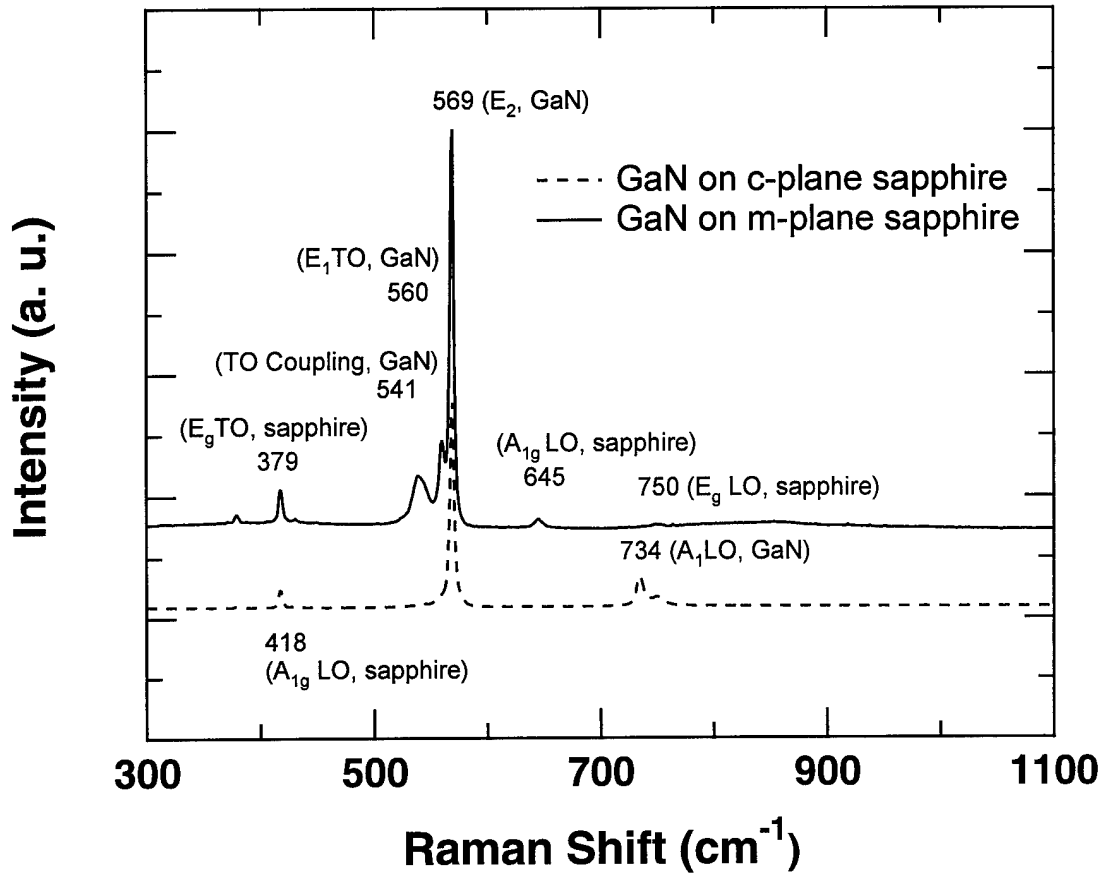


Fig. 2. Optical phonons of GaN films. Dash line is for GaN on c-plane sapphire; solid line is for GaN on m-plane sapphire. 541 cm^{-1} is the coupled TO phonon of A_1 and E_1 TOs.

cm^{-1} LO of sapphire is forbidden when $\langle c \rangle_s$ perpendicular to the polarization (dash line), and it is allowed as $\langle c \rangle_s$ parallel to the polarization (solid line). Therefore a reference plane can be formed by $\langle q \rangle$ and $\langle c \rangle_s$, which is perpendicular to the sample surface. The task now is to determine where the $\langle c \rangle_g$ locates at, either in the reference plane or in the plane which is perpendicular to both sample surface and the reference plane, or in some intermediate plane. This problem can be solved by tilting the sample to change the angle θ . If $\langle c \rangle_g$ is in the reference plane, by rotating the sample about the x-axis which is perpendicular to the reference plane will result in a maximum angle θ change, which should create a different coupled TO phonon according to the equation (9). But the coupled TO frequency will keep unchanged when rotate the sample about the $\langle c \rangle_s$. In fact, this is the case for the GaN/m-sapphire sample we have, as shown in Fig. 4 (a). The solid line refers to the Raman data of the untilted sample case, which has the coupled TO at 541 cm^{-1} . The other dash lines refer to the -20° , -30° , 20° , and 30° tilted sample cases, which show that the coupled TO phonon moves either to higher or lower wave number indicating the angle θ is changed correspondingly with the sample rotations. The coupled TO wave number keeps unchanged while rotates the sample about the $\langle c \rangle_s$ in our experiment. The calculated and experimental values of the coupled TO phonon frequency as a function of angle θ is plotted in Fig. 4 (b). Notice that the relation between θ and α is untrue for

$$\theta = 58^\circ \pm \alpha, \quad (11)$$

where α is the tilting angle. In stead,

$$\theta = 58^\circ \pm \arcsin[\sin(\alpha) / n_g] \quad (12)$$

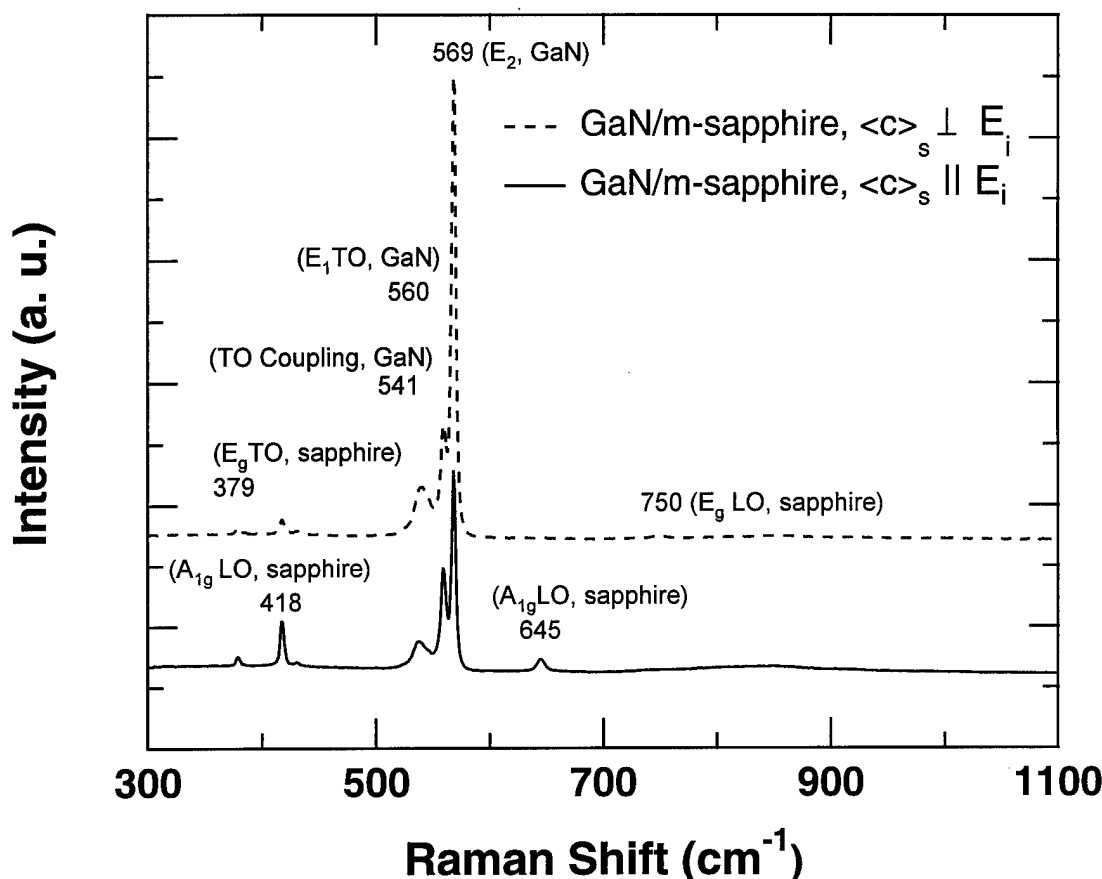


Fig. 3. Optical phonons of GaN film grown on m-plane sapphire substrate at two sample positions respect to the polarization. Dash line represents $\langle c \rangle_s \perp E_i$ case where 645 cm^{-1} LO of sapphire is forbidden, and solid line represents $\langle c \rangle_s \parallel E_i$ case, where the 645 cm^{-1} LO of sapphire is allowed.

is true when the sample is tilted away α degree. Where $n_g = 2.4$ is the refractive index of GaN at the probe laser wavelength (488nm). By taking account the interface refraction effect on the $\langle q \rangle$ direction, the experimental data is in good agreement with the theory.

4.2. Generalized ellipsometry of GaN/m-sapphire

Optical anisotropy can also be measured by generalized ellipsometry, especially the transmission type measurements for transparent materials. The TVASE data of an a-plane sapphire are shown in Fig. 5 as a good example. The data were obtained at 0° , 1° and 60° sample positions in the range of 0.75 eV to 5.8 eV. The angle of incidence are 20° and 30° , respectively. It can be seen clearly in Fig. 5 (c) that the off-diagonal elements A_{pst} and A_{spt} of the Jones matrix have large ψ values indicating the existence of the optical anisotropy in sapphire crystal. The magnitude of the off-diagonal signal in Fig. 5 (b) is still in reasonable size even for only about 1° difference between $\langle c \rangle_s$ and x-axis. The zero A_{pst} and A_{spt} in Fig. 5 (a) are obtained at the sample position of $\langle c \rangle_s \parallel x$ (the same result for $\langle c \rangle \perp x$). By finding the zero A_{pst} and A_{spt} position, the optical axis of sapphire can thus be fully determined. The results from Fig. 5 agree each other very well with Raman analysis in Fig. 1, but with more accuracy ($<1^\circ$). The one drawback of TVASE method for determining the optical axis is that TVASE can not distinguish the 0° and 90° position since all the off-diagonal elements are zero at these two positions.

In order to reveal the optical anisotropy of GaN, a series of anisotropic mode TVASE measurements have been made on the GaN/m-sapphire sample, as shown in Fig. 6. The selected typical data here are taken from four sample positions: 0° , 1° , 90°

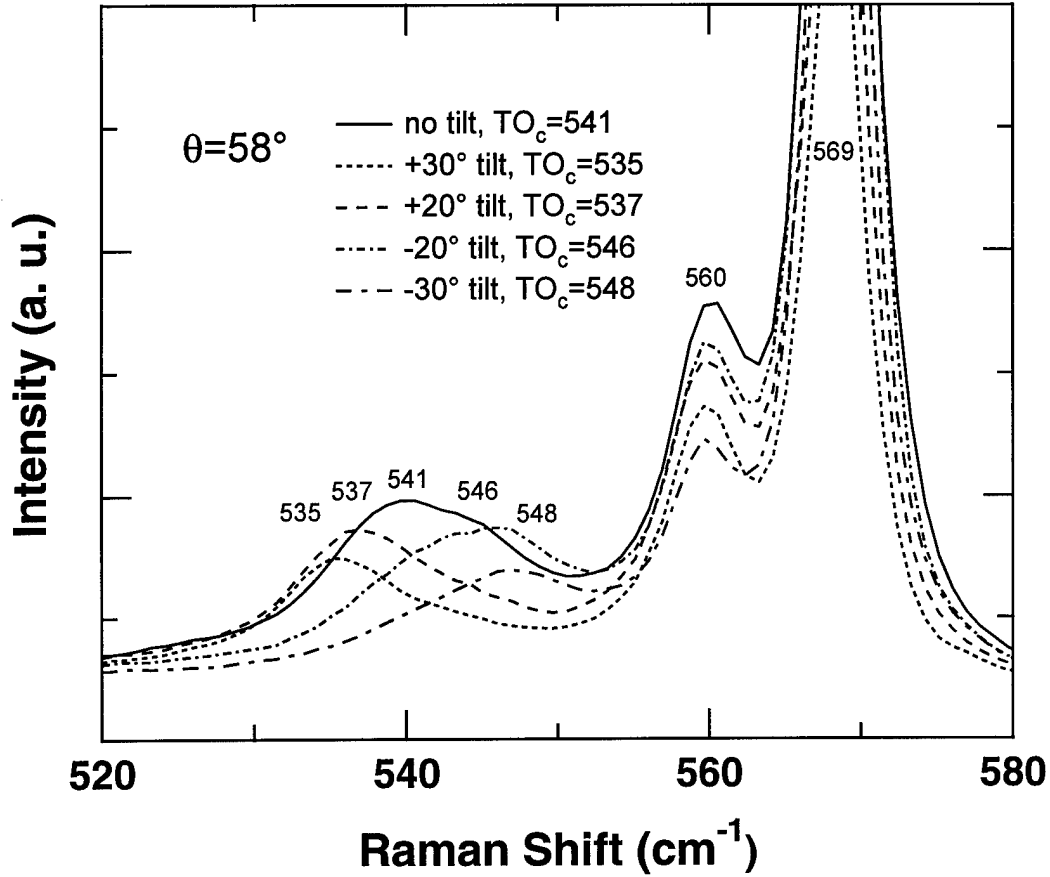


Fig 4. (a) Anisotropic angular dependence of the coupled TO phonon of GaN grown on m-plane sapphire. The sample was rotated about the x-axis which is in the sample surface plane and perpendicular to the sapphire optical axis $\langle c \rangle_s$.

and 92° , as shown in Fig. 6. The angle α is between $\langle c \rangle_s$ and x-axis. The spectra are cut off at about 3.4 eV since no transmission above the GaN band gap. Multiple angles of incidence (0° , 10° , 20° and 30°) have been used for collecting strong off-diagonal signal. At 0° position shown in Fig. 6 (a), the off-diagonal elements A_{pst} and A_{spt} are all zero. A clear conclusion can be drawn from Fig. 6 (a) is that the optical axis of GaN $\langle c \rangle_g$ must lay in the plane of incidence somewhere between x-axis and z-axis, since $\langle c \rangle_g$ could be along neither x-axis nor y-axis direction for the zero A_{pst} and A_{spt} , and we already know from Raman scattering that the angle between $\langle c \rangle_g$ and $\langle c \rangle_s$ is larger than zero and less than 90° . Recall the calculation result based on the coupled TO phonon mode at 541 cm^{-1} and equation (9), the angle θ between $\langle q \rangle$ and $\langle c \rangle_s$ is about 58° . We now also know that the so-called reference plane formed by $\langle q \rangle$ and $\langle c \rangle_s$ defined previously is the plane of incidence. Therefore, The orientation of $\langle c \rangle_g$ can be fully determined, which is in the reference plane (or the plane of incidence) and 32° away from $\langle c \rangle_s$ (or x-axis). To test the accuracy of this measurement, another TVASE data was taken at 1° position as shown in Fig. 6 (b). The sizable A_{pst} and A_{spt} were detected at all the angles of incidence indicating the sensitivity of TVASE is high enough. At a larger angle position, much bigger pairs of A_{pst} and A_{spt} can be obtained, which is a good evidence of the optical anisotropy of the whole structure. However, it is difficult to know how much anisotropy comes from GaN at these positions. Because of the special orientation relationship between $\langle c \rangle_g$ and $\langle c \rangle_s$ for GaN on m-plane sapphire, the 90° position can serve very well for this purpose as shown in Fig. 6 (c). The nonzero A_{pst} and A_{spt}

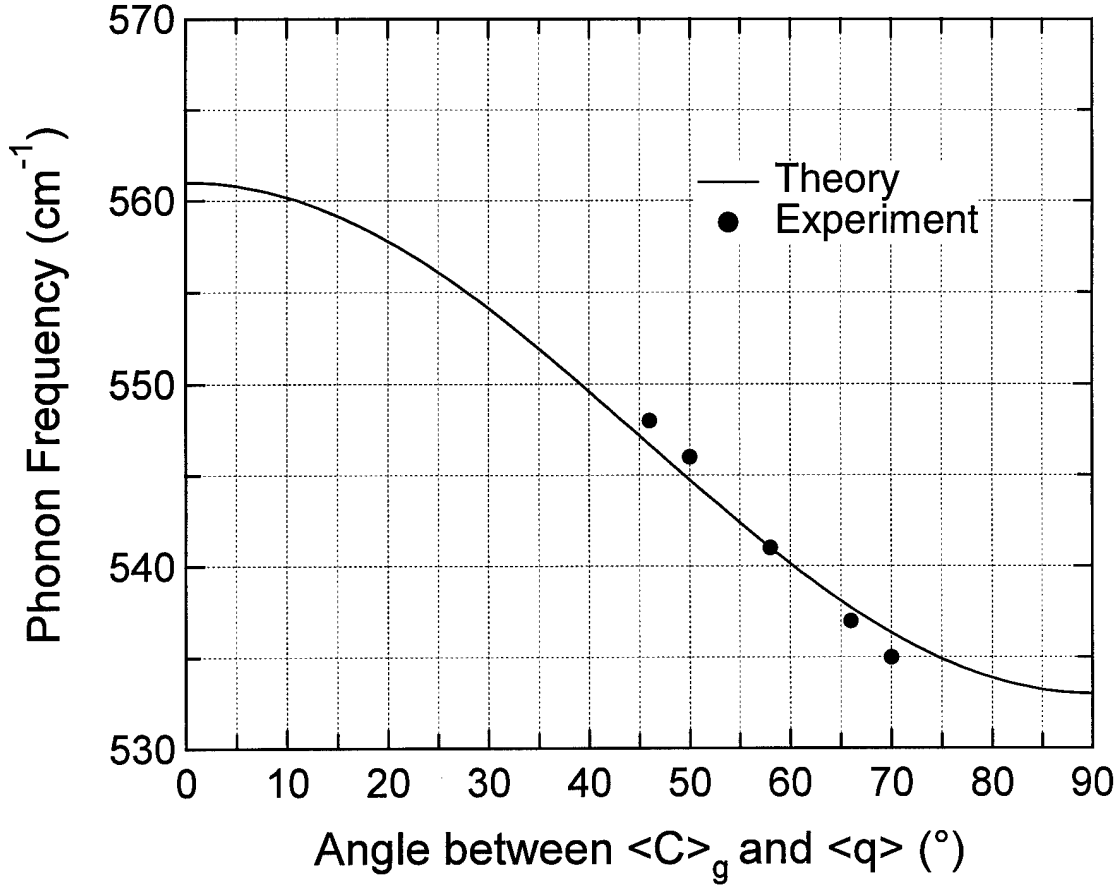


Fig. 4 (b) A comparison of the coupled TO positions from the theoretical calculation and the experimental data.

appeared in Fig. 6 (c) are purely due to the anisotropy of GaN film, since the contribution from sapphire substrate to the A_{pst} and A_{spt} is zero. Data in the Fig. 6 (c) is very valuable especially for GaN dielectric functions study. Only two degree away from the 90° position, the A_{pst} and A_{spt} are modified by the sapphire substrate dramatically as shown in Fig. 6 (d). This indicates that the optical axis orientation of GaN can be determined accurately.

The angle of incidence dependence of the optical anisotropy is showed in Fig. 7 (a) and (b) refer to two sample positions, 0° and 90° , respectively. The TVASE data was taken at three photon energies of 1.0 eV, 1.6 eV, and 2.2 eV (arbitrary chosen below GaN band gap). The angular increment is 1° . In Fig. 7 (a), the off-diagonal elements are zero in the whole angular range. This is due to that the $\langle c \rangle_g$ and $\langle c \rangle_s$ are all in the plane of incidence. In Fig. 7 (b). A different behavior is observed for the same three wavelengths below the band gap. This is because that the optical axis of GaN is in the plane perpendicular to both the sample surface and the plane of incidence. As discuss previously the magnitude of A_{pst} and A_{spt} are all contributed by GaN. The A_{pst} and A_{spt} are zero at normal incidence at 90° position which is again the proof of $\langle c \rangle_g$ in the reference plane. The bigger A_{pst} and A_{spt} values at larger angle of incidence suggest that a large angle of incidence is usually a better choice for measuring the optical anisotropy by TVASE.

According to the data analysis of both Raman scattering and TVASE, the growth configuration of this GaN/m-sapphire sample is $(01\bar{1}3)/(0001)$ as the interface plane, and $[03\bar{3}2]/[01\bar{1}0]$ as the in-plane orientation preference, which is different from the reported structure configuration $(01\bar{1}3)/(01\bar{1}0)$ as the interface plane, and $[03\bar{3}2]/[2\bar{1}\bar{1}0]$ as the in-plane orientation preference. we consider this is the other option for GaN grow on m-plane sapphire substrates.

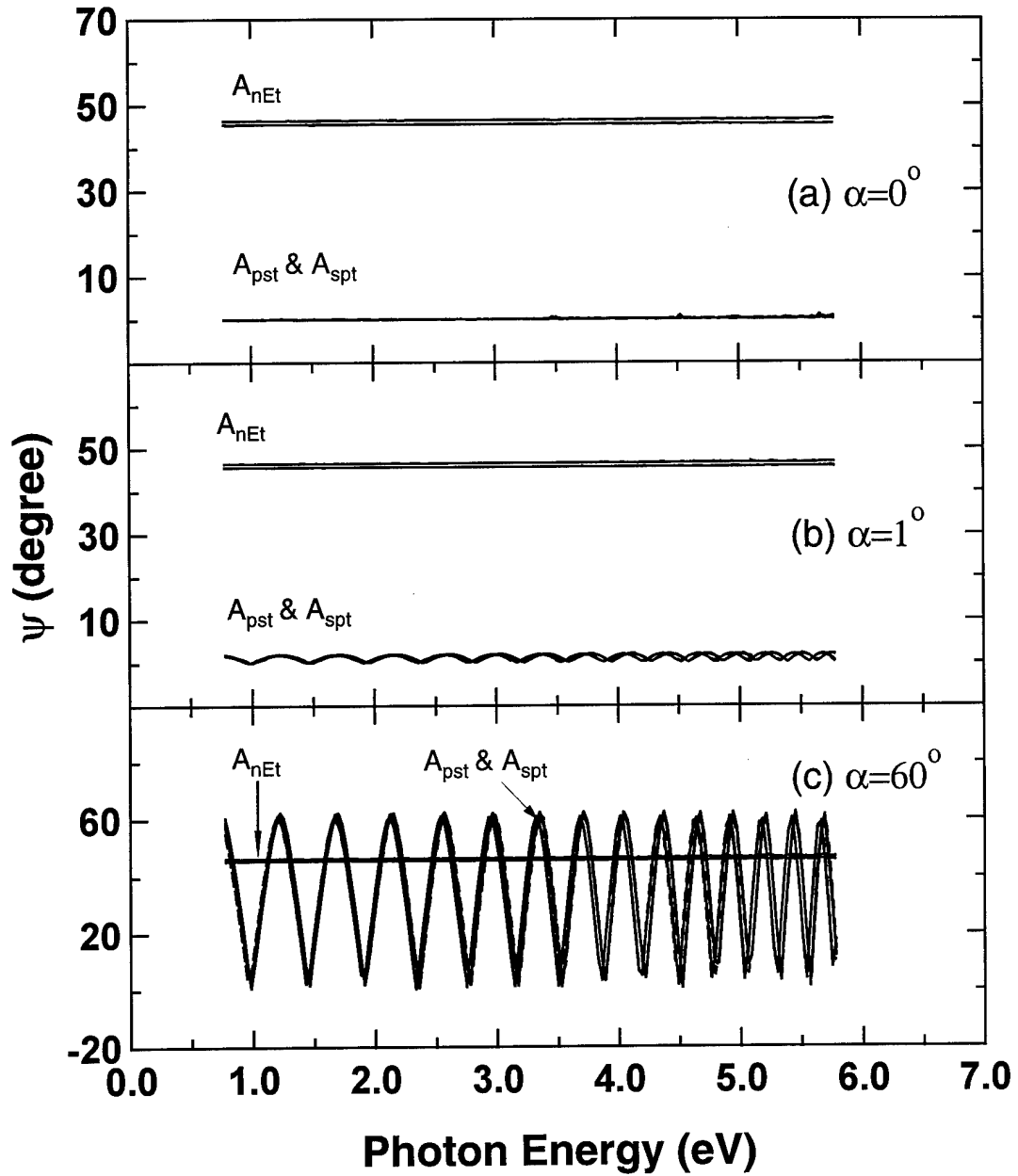


Fig.5. Transmission VASE data of an a-plane sapphire at the angle of incidence of 20° and 30°, respectively. (a) $\alpha=0^\circ$; (b) $\alpha=1^\circ$; (c) $\alpha=60^\circ$. α is the angle between the optical axis and x-axis of the lab coordinates.

5. Summary

Optical anisotropy nature of GaN films grown on m-plane sapphire substrates was characterized by Raman scattering and generalized variable angle spectroscopic ellipsometry. A 541 cm^{-1} phonon of GaN due to the TO coupling was observed experimentally and it agrees very well with the theoretical prediction. The coupled TO phonon of GaN film grown on m-plane sapphire substrate is a good signature of its optical anisotropy, and the angular dependence relation can be used to

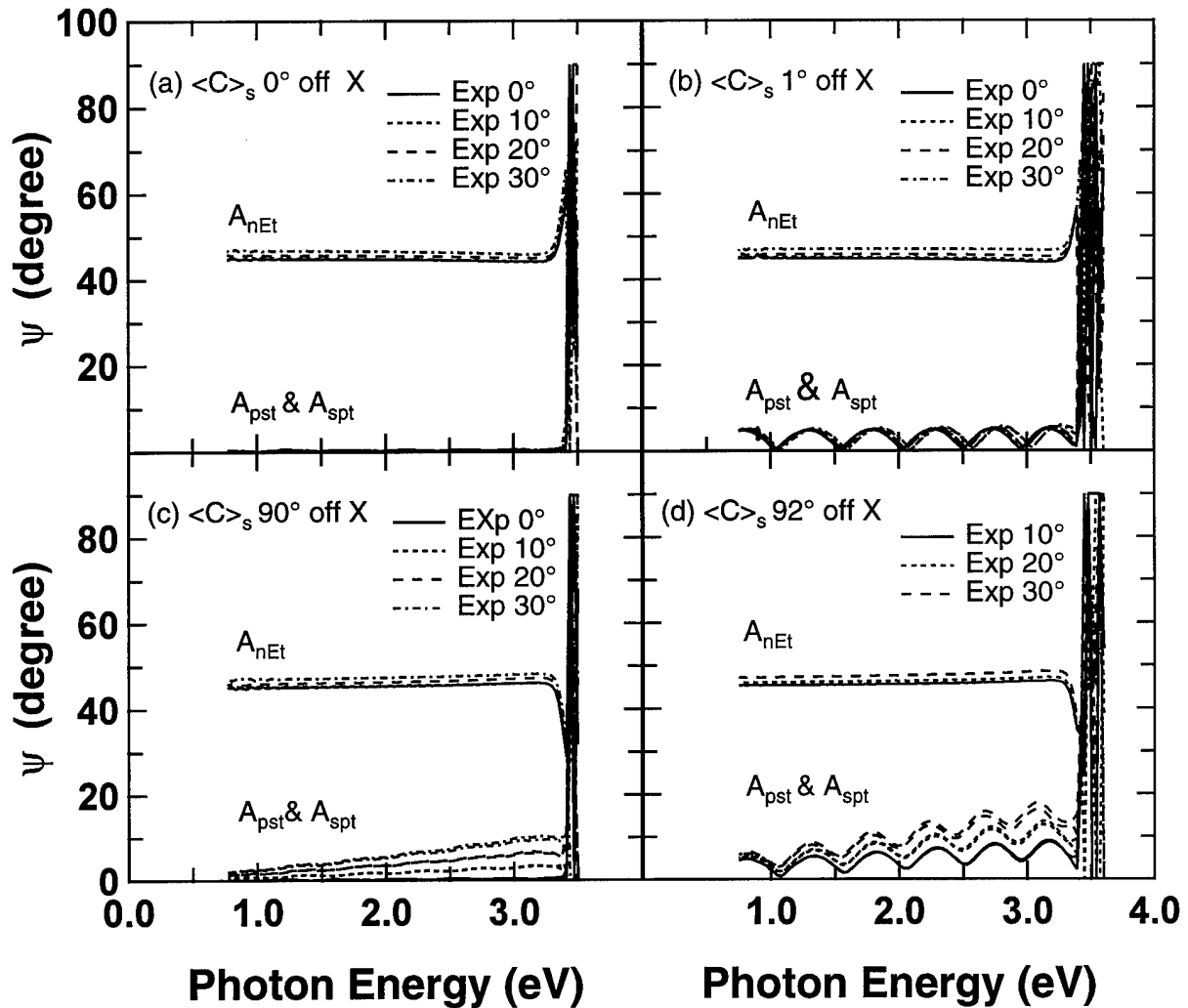


Fig. 6. Transmission VASE data of GaN/m-sapphire at the angle of incidence of 0°, 10°, 20° and 30°, respectively. (a) $\langle C \rangle_s$ 0° off X-axis; (b) $\langle C \rangle_s$ 1° off X-axis; (c) $\langle C \rangle_s$ 90° off X-axis; (d) $\langle C \rangle_s$ 92° off X-axis. A_{pst} and A_{spt} are the off-diagonal elements of transmission Jones matrix.

determine the location of $\langle c \rangle_g$. It is also found that the off-diagonal elements of transmission type Jones matrix are very sensitive to both the sample position and the angle of incident. The optical axis of GaN is fully determined by using the null A_{pst} and A_{spt} position at 0°, which is in good agreement with the result from the angular dependence Raman scattering. According to the analysis of both Raman and TVASE, the $\langle c \rangle_g$ of GaN on m-plane sapphire lies in the reference plane defined by $\langle q \rangle$ and $\langle c \rangle_s$, and it is 32° away from the $\langle c \rangle_s$. TVASE measurement at 90° position has given non-zero A_{pst} and A_{spt} which are purely due to the anisotropy of GaN film, this kind of data will be very important for the future studies of anisotropic dielectric functions of GaN. A new growth configuration of GaN on m-plane sapphire has been observed as (01 $\bar{1}$ 3) / (0001), and [03 $\bar{3}$ 2] / [0 $\bar{1}$ 10] for the interface plane and in-plane orientation preferences.

Acknowledgments

This work was supported by US Army Research Office under Grant No. DAAG55-98-1-0462. We thank Dr. Richard J. Molnar at MIT Lincoln Laboratories for providing GaN/m-sapphire samples for this study.

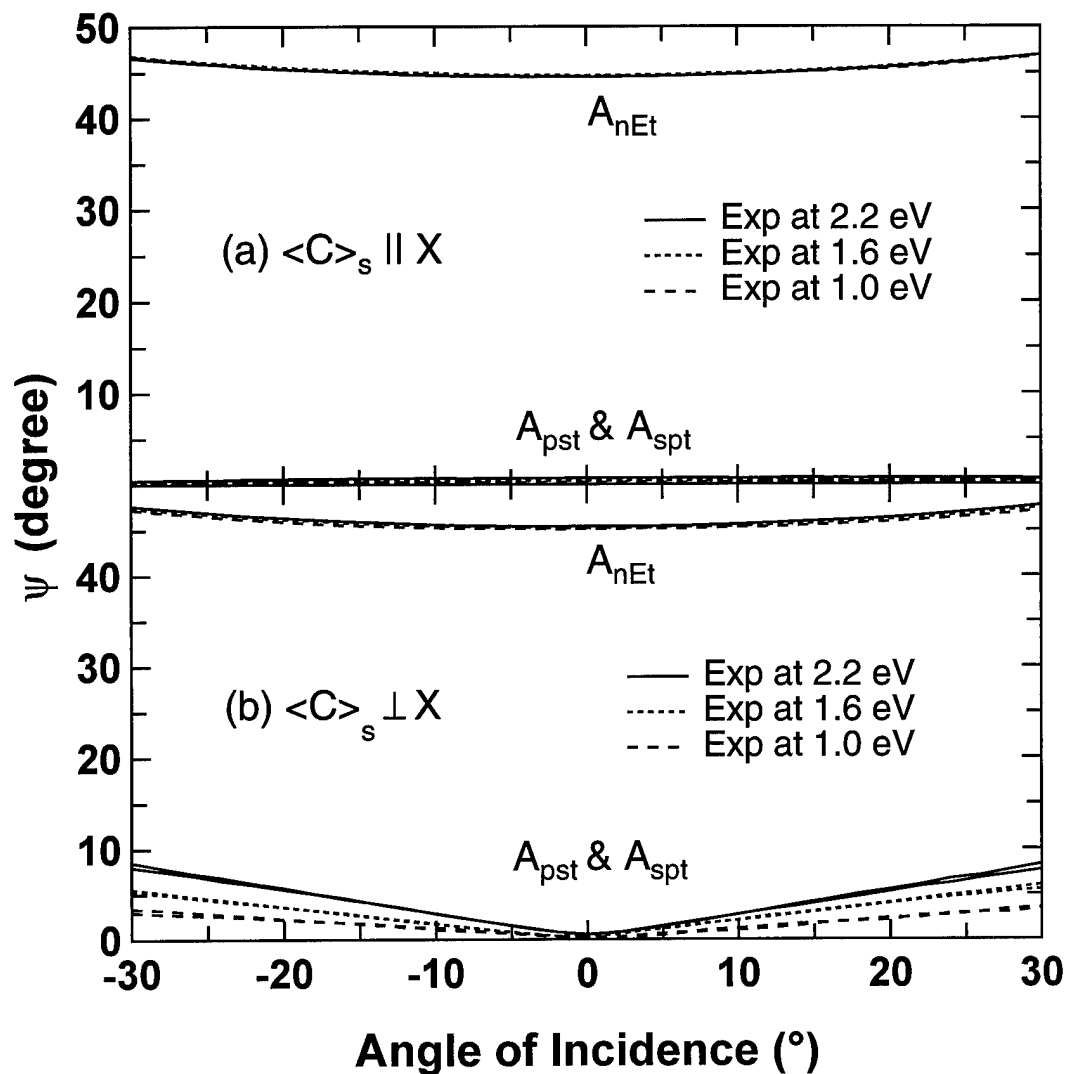


Fig. 7. Incident angular dependence of A_{pst} and A_{spt} of GaN/m-sapphire at 1.0, 1.6, and 2.2 eV, respectively. (a) $\langle c \rangle_s \parallel x$, (b) $\langle c \rangle_s \perp x$.

References

1. H. Morkoc, S. Strite, G. B. Gao, M. E. Lin, B. Sverdlov, and M. Burns, "Large-band-gap SiC, III-V nitride, and II-VI ZnSe-based semiconductor device technologies," *J. Appl. Phys.* **76**, pp. 1363-1398, 1994.
2. S. Nakamura, T. Mukai, and M. Senoh, "Candela-class high-brightness InGaN/AlGaIn double-heterostructure blue-light-emitting diodes," *Appl. Phys. Lett.* **64**, pp. 1687-1679, 1994.
3. S. Nakamura, M. Senoh, N. Iwasa, and S. Nagahama, "High-Brightness InGaIn Blue, Green and Yellow Light-Emitting Diodes with Quantum Well Structures," *Jpn. J. Appl. Phys.* **34**, pp. L797-L799, 1995.
4. S. Nakamura, M. Senoh, S. Nagahama, N. Iwasa, T. Yamada, T. Matsushita, H. Kiyoku and Y. Sugimoto, "InGaIn-Based Multi-Quantum-Well-Structure Laser Diodes," *Jpn. J. Appl. Phys.* **35**, pp. L74-L76, 1996.
5. S. Nakamura, M. Senoh, S. Nagahama, N. Iwasa, T. Yamada, T. Matsushita, H. Kiyoku, Y. Sugimoto, T. Kozaki, H. Umemoto, M. Sano, and K. Chocho, "Continuous-wave operation of InGaIn/GaN/AlGaIn-based laser diodes grown on GaN substrates," *Appl. Phys. Lett.* **72**, pp. 2014-2016, 1998.

6. Z. C. Feng, M. Schurman, R. A. Stall, M. Pavlosky and A. Whitley, "Raman scattering as a characterization tool for epitaxial GaN thin films grown on sapphire by turbo disk metal-organic chemical vapor deposition," *Applied Optics* **36**, pp. 2917-2922, 1997.
7. T. Kawashima, H. Yoshikawa, S. Adachi, S. Fuke, and K. Ohtsuka, "Optical properties of hexagonal GaN," *J. Appl. Phys.* **82**, pp. 2528-3535, 1997.
8. T. Matsuoka, "Lattice-matching growth of InGaAlN systems," *Mat. Res. Soc. Symp. Proc.* **395**, pp. 39-50, 1996.
9. H. Yao, C. H. Yan, S. P. Denbaars, J. M. Zavada, "Optical anisotropy studies of sapphire by Raman scattering and spectroscopy transmission ellipsometry," *Mat. Res. Soc. Symp. Proc.* **512**, pp. 411-416, 1998.
10. S. P. S. Porto and R. S. Krishnan, "Raman effect of corundum," *J. Of Chem. Phys.* **47**, pp. 1009-1012, 1967.
11. T. Azuhata, T. Sota, K. Suzuki and S. Nakamura, "Polarized Raman spectra in GaN," *J. Phys.: Condens. Matter* **7**, pp. L129-L133, 1995.
12. R. M. A. Azzam and N. M. Bashara, *Ellipsometry and Polarized Light*, North-Holland, Amsterdam, 1977.
13. M. Schubert, B. Rheinlander, J. A. Wollam, B. Johs, and C. M. Herzinger, "Extension of rotating analyzer ellipsometry to generalized ellipsometry: determination of the dielectric function tensor from uniaxial TiO₂," *J. Opt. Soc. Am.* **A13**, pp. 875-883, 1996.
14. R. M. A. Azzam, and N. M. Bashara, "Generalized ellipsometry for surface with directional preference: application to diffraction gratings," *J. Opt. Soc. Am.* **62**, pp. 1521-1523, 1972.
15. D. W. Berreman, "Optics in stratified and anisotropic media: 4x4 matrix formulation," *J. Opt. Soc. Am.* **62**, pp. 502-510, 1972.
16. M. Schubert, "Polarization dependent parameters of arbitrarily anisotropic homogeneous layered systems," *Phys. Rev. B*, **53**, pp. 4265-4274, 1996.
17. G. H. Wei, J. Zi, K. M. Zhang, X. D. Xie, "Zone-center optical phonons in wurtzite GaN and AlN," *J. Appl. Phys.* **82**, pp. 4693-4695, 1997.
18. R. Loudon, "The Raman effect in crystals," *Advan. Phys.* **13**, pp. 423-482, 1964.

Anisotropic optical responses of sapphire (α -Al₂O₃) single crystals

H. Yao^{a)} and C. H. Yan

Center for Microelectronic and Optical Materials Research, and Department of Electrical Engineering, University of Nebraska-Lincoln, Lincoln, Nebraska 68588-0511

(Received 6 January 1999; accepted for publication 20 January 1999)

Anisotropic dielectric functions of sapphire have been determined by both reflection and transmission variable angle spectroscopic ellipsometry. The measurements were made on *a*-plane (2 $\bar{1}\bar{1}$ 0) sapphire substrates in the energy range of 0.75–6.5 eV at room temperature. The orientation of the optic axis of the *a*-plane sapphire sample was determined by polarized Raman scattering based on which the Euler angles are set for the fitting model. Two pairs of Cauchy user-defined functions were constructed to describe the optical constants of both ordinary $n_{\perp}(\omega)$ and extraordinary $n_{\parallel}(\omega)$ rays, respectively. As a result the optical constants from the generalized ellipsometry analysis are in good agreement with the reported data. The Kramers–Kronig (KK) relation between the real and the imaginary part have been carefully checked for both ordinary and extraordinary rays. The perfect fitting between the calculated and experimental $\epsilon_1(\omega)$ function indicates that both functions of ordinary and extraordinary rays are KK consistent. The refractive index difference between the ordinary and extraordinary rays is close to a constant (+0.008), which is determined mainly by the off-diagonal signal of the transmission ellipsometry data. The extinction coefficients are zero below 6 eV, and increase rapidly above 6 eV. © 1999 American Institute of Physics. [S0021-8979(99)01409-7]

I. INTRODUCTION

Sapphire crystals have many attractive properties that make them widely applied in solid-state device fabrications. More recently, due to the dramatic progress in the GaN related blue light emitting diodes (LEDs) and lasers field, sapphire as a good substrate candidate has become even more important than in the past since its crystal structure is similar to GaN and allows us to realize a small lattice mismatch growth.

It is essential to have precise measurements of the optical constants of sapphire for further optical study on GaN and related materials, since the optical dielectric response is of utmost importance for optoelectronic device design. Because of the rhombohedral structure of both GaN and sapphire crystal, they are optically anisotropic (uniaxial). To study the optical properties of GaN film grown on sapphire substrate, it is necessary to have the knowledge of the optical response of sapphire. This is the main purpose of our study on sapphire. Although the optical properties of sapphire have been studied since 1958¹ and continue to receive attention,^{2–4} most of the results are about the ordinary optical response (the optical axis is perpendicular to the light polarization). The current state of the optical measurements of the extraordinary response is still less than adequate; only several discrete values are available which were obtained by the traditional prism method.⁵ Another work⁶ does present the extraordinary response in a fairly wide energy range, but the range of experimental data is limited to 1.2–5.4 eV, and only the normal reflection ellipsometry was employed in their work, which does not have very high sensitivity for the de-

termination of the difference of the refractive index between the ordinary and extraordinary rays. Therefore, more precise optical measurements are needed to determine accurately the anisotropic response in a wider photon energy range.

In this work, we report the determination of room-temperature anisotropic optical constants of sapphire crystal in the energy range of 0.75–6.5 eV by intensity transmission, reflection variable angle spectroscopic ellipsometry (R-VASE), and transmission VASE (T-VASE). All the measurements were taken from *a*-plane sapphire samples. The optical constants were extracted from VASE analysis of all three types of measurements by a multiple-sample, multiple-model method.

II. EXPERIMENTS

Two pieces of *a*-plane (2 $\bar{1}\bar{1}$ 0) sapphire substrates were used in our optical measurements. A single-side polished one was for R-VASE, and the other double-side polished one was for intensity transmission and T-VASE measurements. For these *a*-plane samples, the optic axis $\langle c \rangle$ is parallel to the sample surface, and it will be shown later how the $\langle c \rangle$ orientation is determined by Raman scattering.

The optical measurements were performed in the energy range of 0.75–6.5 eV with a 0.03 eV increment. The intensity transmission data were taken under both $\langle c \rangle \perp E_i$ ($\langle c \rangle$ is the optic axis, and E_i is the electric field direction of the incident light) and $\langle c \rangle \parallel E_i$ conditions. The optic axis was set at 45° horizontal for the R-VASE measurements. A series of angle of incidences were used from 65° to 75°. The most important T-VASE measurements were taken at three sample positions, the angles between $\langle c \rangle$ and E_i being 1°, 60°, and

^{a)}Electronic mail: hyao@unl.edu

90°, respectively. Two angles (20° and 30°) of incidence were used at each sample position.

Polarized Raman scattering was used as a complementary tool to determine the optic axis orientation of the *a*-plane sapphire samples. The probe light was a 488 nm argon laser beam. The scattered light was detected by a charge coupled device (CCD) camera under a backscattering geometry.

III. ELLIPSOMETRY BASICS

A. Standard ellipsometry

The variable angle spectroscopic ellipsometry is designed to accurately determine the values of two standard ellipsometry parameters ψ and Δ , which are related to the complex ratio of reflection (or transmission) coefficients for light polarized parallel (*p*) and perpendicular (*s*) to the plane of incidence.⁷ For the isotropic material system

$$\rho = \frac{R_p}{R_s} = \tan(\psi)e^{i\Delta}. \quad (1)$$

The electric field reflection coefficient at an incident angle of ϕ is defined as $R_p(R_s)$ for *p*(*s*)-polarized light. They are the diagonal elements of the Jones matrix as

$$[J]_{\text{sample}} = \begin{bmatrix} R_p & 0 \\ 0 & R_s \end{bmatrix}. \quad (2)$$

The ψ and Δ are not only dependent on dielectric functions, but also on the surface condition, sample structure, and other properties such as the optical anisotropy of the material.

The pseudodielectric function $\langle\epsilon\rangle$ can be obtained directly from the measured ψ and Δ values

$$\langle\epsilon\rangle = \langle\epsilon_1\rangle + i\langle\epsilon_2\rangle = \sin^2\phi \left[1 + \tan^2\phi \left(\frac{1-\rho}{1+\rho} \right)^2 \right]. \quad (3)$$

In the case of an air ambient over a bare bulk material with an ideal smooth surface, the pseudodielectric and intrinsic dielectric functions are identical. To determine optical constants of a sample with more complicated structure, VASE data must be analyzed using a parametric model that is adjusted to fit the measured data.⁷

For the anisotropic material system, the off-diagonal elements of the Jones matrix are no longer zero. In the reflection VASE configuration, it can be written as

$$[J]_{\text{sample}} = \begin{bmatrix} R_{pp} & R_{sp} \\ R_{ps} & R_{ss} \end{bmatrix}. \quad (4)$$

By using the same approach with considerably more algebra involved, we can still predict the ψ and Δ values, but the Fourier coefficients related to ψ and Δ become more complicated,⁸ and similar treatments are needed for the transmission VASE.

B. Generalized ellipsometry

In principle standard ellipsometry, which is related to structures which reflect or transmit *p*- or *s*-polarized light into *p*- or *s*-polarized light, respectively, can be used to determine both ordinary and extraordinary constants of an an-

isotropic sample by mounting it in a special manner so that the optic axis is strictly either perpendicular or parallel to the electric field of the incident beam.^{6,9} The Jones matrix in this case is strictly diagonal. But there are several problems for this application. (1) It is hard to make a perfect alignment since the crystal is usually cut with up to an error of several degrees so that the off-diagonal elements of the Jones matrix will not vanish completely. (2) R-VASE cannot directly give the information of the difference of n_{\perp} and n_{\parallel} . Especially for a very small $n_{\perp} - n_{\parallel}$, e.g., $n_o - n_e = 0.008$ for sapphire, it is not reliable to determine the $n_{\perp} - n_{\parallel}$ only by the standard R-VASE data which are dominant by the diagonal elements. (3) For most material analysis, we may deal with thin films grown on substrates, like GaN on sapphire. This is the system which has an anisotropic material on another anisotropic material, and even if we know the orientation of the optic axis of the substrate, the optic axis of the GaN film is probably unknown, and in general it may not overlap with the substrate optic axis. In this situation, the standard R-VASE is no longer adequate. Therefore, we need a technique which is able to detect the off-diagonal elements and also has a corresponding model to analyze the data.

Generalized ellipsometry, which was first introduced by Azzam and Bashara¹⁰ can serve this purpose. The recent developments make this technique more complete and powerful.^{11,12} In a word, the generalized ellipsometry is a technique which can be used to determine all the elements of the Jones matrix of arbitrarily anisotropic and homogeneous layered systems with nonscalar dielectric susceptibilities.

C. Data type and modeling

Within the generalized ellipsometry, several new terms have been defined. For reflection ellipsometry, the elements of the Jones matrix are A_{nE} , A_{ps} , and A_{sp}

$$\begin{aligned} [J]_{\text{sample}} &= \begin{bmatrix} R_{pp} & R_{sp} \\ R_{ps} & R_{ss} \end{bmatrix} = R_{ss} \begin{bmatrix} \frac{R_{pp}}{R_{ss}} & \frac{R_{sp}}{R_{ss}} \\ \frac{R_{ps}}{R_{pp}} & \frac{R_{pp}}{R_{ss}} \end{bmatrix} \\ &= R_{ss} \begin{bmatrix} A_{nE} & A_{sp} \\ A_{ps}A_{nE} & 1 \end{bmatrix}. \end{aligned} \quad (5)$$

The A_{nE} parameter is the complex ratio of reflection coefficients similar to ρ of the isotropic material case. But the A_{ps} and A_{sp} are the ratios counting the amount of *p*- (or *s*-) polarized light that converts to *s*- (or *p*-) polarized light after the reflection from an anisotropic material system. In the generalized VASE, three pairs of ψ and Δ are the measured parameters, which associate with A_{nE} , A_{ps} , and A_{sp} , respectively. In the same manner, the Jones matrix elements of transmission VASE are defined as A_{nEt} , A_{pst} , and A_{spt} , respectively. They also have three pairs corresponding to ψ and Δ as the measured parameters.

In order to obtain the optical constants by analyzing the experimental data, an optical model containing the fitting parameters that can fully describe sapphire optical property is needed. Since sapphire is a uniaxial crystal, i.e., it has an optical axis that is associated with the optical anisotropy. In

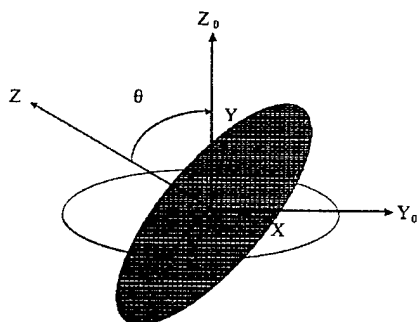


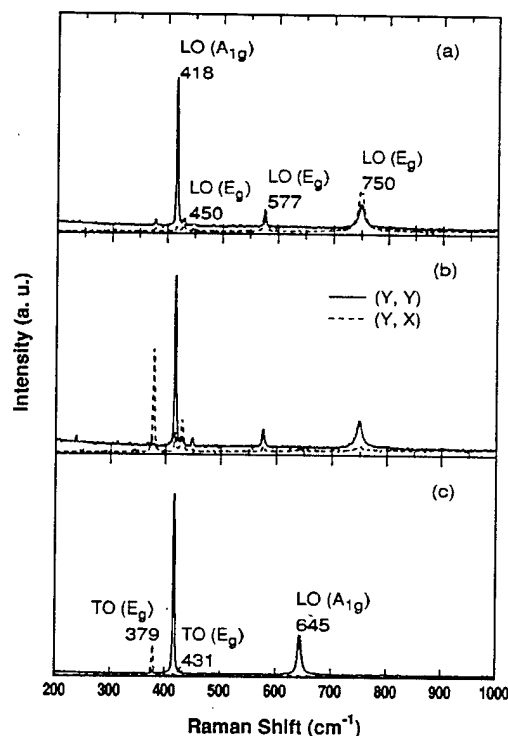
FIG. 1. The Eulerian angles and related coordinates.

addition, since sapphire ($\alpha\text{-Al}_2\text{O}_3$) is chemically stable in air, no surface oxide layer was considered in the model. Therefore an one-layer uniaxial sapphire model can be constructed by the sample thickness and two sets of optical constants, ordinary $n_{\perp}(\omega)$, $k_{\perp}(\omega)$ and extraordinary $n_{\parallel}(\omega)$, $k_{\parallel}(\omega)$. Once the lab coordinate is selected, the relative spatial orientation of the optical axis of the sapphire sample can be located by using Euler angles ϕ , θ , and ψ , as shown in Fig. 1. Our lab-fixed axes are the X_0 , Y_0 , Z_0 . The Z_0 axis is normal to the sample surface. The X_0 and Z_0 axes are in the plane of incidence. The Y_0 axis is perpendicular to the plane of incidence. The sample unit-cell-fixed axes are X , Y , and Z . As shown in Fig. 1, Euler angles ϕ , θ , and ψ correspond to rotations about the Z axis, then about the new X axis, and then again about the new Z axis. The uniaxial sapphire model can be constructed either based on c -plane or a -plane configurations. If an a plane is selected, we may choose the electric field of the extraordinary ray parallel to the Y_0 direction (or X_0 direction), thus the X_0 (Y_0) and Z_0 directions are correspond to the E fields of the ordinary ray. If the a -plane sample is mount with its optic axis parallel to the Y_0 direction, all the Euler angles are zero under such conditions. In general, the optic axis of a sample may lie in an arbitrary direction and the Euler angles have nonzero values. For instance, if $\phi=20^\circ$ and $\theta=\psi=0^\circ$, it means that the n_{\perp} of sapphire is orientated 20° from the X_0 axis in the sample surface plane, the n_{\parallel} is orientated 20° from the Y_0 axis, and the $n_z=n_{\perp}$ is still normal to the sample surface.

IV. RESULTS AND DISCUSSION

A. Optic axis determination by polarized Raman scattering

In our study, a -plane substrates ($2\bar{1}\bar{1}0$) were selected in order to determine the optical constants of both ordinary $n_{\perp}(\omega)$ and extraordinary $n_{\parallel}(\omega)$. As mentioned earlier in the modeling part, the Euler angles in the model depend on the location of the optic axis. Therefore how to determine the orientation of the optic axis becomes very important. For a given small piece of an a -plane sapphire sample, its optic axis can be determined by polarized Raman scattering. The selection rules of Raman scattering on both c -plane and a -plane samples are shown in Fig. 2 for a comparison. The three pair spectra refer to two backscattering geometry,

FIG. 2. Polarized Raman effect of c -plane and a -plane sapphire samples: (a) $\langle c \rangle \perp E_i$, c plane; (b) $\langle c \rangle \perp E_i$, a plane; (c) $\langle c \rangle \parallel E_i$, a plane.

$Z(Y,Y)\bar{Z}$ (solid line) and $Z(Y,X)\bar{Z}$ (dashed line). Figure 2(a) is from a c -plane sample, Figs. 2(b) and 2(c) are from an a -plane sample, but with a 90° sample rotation between Figs. 2(b) and 2(c). The similar phonon spectra of Figs. 2(a) and 2(b) indicate that the optic axis of the a -plane sample in Fig. 2(b) geometry is perpendicular to the electric field of the incident laser beam E_i . The new strong 645 cm^{-1} longitudinal optical (LO) phonon peak in the Fig. 2(c) refers that the optic axis is parallel to the incident E field. It is the characteristic phonon peak of the lattice vibration along the optic axis direction. Therefore, by either minimizing or maximizing the 645 cm^{-1} peak intensity through the sample rotation, the optic axis of an a -plane sample can be easily located by polarized Raman scattering.

B. VASE data and analysis

Sapphire is a colorless, transparent material with very low reflectivity. The reflectivity of the off-diagonal elements are too small to detect. The reflection VASE data of both a c -plane and an a -plane sample are shown in Fig. 3. In theory, both A_{ps} and A_{sp} should be zero for the a c -plane sample, but they should not be zero for an a -plane sample. The near zero A_{ps} and A_{sp} we have seen in Fig. 3(b) is simply due to the weak reflectivity (about 1×10^{-6}). In order to collect all the information of the Jones matrix, a R-VASE, three T-VASE, and two intensity transmission measurements have been performed on two a -plane sapphire samples, the data and fittings of these three types are shown in Figs. 4, 5, and 6,

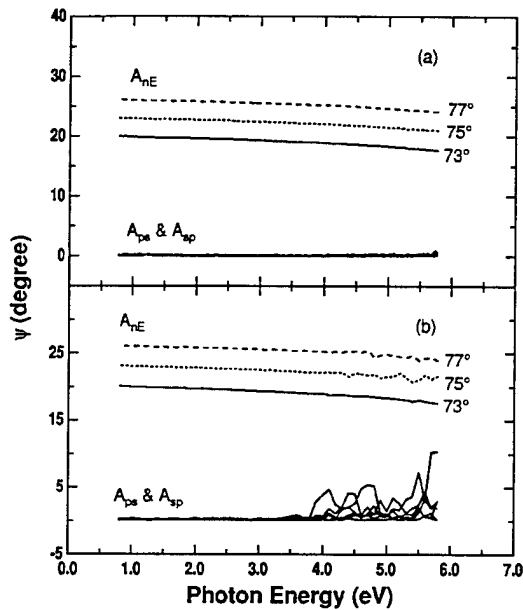


FIG. 3. Reflection-VASE data of: (a) *c*-plane, and (b) *a*-plane ($\langle c \rangle$ off E_i 45°) sapphire samples.

respectively. It can be seen clearly in Fig. 5(b) that the off-diagonal elements A_{pst} and A_{spt} of the T-VASE data have very big ψ values indicating the existence of the optical anisotropy in sapphire material. The magnitude of the off-diagonal signal as shown in Fig. 5(a) is still reasonable in size for only about 1° difference between $\langle c \rangle$ and E_i . The zero A_{pst} and A_{spt} in Fig. 5(c) are obtained at the sample position of $\langle c \rangle \perp E_i$ (the same result for $\langle c \rangle \parallel E_i$). The optic axis orientation is in well agreement with that determined from Raman measurements. The nearly identical intensity transmission spectra of Figs. 6(a) and 6(b) indicate that the difference between n_{\perp} and n_{\parallel} is very small even when using a quite thick sample (0.332 mm). The best model fit results for the three data types are also presented in the solid line in Figs. 4, 5, and 6, respectively. The excellent data fit indicates

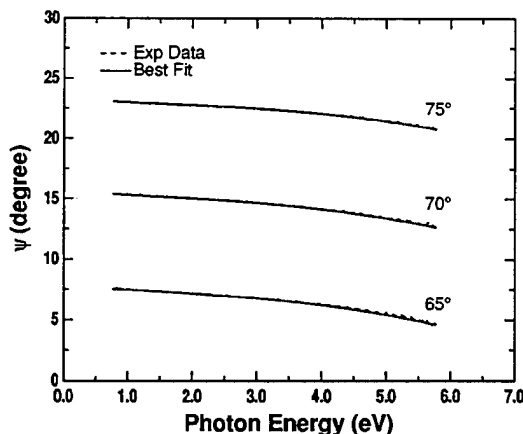


FIG. 4. Reflection VASE data and fittings of *a*-plane sapphire, $\langle c \rangle$ off E_i 45°.

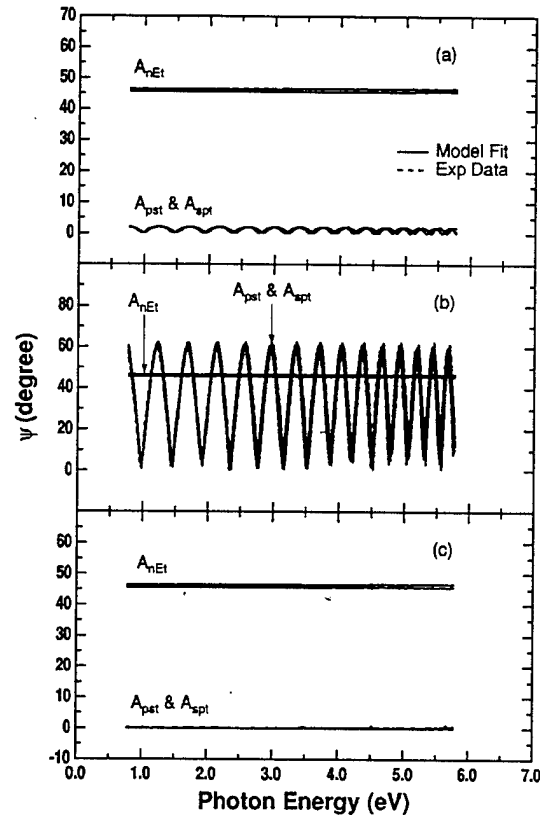


FIG. 5. Transmission VASE data and fittings of *a*-plane sapphire: (a) $\langle c \rangle$ off E_i 1°; (b) $\langle c \rangle$ off E_i 60°; (c) $\langle c \rangle$ off E_i 90°.

that our model correctly describes the optical anisotropy of the sapphire material.

In the uniaxial sapphire model, the known parameters are sample thickness which was measured by a micrometer, and the Euler angles based on the Raman measurements. The

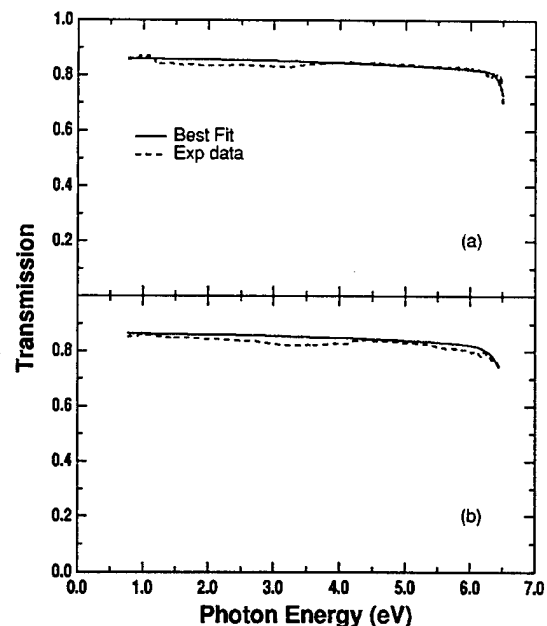


FIG. 6. Intensity transmission data and fittings: (a) ordinary ray ($\langle c \rangle \perp E_i$) and (b) extraordinary ray ($\langle c \rangle \parallel E_i$).

TABLE I. Best fitting parameters of the anisotropic sapphire optical constants in the energy range of 0.75–6.5 eV.

	A	B	C	D	E
n_{\perp}	1.734 94	0.025 60	-0.008 24	0.002 71	-0.000 13
n_{\parallel}	1.727 00	0.026 85	-0.008 41	0.002 71	-0.000 13
...	a	b	c	d	...
k_{\perp}	2.3279×10^{-7}	0.281 23	0.037 06	0.000 00	...
k_{\parallel}	4.3854×10^{-7}	0.280 72	0.043 70	0.000 00	...

four unknown quantities are n_{\perp} , k_{\perp} , and n_{\parallel} , k_{\parallel} described by two user-defined Cauchy functions which are shown below:

$$n = A + \frac{B}{\lambda} + \frac{C}{\lambda^2} + \frac{D}{\lambda^3} + \frac{E}{\lambda^4}, \quad (6)$$

$$k = (1 \times 10^{-5}) \times a \times \exp\{-(\lambda - b)/c\}^3 + d, \quad (7)$$

where λ is wavelength in μm . All the constants obtained from the best fitting are listed in Table I. Notice that we did not simply make the $k_{\perp} = k_{\parallel} = 0$ assumption in our data fitting since the k value may be detectable at high photon energy close to the band edge (about 9 eV)^{2,13} in a thick sample. In fact, the k values of larger than 1×10^{-6} were measured and they showed a non-negligible effect on all the transmission-type data. Therefore the $k=0$ assumption may bring a large error on the n results above 6 eV, since the intensity transmission is sensitive to sample thickness and nonzero k values. With an accurate thickness, both k_{\perp} and k_{\parallel} can be accurately determined by the intensity transmission spectra. The amplitude of n_{\perp} and n_{\parallel} are basically controlled by both A_{nE} and A_{nEt} , and the difference of n_{\perp} and n_{\parallel} is the key source of the big A_{pst} and A_{spt} values.

C. Kramers–Kronig consistency check

For a set of correct complex dielectric functions $\epsilon = \epsilon_1 + i\epsilon_2$ of any material, its real and imaginary parts by nature obey the Kramers–Kronig (KK) relation:^{9,14}

$$\epsilon_1(E) - 1 = \frac{2}{\pi} P \int_0^{\infty} \frac{E' \epsilon_2(E')}{E'^2 - E^2} dE'. \quad (8)$$

In our application, due to the limited measurement range of 0.75–6.5 eV, a modified form of the KK relation was used to check the KK consistency of a set of optical constants:

$$\epsilon_1^{kk}(E) = \epsilon_1^{\text{offset}} + \sum_{i=1}^2 \frac{A_i}{E_i^2 - (E)^2} + \frac{2}{\pi} P \int_{0.75 \text{ eV}}^{6.5 \text{ eV}} \frac{E' \epsilon_2^{\text{meas}}(E')}{E'^2 - (E)^2} dE'. \quad (9)$$

For a specified material, the KK integral is numerically evaluated to calculate ϵ_1 values from ϵ_2 . Two zero-broadening oscillators and a fixed offset are employed to represent the spectral response outside the range of experimental measurement. E_i is the center energy location of a zero-broadening oscillator; and A_i is the amplitude of the zero-broadening oscillator located at the E_i position. The calculated values ϵ_1^{kk} were compared with VASE determined by

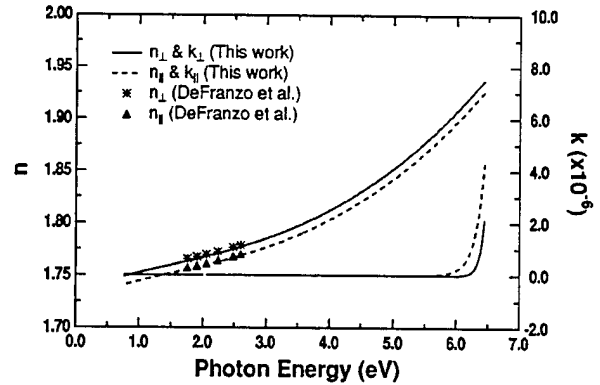


FIG. 7. Optical constants of sapphire for both ordinary and extraordinary rays with reference data.

ϵ_1^{meas} through a regression analysis by varying the values of A_1 , E_1 , and $\epsilon_1^{\text{offset}}$ until calculated and measured values match as close as possible.

Figures 7(a) and 7(b) show a comparison of the measured values ϵ_1^{meas} and the calculated values ϵ_1^{kk} of the ordinary ray and the extraordinary ray, respectively. Also the fitting parameters of KK transformation are listed in Table II. In our calculation two zero-broadening oscillators were used outside the measured region. The perfect match of the two curves in Fig. 7 indicates that the dielectric functions of sapphire obtained from our VASE analysis are KK consistent.

D. Anisotropic sapphire optical constants

Two pairs of sapphire optical constants of both ordinary $n_{\perp}(\omega)$ and extraordinary $n_{\parallel}(\omega)$ rays are shown in Fig. 8. It is necessary to point out that n_{\perp} is slightly larger than n_{\parallel} , which is consistent with other reports.^{5,15} The difference between them is close to a constant value 0.008, which is also in well agreement with References 5 and 15. The symbolized data points with * and ▲ are the n_{\perp} and n_{\parallel} values from DeFranzo and Pazol, in which the traditional prism method was employed. It also can be seen that k is equal to zero at the energies below 6 eV, but it rapidly increases above 6 eV indicating that the absorption tail can start well below the band edge (9 eV).

V. SUMMARY

In summary, we have studied the anisotropic optical response of sapphire single crystal by generalized ellipsometry with three different types of measurement, R-VASE, T-VASE, and intensity transmission. Polarized Raman scat-

TABLE II. Fitting parameters in the Kramers–Kronig's self-consistency check.

	Fitting parameters	E_i (eV)	A_i	$\epsilon_1^{\text{offset}}$ (eV)
Ordinary	Pole No. 1	0.053 01	0.462 27	1.4061
	Pole No. 2	11.955	31.363	1.4061
Extraordinary	Pole No. 1	0.034 03	0.734 74	1.4299
	Pole No. 2	11.929	30.346	1.4299

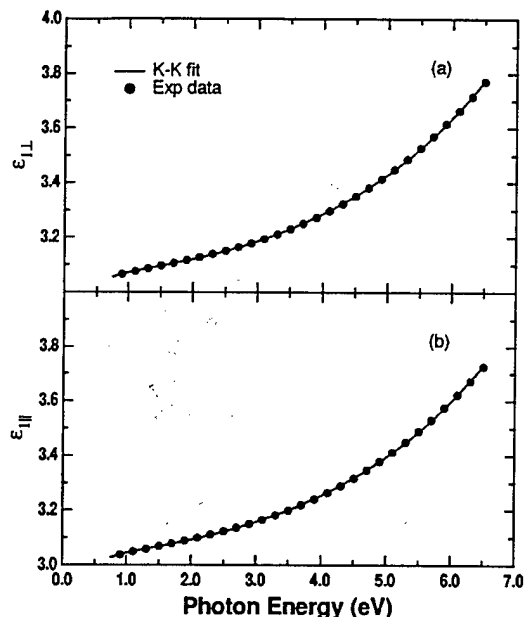


FIG. 8. KK consistency check of the dielectric functions of sapphire: (a) KK fitting of the ordinary dielectric function, (b) KK fitting of the extraordinary function.

tering as a convenient and nondestructive tool was used to determine the optic axis location of the *a*-plane sapphire samples. For the transparent sapphire crystal, the T-VASE measurement is critically important for collecting entire information of the Jones matrix, and it is especially helpful for extracting the small difference between n_{\perp} and n_{\parallel} . The two sets of optical constants, both ordinary $n_{\perp}(\omega)$ and extraordinary $n_{\parallel}(\omega)$, in the energy range of 0.75–6.5 eV resulted from our best model fit are in well agreement with the available discrete data in recent reports. The KK check further confirms that the resulting dielectric functions of sapphire

are Kramers–Kronig self-consistent. The difference of the refractive index between the ordinary and the extraordinary is about a constant of 0.008 in the range of 0.75–6.5 eV. The extinction coefficients of both ordinary and extraordinary rays are close to zero below 6 eV, but they increase rapidly above 6 eV showing a non-negligible absorption tail below the band edge. Combining polarized Raman scattering and the generalized ellipsometry technique could allow us to study the optical anisotropy of any crystal with arbitrary optic axis orientation.

ACKNOWLEDGMENTS

The authors would like to acknowledge Professor S. P. Denbarrs for providing sapphire samples. This work was supported by the U.S. Army Research Office under Contract No. DAAG55-98-1-0462.

- ¹I. H. Malitson, F. V. Murphy, Jr., and W. S. Rodney, *J. Opt. Soc. Am.* **48**, 72 (1958).
- ²M. L. Lang and W. L. Wolfe, *Appl. Opt.* **22**, 1267 (1983).
- ³F. Gervais, in *Handbook of Optical Constants of Solids II*, edited by E. D. Palik (Academic, San Diego, 1991), p. 761.
- ⁴T. Tomiki *et al.*, *J. Phys. Soc. Jpn.* **62**, 573 (1993).
- ⁵A. C. DeFranzo and B. G. Pazol, *Appl. Opt.* **32**, 2224 (1993).
- ⁶A. K. Harman, S. Ninomiya, and S. Adachi, *J. Appl. Phys.* **76**, 8032 (1994).
- ⁷R. M. A. Azzam, and N. M. Bashara, *Ellipsometry and Polarized Light* (North-Holland, New York, 1977), Chap. 4.
- ⁸M. Schubert, B. Rheinländer, J. A. Woollam, B. Johs, and C. M. Herzinger, *J. Opt. Soc. Am. A* **13**, 875 (1996).
- ⁹H. Yao, B. Johs, and R. B. James, *Phys. Rev. B* **56**, 9414 (1997).
- ¹⁰R. M. A. Azzam and N. M. Bashara, *J. Opt. Soc. Am.* **62**, 1521 (1972).
- ¹¹D. W. Berreman, *J. Opt. Soc. Am.* **62**, 502 (1972).
- ¹²M. Schubert, *Phys. Rev. B* **53**, 4265 (1996).
- ¹³E. T. Arakawa and M. W. Williams, *J. Phys. Chem. Solids* **29**, 735 (1968).
- ¹⁴C. F. Klingshirn, *Semiconductor Optics* (Springer, New York, 1995), Chap. 8.
- ¹⁵D. S. Kliger, J. W. Lewis, and E. Randall, *Polarized Light in Optics and Spectroscopy* (Academic, San Diego, 1990), p. 41.

NONDESTRUCTIVE CHARACTERIZATION OF GaN FILMS GROWN AT LOW AND HIGH TEMPERATURES

C.H. YAN^{a)}, H.W. YAO^{a)}, J.M. VAN HOVE^{b)}, A.M. WOWCHAK^{b)}, P.P. CHOW^{b)}, J. HAN^{c)}, J.M. ZAVADA^{d)}

a) University of Nebraska, Center for Microelectronic and Optical Material Research,
and Department of Electrical Engineering, Lincoln, NE 68588, hyao@unl.edu

b) SVT Associated, Eden Prairie, MN

c) Sandia National Laboratories, Albuquerque, NM

d) US Army European Research Office, London, UK

ABSTRACT

GaN films grown on GaAs and sapphire substrates by molecular beam epitaxy (MBE) and metalorganic vapor phase epitaxy (MOVPE) at both low and high temperatures (LT and HT) were characterized by Raman scattering and variable angle spectroscopic ellipsometry (VASE). Optical phonon spectra of GaN films are obtained through back-scattering geometry. Crystal quality of these films was qualitatively examined using phonon line-width. Phonon spectra showed that the HT GaN has wurtzite crystal structure, while LT GaN and GaN/GaAs have cubic-like structures. Thickness nonuniformity and defect-related absorption can be characterized by pseudo dielectric functions directly. Surface roughness also can be determined by using an effective-medium approximation (EMA) over-layer in a VASE analysis. Anisotropic optical constants of GaN, both ordinary and extraordinary, were obtained in the spectral range of 0.75 to 6.5 eV with the consideration of surface roughness, through the small and large angles of incidence, respectively. The film thickness of the GaN was accurately determined via the analysis as well.

INTRODUCTION

GaN and related III-nitrides wide band gap semiconductors have attracted much attention recently due to the successes of blue light emitting diode (LED) and laser diode (LD) fabrications [1]. However, there are many unsolved problems in the nitride film growth field, such as high dislocation density, cracks, and lack of surface flatness [2]. In order to improve the film quality, more advanced and sensitive film characterizations are highly required, especially in nondestructive ways. By measuring the phonon spectrum of a film, Raman scattering can reveal its crystalline quality, crystal structure, alloy composition, optical anisotropy, and many others. Spectroscopic ellipsometry, on the other hand, not only can measure the film optical constants and its thickness, but also determine the surface roughness, thickness uniformity, and defect related absorption. In this paper, we report phonon spectra of LT and HT GaN films. The anisotropic optical constants along with film thickness, surface roughness, and thickness nonuniformity of the HT GaN are studied by VASE as well.

THEORY

It is well known that α -GaN is optically anisotropic (uniaxial) material due to its wurtzite crystal structures. Group theoretical analysis shows that the irreducible representation for the optical modes of Wurtzite GaN [3]

$$\Gamma = A_1(z) + 2B_1 + E_1(x, y) + 2E_2, \quad (1)$$

for phonon propagating along or perpendicular to the optical axis $\langle c \rangle$. Where x, y, z in parentheses represent the directions of phonon polarization. The A_1 and E_1 modes are both Raman and infrared active, two E_2 modes are only Raman active, and B_1 modes are both Raman and IR silent.

Spectroscopic ellipsometry is another powerful nondestructive method that can be used to study the optical and structural properties of crystals. Two standard ellipsometric parameters ψ and Δ are

related to the complex ratio of reflection (or transmission) coefficients for light polarized parallel (p) and perpendicular (s) to the plane of incidence [4]. For isotropic material systems, ψ and Δ are defined as

$$\rho = \frac{R_p}{R_s} = \tan(\psi)e^{i\Delta}. \quad (2)$$

The electric-field reflection coefficient at an incident angle of ϕ is defined as R_p (R_s) for p (s)-polarized light. ψ and Δ are not only dependent on dielectric functions, also sensitive to the surface conditions, sample structure, and other properties such as the optical anisotropy.

The pseudodielectric function $\langle \epsilon \rangle$ can be obtained directly from the measured ψ and Δ values:

$$\langle \epsilon \rangle = \langle \epsilon_1 \rangle + i \langle \epsilon_2 \rangle = \sin^2 \Phi \left[1 + \tan^2 \Phi \left(\frac{1 - \rho}{1 + \rho} \right) \right]. \quad (3)$$

For the case of an air ambient over a bare bulk material with a perfectly smooth surface, the pseudo dielectric and intrinsic dielectric function are identical. To determine the optical constants of a thin film on a substrate, VASE data must be analyzed using a parametric model that is adjusted to fit the measured data. A regression analysis is usually used to vary the model parameters (e.g., optical constants or layer thickness, etc.) until the calculated and measured values match as closely as possible.

EXPERIMENTAL

GaN films used in this study were grown on c-plane (0001) sapphire and (001) GaAs substrates by molecular beam epitaxy (MBE) at high ($\sim 700^\circ\text{C}$) temperature, and by metalorganic vapor phase epitaxy (MOVPE), at low ($\sim 550^\circ\text{C}$) temperature. These samples are all one-side polished to meet the need of reflection ellipsometry measurements.

The Raman spectra were taken at room temperature with a SPEX 1877E triple spectrometer equipped with a liquid-nitrogen cooled CCD camera. The excitation light source was the Coherent Innova 300 Ar^+ laser operating at 514.5 nm with the output power kept at 300mW. A back scattering geometry was employed for all the Raman measurements. Most of the measurements were performed from the front surfaces with the focusing spot less than 1 μm in diameter. Micro-Raman measurements were also made on the cross-section, so that the anisotropic optical phonons were observed.

The standard reflection variable angle spectroscopic ellipsometry (RVASE) measurements were performed in the spectral range of 0.75eV to 6.5 eV with a 0.02eV increment. Small angles of incidence (20° and 40°) were used to determine the ordinary optical constants, while the extraordinary optical constants of GaN were determined from the VASE data at the near-Brewster angles of incidence (60° , 70° , and 80°).

RESULTS AND DISCUSSION

GaN films grown on c-plane (0001) sapphire substrates usually have hexagonal structure and its optical axis is parallel to the optical axis $\langle c \rangle$ of sapphire. Optical phonons obtained from a HT GaN film grown on c-sapphire are shown in Fig. 1 (a). The solid line represents the phonon spectrum taken from the sample surface, in which two GaN related optical phonons (E_2 569 cm^{-1} and A_1 LO 736 cm^{-1}) are observed. In this case the optical axis of GaN film is perpendicular to the laser polarization. The 418 cm^{-1} and 750 cm^{-1} phonons are due to sapphire substrate. When the laser beam was focused on the cross-section of the GaN film and let the optical axis of GaN (sample surface normal) be parallel to the laser polarization, another set of phonons was obtained as indicated by the dash line in Fig. 1 (a). The existence of A_1 TO (533 cm^{-1}), E_1 TO (561 cm^{-1}) and LO (742 cm^{-1}) indicates that this GaN film has hexagonal structure. The narrow line-widths indicate a good crystalline quality. Unlike the HT GaN/c-sapphire sample, phonon spectra from a LT GaN/c-sapphire and a GaN/GaAs show that they all have cubic-like structures [5], as shown in Fig. 1 (b). The broad peaks of TO 554 cm^{-1} and LO 732 cm^{-1} indicate that the crystal defect density in both films is high either due to a large lattice mismatch or the low temperature growth.

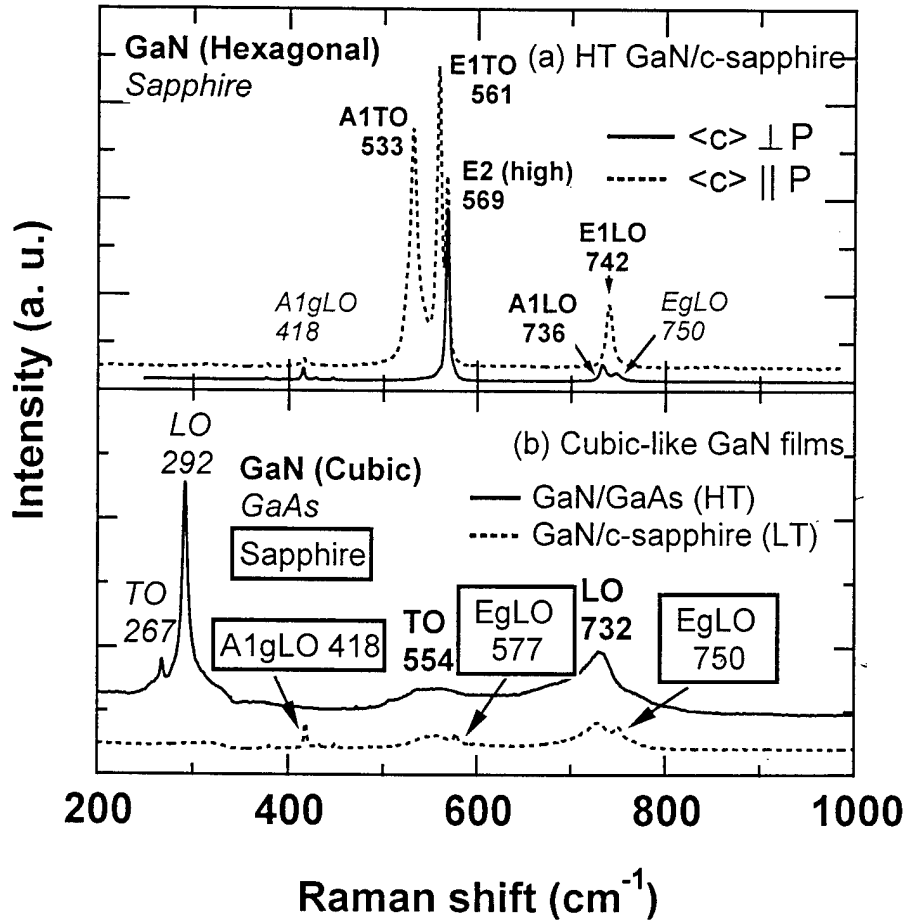


Fig. 1 Optical phonon spectra of GaN films obtained under backscattering geometry [$Z(Y, Y+X)\bar{Z}$]. (a) Phonon spectra from a hexagonal GaN film. (b) Phonon spectra from cubic-like GaN films.

Fig. 2 shows the pseudo dielectric functions of three GaN films, a 1 μm HT GaN on c-sapphire (#1) in Fig. 2 (a), a 2 μm HT GaN on c-sapphire (#2) in Fig. 2 (b), and a 0.2 μm LT GaN on c-sapphire in Fig. 2 (c). The solid lines represent the real part of the pseudo dielectric functions of each film. The dash lines represent the imaginary part. As showed in Fig. 1 (a), the high quality of the #1 HT GaN film can also be seen from its pseudo dielectric functions in Fig. 2 (a). Comparing with Fig. 2 (a), the #2 HT GaN film shows some different properties. The severe amplitude damping of the interference fringes on both $\langle \epsilon_1 \rangle$ and $\langle \epsilon_2 \rangle$ in Fig. 2 (b) indicates the poor thickness uniformity of this film. Also the average value of $\langle \epsilon_2 \rangle$ in the near below band gap (3.4 eV) region is much larger for #2 HT GaN than that for #1 HT GaN. In general, the $\langle \epsilon_2 \rangle$ values below band gap for a perfect GaN should be zero. This high $\langle \epsilon_2 \rangle$ tail may be caused by the crystal defect absorption. An even higher $\langle \epsilon_2 \rangle$ tail was observed in the LT GaN showed in Fig. 2 (c). This is not a surprise for a low temperature grown film. The non-damping interference fringes indicate that the LT GaN film has good thickness uniformity.

Surface morphology is an important issue for III-V semiconductor epitaxial layers, especially for III-nitrides. Usually the thickness of surface rough layer is ranging from a few nm to tens of nm [6, 7]. Quick and nondestructive measurement of the surface roughness along with film thickness and other optical properties is the big advantage of spectroscopic ellipsometry. Ellipsometry is a surface sensitive technique because it not only measures the light intensity, but also measures the phase change after the reflection (or transmission). To study the incident angle dependence of surface over layer thickness, a series of model simulations were performed at 5.0 eV (above the band gap). The calculated Ψ and Δ spectra are showed in Fig. 3 (a) and (b). A three-phase model (surface over-layer, 1.0 μm GaN film, and c-sapphire substrate) was used in the simulations. Anisotropic optical constants of sapphire were used in the calculations [8]. Both Ψ and Δ spectra at near the pseudo Brewster angle region show great sensitivity to the roughness layer thickness. With the increase of the roughness

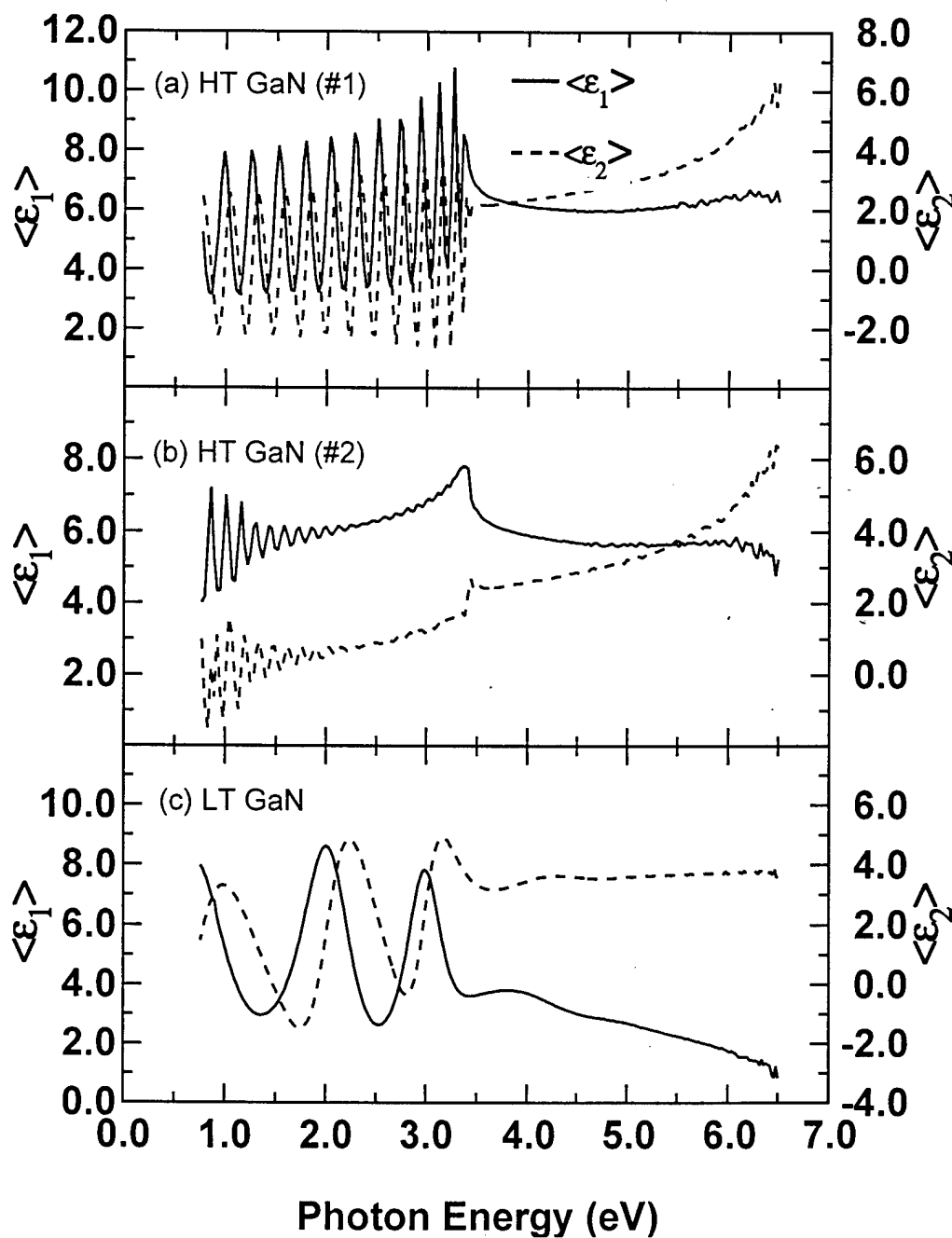


Fig. 2 Pseudo dielectric functions of GaN/c-sapphire structures. (a) 1 μm high quality HT GaN on c-sapphire; (b) 2 μm HT GaN on c-sapphire; (c) 0.2 μm LT GaN on c-sapphire.

layer thickness, the Δ spectrum as a function of incident angle no longer has the abrupt turn feature near the pseudo Brewster angle. This could be a useful sign for monitoring the surface roughness. The full spectral simulations of Ψ and Δ with or without surface roughness layer are shown in Fig. 3 (c) and (d). It shows clearly that Ψ and Δ are much more sensitive to the roughness layer thickness in the above gap region than below gap. It is due to the small penetration depth of photons with energies above the band gap under strong absorption. On the other hand, photons with energies below the band gap can almost see the whole structure. Therefore, it allows us to measure the film thickness.

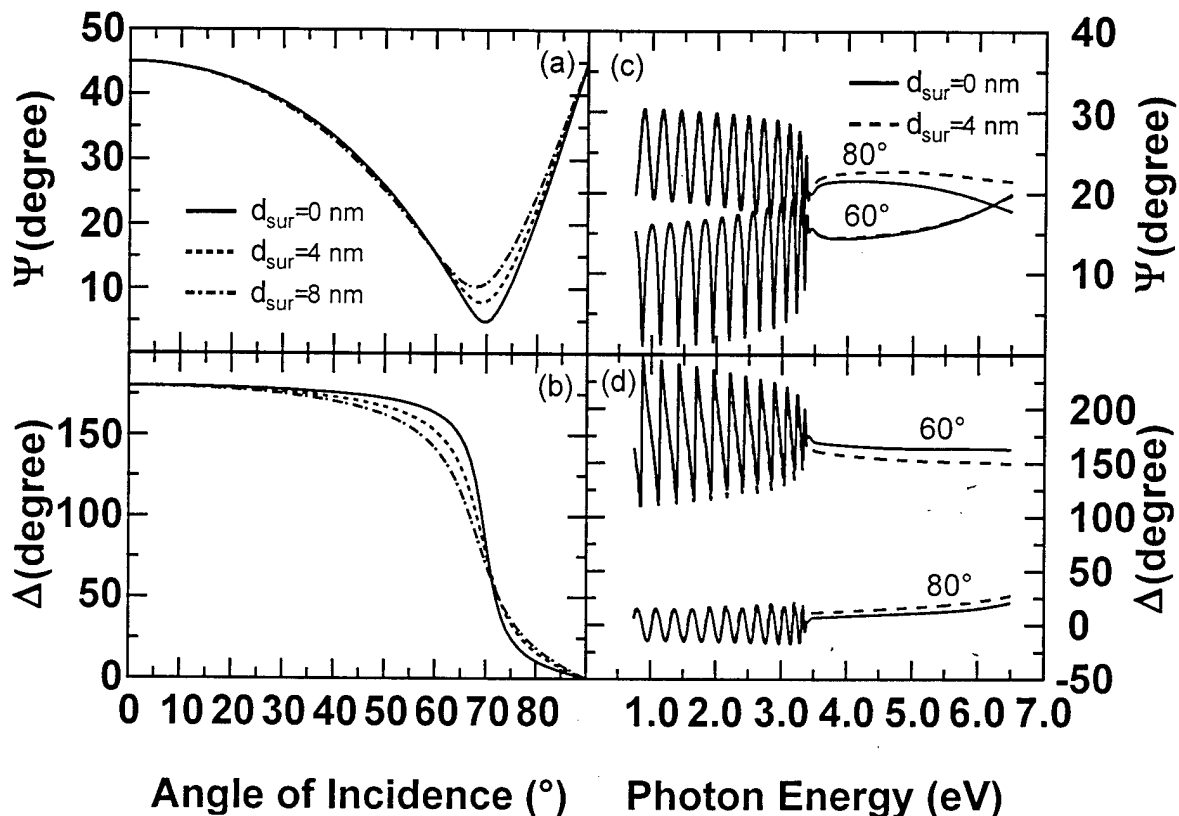


Fig. 3 VASE model simulations of the surface roughness effect. d_{sur} is the surface roughness layer (EMA with 50% voids and 50% GaN) thickness. The model is a three-phase structure (surface rough layer(d_{sur})/GaN (1 μm)/c-sapphire). (a) & (b) As a function of angle of incidence at 5.0 eV; (c) & (d) As a function of photon energy at 60° and 80° angles of incidence.

The ordinary and extraordinary optical constants of a high quality HT GaN grown on c-sapphire are shown in Fig. 4 (a). The results were extracted from a multiple angle VASE data analysis using two parametric semiconductor models for GaN. The indices of refraction of extraordinary are about 3.5% higher than its ordinary counterpart throughout the whole spectrum. The zero k below band gap indicates that this HT GaN film has very low defect density. A comparison of optical constants of a HT and a LT GaN film grown on sapphire substrates is shown in Fig. 4 (b). The broadening of n and k spectra at critical points indicates the existence of high densities of structural defects in the LT GaN film.

SUMMARY

In summary, we have studied the optical properties of HT and LT GaN films by both Raman scattering and variable angle spectroscopic ellipsometry. It has been observed that HT GaN grown on c-sapphire has hexagonal structure, while GaN grown on GaAs and LT GaN on c-sapphire may have cubic-like structure that strongly depends on the growth conditions. Defect density and thickness nonuniformity can be characterized using VASE by monitoring the pseudo dielectric function line shapes. VASE is also a surface-roughness sensitive technique which can precisely determined the surface over layer at near pseudo Brewster angle region in the above band gap spectral range. The ordinary and extraordinary optical constants of a high quality HT GaN were fully determined by a multiple angle VASE data analysis. The indices of refraction for extraordinary ray are about 3.5% larger than that of the ordinary.

ACKNOWLEDGEMENTS

This work was supported in part by US Army Research Office under contract No. DAAG55-98-1-0462.

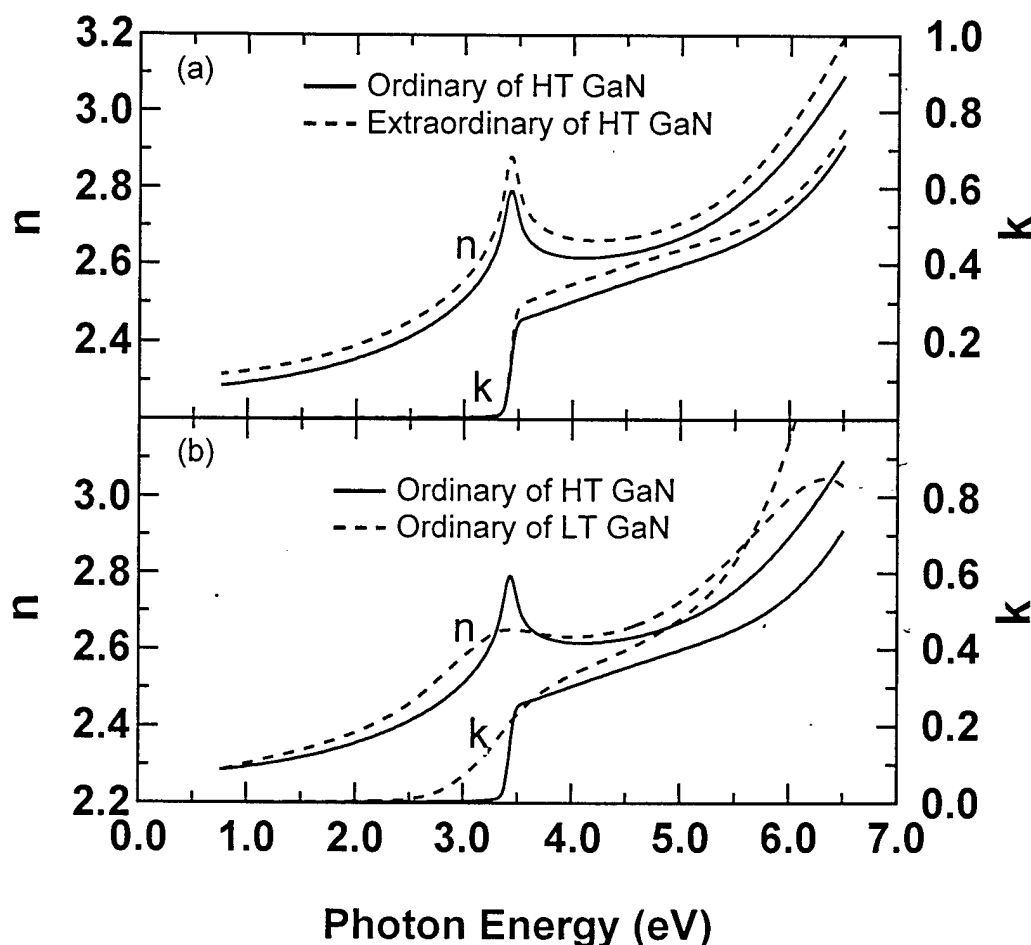


Fig. 4 Optical constants of GaN films obtained from a multiple angle VASE data analysis. (a) Ordinary and extraordinary optical constants of a HT GaN film; (b) Ordinary optical constants of a HT and LT GaN films.

REFERENCES

1. S. Nakamura, MRS Bulletin **22**(2), p.29 (1997).
2. I. Akasaki, 2nd Intern. Symp. On Blue Laser and Light Emitting Diodes, Chiba, Japan, Sept. 29-Oct. 2, 1998. p. 9-14.
3. T. Azuhata, T. Sota, K. Suzuki and S. Nakamura, J. Phys.: Condens. Matter **7**, p. L129 (1995).
4. R. M. A. Azzam and N. M. Bashara, *Ellipsometry and Polarized Light*, North-Holland, Amsterdam, 1977, pp. 287-288.
5. A. Tabata, R. Enderlein, J. R. Leite, S. W. da Silva, J. C. Galzerani, D. Schikora, M. Kloidt, and K. Lischka, J. Appl. Phys. **79** (8), p. 4137 (1996).
6. T. Kawashima, H. Yoshikawa, S. Adachi, S. Fuke, K. Ohtsuku, J. Appl. Phys. **82** (7), p. 3528 (1997).
7. S. Shokhovets, R. Goldhahn, V. Cimalla, T. S. Cheng, C. T. Foxon, J. Appl. Phys. **84** (3), p. 1561 (1998).
8. H. Yao, C.H. Yan, J. Appl. Phys. **85**, p. 6717 (1999).

Optical properties of AlN/sapphire grown at high and low temperatures studied by variable angle spectroscopic ellipsometry and micro Raman scattering

C. H. Yan^a, H. Yao^a, A. C. Abare^b, S. P. Denbaars^b, J. J. Klaassen^c, M. F. Rosamond^c,
P. P. Chow^c, J. M. Zavada^d

^aUniversity of Nebraska, Center for Microelectronic and Optical Material Research,
and Department of Electrical Engineering, Lincoln, NE 68588

^bUniversity of California at Santa Barbara, CA

^cSVT Associates, Eden Prairie, MN

^dUS Army European Research Office, London, UK

ABSTRACT

Variable angle spectroscopic ellipsometry (VASE) and micro Raman scattering have been employed to study the optical anisotropy and optical constants of AlN films grown at high and low temperatures (HT and LT). The AlN films were grown by metalorganic vapor phase epitaxy (MOVPE) and molecular beam epitaxy (MBE) on c-plane sapphire (α -Al₂O₃) substrates, respectively. Anisotropic optical phonon spectra of AlN have been measured along two directions so that the optical axis $\langle c \rangle$ of AlN is either perpendicular or parallel to the polarization of the incident beam. Nonzero off-diagonal elements A_{ps} and A_{sp} of Jones matrix in the reflection VASE (RVASE) measurements indicate that the $\langle c \rangle$ of AlN is slightly away from surface normal due to substrate miscut. The ordinary optical constants of both HT AlN have been determined spectroscopically at small angles of incidence so that the extraordinary response is greatly reduced. The film thickness along with the surface overlayer was determined via the VASE data analysis as well.

Keywords: AlN, sapphire, Raman scattering, spectroscopic ellipsometry, optical anisotropy, optical constants.

1. INTRODUCTION

The wide band gap AlN along with GaN and InN, are the important building blocks for both high temperature electronic devices and short wave-length optical emitters.^{1,2} AlN films grown on c-plane sapphire usually have wurtzite crystal structure (α -AlN), which is anisotropic (uniaxial). There are some valuable optical property studies have been carried out on textured³ and single crystal^{4,5} AlN films by various kinds of techniques. For instance, prism-coupling^{3,4} can give very accurate values of reflective index at several discrete wavelengths but lacks spectroscopic information. Transmittance and reflectance⁵ can obtain spectroscopic data but do not have enough sensitivity on surface overlayer since it does not contain the phase information. Ellipsometry, on the other hand, is an ideal choice for measuring the spectroscopic optical constants and structural parameters of thin films, especially when the films have interface or surface roughness. In this work, the ordinary optical constants of both HT and LT AlN thin films were accurately determined by transmission variable angle spectroscopic ellipsometry (TVASE) and reflection VASE (RVASE). The extraordinary optical response from the uniaxial AlN films was greatly reduced by using small angle of incidence. Small angle of incidence is also good for minimizing the error caused by the substrate miscut that can result in non-zero off-diagonal elements of Jones matrix. Surface and interface roughness were carefully considered in the VASE model analysis using the effective medium approximation (EMA).⁶

* Correspondence: Email: hyao@unl.edu; Telephone: 402-472-5914; Fax: 402-472-4732

2. Theory

2.1 Raman Scattering

The irreducible representation of Wurtzite AlN optical phonons is:⁷

$$\Gamma = A_1(z) + 2B_1 + E_1(x, y) + 2E_2, \quad (1)$$

for phonon propagating along or perpendicular to the optical axis $\langle c \rangle$. Where x, y, z in parentheses represents the directions of phonon polarization. A_1 and E_1 modes are polar modes and each split into a propagation-parallel longitudinal optical (LO) and a propagation-perpendicular transverse optical (TO) mode. The A_1 and E_1 modes are both Raman and infrared active, two E_2 modes are only Raman active, and B_1 modes are both Raman and IR silent. Therefore, there are total six active Raman phonon modes in the AlN crystal.

2.2 Generalized Ellipsometry

The variable angle spectroscopic ellipsometry is designed to accurately determine the values of two standard ellipsometry parameters ψ and Δ , which are related to the complex ratio of reflection (or transmission) coefficients for light polarized parallel (p) and perpendicular (s) to the plane of incidence.⁸ For isotropic material systems,

$$\rho = \frac{R_p}{R_s} = \tan(\psi)e^{i\Delta}. \quad (2)$$

The electric-field reflection coefficient at an incident angle of ϕ is defined as r_p (r_s) for p (s)- polarized light. They are the diagonal elements of Jones matrix.

$$[J]_{\text{sample}} = \begin{bmatrix} r_p & 0 \\ 0 & r_s \end{bmatrix} \quad (3)$$

The ψ and Δ are not only dependent on dielectric functions, also on the surface condition, sample structure, and other properties such as the optical anisotropy.

Generalized ellipsometry was first introduced by Azzam and Bashara.⁹ The recent developments makes this technique more complete and powerful.^{10,11} In a word, the Generalized ellipsometry is a technique which can be used to determined all the elements of Jones matrix of arbitrarily anisotropic and homogeneous layered systems with nonscalar dielectric susceptibilities.

For the anisotropic material system, the non-diagonal elements of Jones matrix are not necessary to be zero. In the reflection VASE configuration,

$$[J]_{\text{sample}} = \begin{bmatrix} r_{pp} & r_{sp} \\ r_{ps} & r_{ss} \end{bmatrix} \quad (4)$$

By using the same approach with considerably more algebra involved, we can still predict the ψ and Δ values, but the Fourier coefficients related to ψ and Δ become more complicated.¹² The generalized ellipsometric parameters are defined as below.

$$A_{nE} = \frac{r_{pp}}{r_{ss}} = \tan \psi_{nE} e^{i\Delta_{nE}} \quad (5)$$

$$A_{ps} = \frac{r_{ps}}{r_{pp}} = \tan \psi_{ps} e^{i\Delta_{ps}} \quad (6)$$

$$A_{sp} = \frac{r_{sp}}{r_{ss}} = \tan \psi_{sp} e^{i\Delta_{sp}} \quad (7)$$

where the A_{ps} and A_{sp} describe how much amount p- or s-polarized light becomes s- or p-polarized light after the reflection, respectively. If the optical axis is strictly perpendicular (perfect c-plane situation) to the electric field of the incident beam, the Jones matrix is strictly diagonal. While it may not be true for real AlN films grown on nominal c-plane sapphire substrates since the substrates are usually miscut within 1° . The off-diagonal elements A_{ps} and A_{sp} are dependent on sample positions, angles of incidence.

3. Experiments

The Raman spectra were taken at room temperature with a SPEX 1877E triple spectrometer equipped with a liquid-nitrogen cooled CCD camera. The excitation light source was the Coherent Innova 300 Ar⁺ laser operating at 488 nm with the output power kept at 150 mW. A back scattering geometry was employed for all the Raman measurements.

Two identical thin AlN films (about 130 nm thick) were grown at high temperature (1070°C) side by side by MOVPE on two c-plane sapphire substrates with polished and unpolished backsides to serve the transmission type and reflection type VASE measurements. About 20 nm thick LT (525°C) GaN nucleation layers were deposited before the HT AlN growth. Another two films were grown by MBE at high (800°C) and low (400°C) temperatures with different thickness, respectively. The very thin (~36 nm) LT AlN film was grown on a one-side polished c-plane sapphire. The thickness of the MBE grown HT AlN film is about 1 μ m. Both isotropic and anisotropic mode VASE measurements were performed in the energy range of 0.75 eV to 6.5 eV with a 0.02 eV increment at room temperature. The range of angle of incidence is from 20° to 80° for reflection VASE, and 0° to 30° for transmission VASE.

4. Results and discussion

4.1. Optical phonons of AlN films

Raman scattering is a nondestructive technique used to detect the lattice vibration modes related with crystal orientation and symmetry. A series of Raman scattering measurements have been carried out on various kinds of AlN samples. The optical phonon spectra of a 1 μ m thick AlN film grown on c-plane sapphire at back-scattering geometry $Z(Y, Y+X)\bar{Z}$ are shown in Fig. 1(a). The solid line was obtained from the front surface, in which the optical axis $\langle c \rangle$ of AlN (and sapphire substrate) is perpendicular to the incident polarization (Y). Three AlN related optical phonon were observed under such condition including 656 cm^{-1} E_2 (high), 888 cm^{-1} A_1 (LO), and a 246 cm^{-1} E_2 (low) which is not shown in this figure. The other two phonons of 577 cm^{-1} E_g (LO) and 750 cm^{-1} E_g (LO) are due to the sapphire substrate. The dash line in Fig. 1(a) was obtained from the side cross-section surface in which the AlN optical axis $\langle c \rangle$ is parallel to the polarization of the incident laser beam. There are three new phonons appeared, 612 cm^{-1} A_1 (TO), 670 cm^{-1} E_1 (TO), and 909 cm^{-1} E_1 (LO). All the above six optical phonons measured from AlN film are in good agreement with the theoretical calculation based on the rigid-ion model.¹³ The comparison is listed in Table 1. Fig. 1 (b) is a phonon line-width comparison of HT and LT AlN films. The solid line represents the thin LT AlN (36 nm) grown by MBE; the dash line represents the thin HT AlN (130 nm) grown by MOVPE. The broadening of AlN E_2 (high) may be due to the high-density structural defects (such as group III vacancies) in LT material and the misfit dislocations due to the large lattice mismatch. It is observable that the AlN E_2 (high) in both thinner films moves to lower frequency comparing with the AlN E_2 (high) in Fig. 1 (a). This may be caused by the partial strain relaxation instead of full relaxation in a thin lattice-mismatched film even for a thickness of 130 nm.

Table 1. Zone-center optical phonons in wurtzite AlN, in cm^{-1} .

Mode	A_1 (LO)	A_1 (TO)	E_1 (LO)	E_1 (TO)	E_2 (low)	E_2 (high)
Theory ¹²	885	614	923	668	252	660
This work	888	612	909	670	246	656

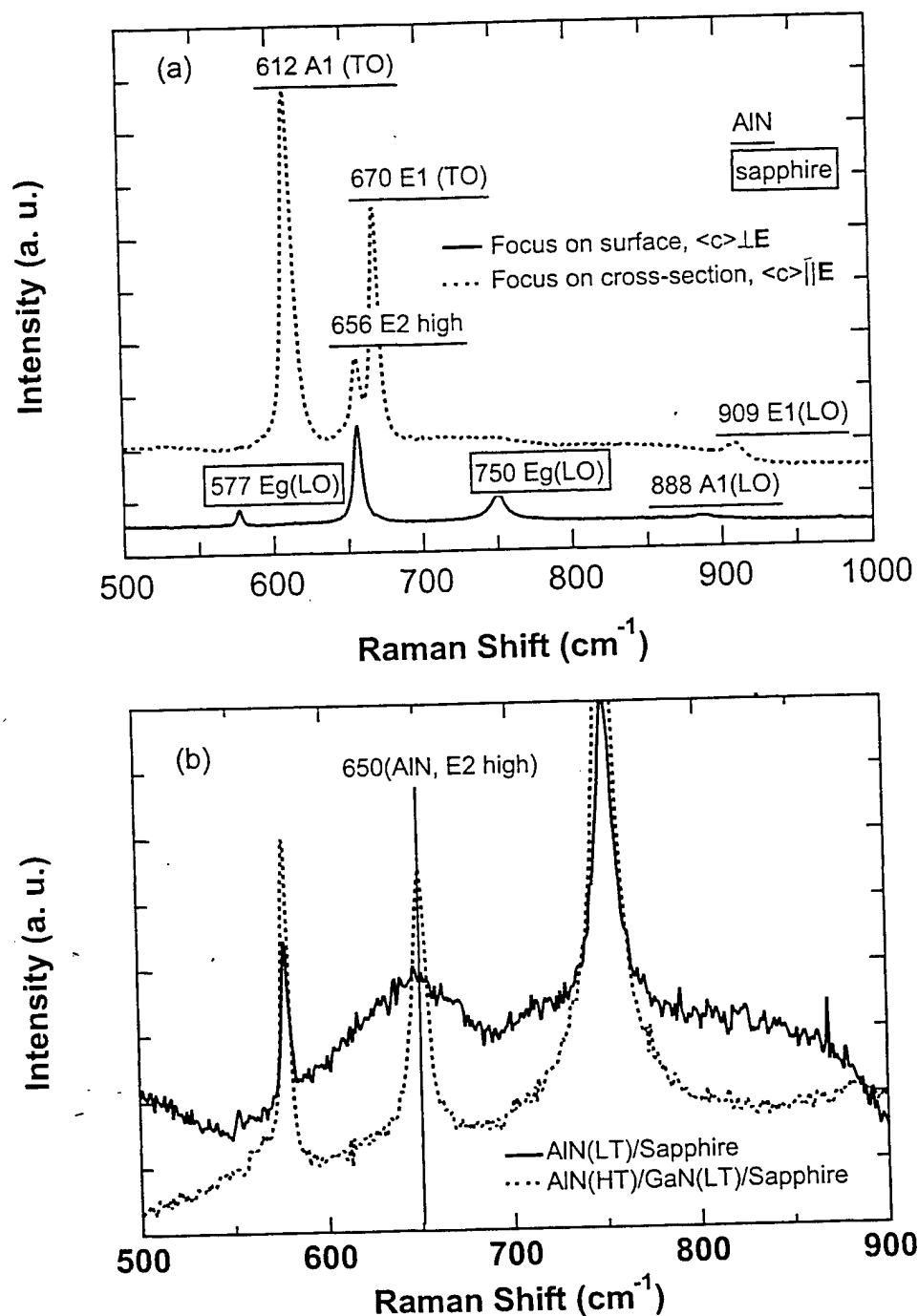


Fig. 1. Optical phonons of HT and LT AlN films. (a) 1 μm thick MBE grown HT AlN film on c-plane sapphire substrate. Solid line and dash line represent that $\langle c \rangle$ is perpendicular and parallel to the incident polarization E , respectively. (b) HT and LT thin MOVPE grown AlN films on c-plane sapphire substrates. Solid line represents 36 nm thick LT AlN film; dash line represents 130 nm thick HT AlN film.

4.2. VASE data analysis

For ideal c-plane samples, its off-diagonal element of Jones matrix must be zero as we pointed out in the theory part. But for real nominal c-plane samples, since there is a small miscut (usually within 1°) on the substrate, the off-diagonal elements

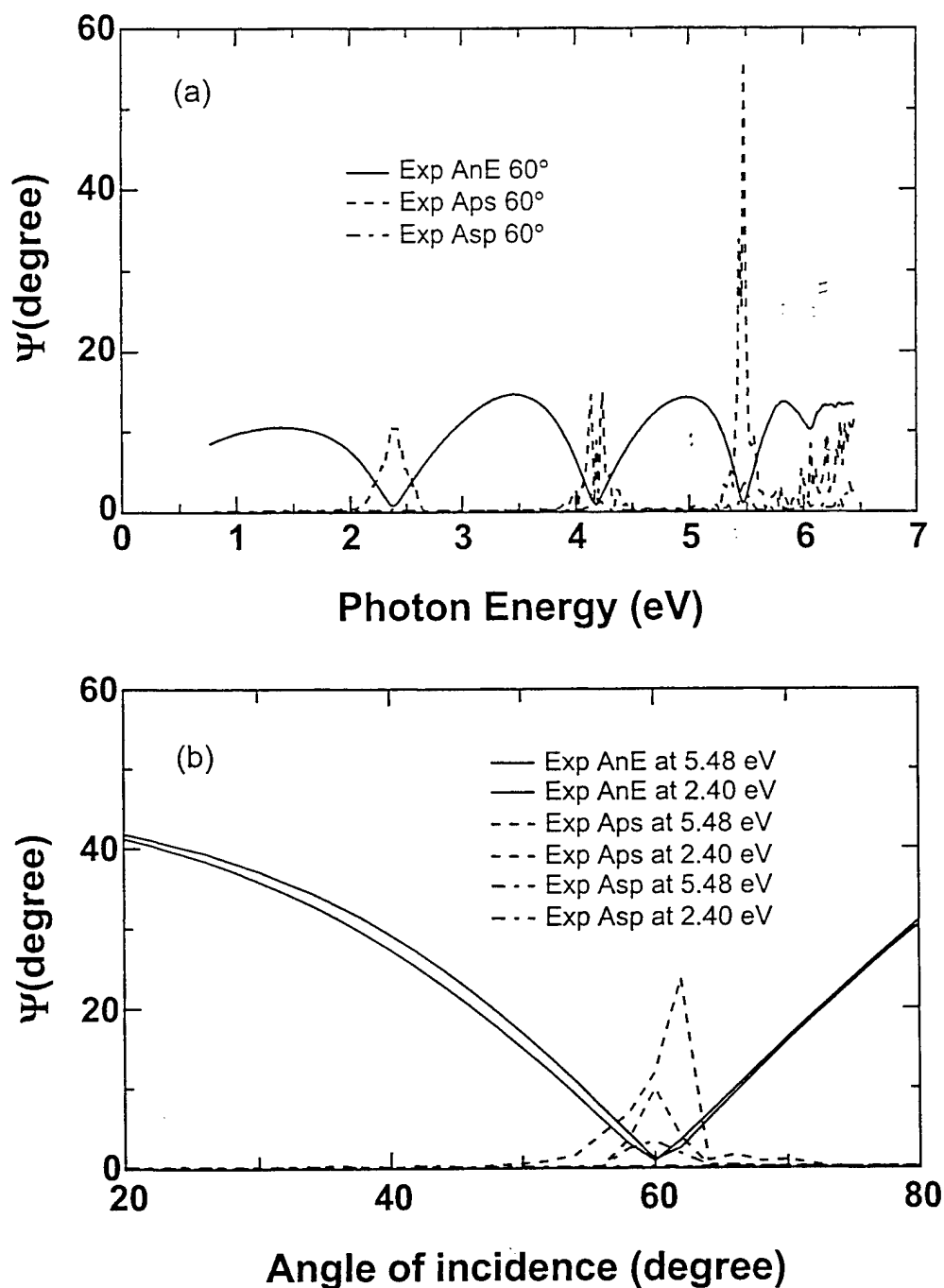


Fig. 3. Anisotropic mode RVASE data of HT AlN/c-sapphire grown by MOVPE. (a) Ψ as a function of photon energy at 60° angle of incidence; (b) Ψ as a function of incident angle at 2.40 and 5.48 eV.

may not vanish completely, as shown in Fig. 2. Fig. 2 (a) is an anisotropic mode RVASE data obtained from a 130 nm MOVPE grown AlN/c-sapphire sample. It was taken at 60° angle of incidence, which is near the pseudo Brewster angle. It can be seen clearly that the off-diagonal elements A_{ps} and A_{sp} are not negligible. The incident angular dependent measurements were made at certain wavelengths (1.4 and 5.48 eV), as shown in Fig. 1 (b). The angular increment was 1°. The off-diagonal elements are detectable in the angle range of 50° to 70°, but they are negligible at the angle of incidence below 40° or above 80°. Therefore, small angle of incidence (<40°) can be used to reduce the cross-conversion of p- to s- or s- to p- polarization caused by the <c> axis offset.

Small angle of incidence is not only good for overcoming the miscut error, but also can greatly reduce the anisotropic effect on the diagonal elements as shown in our previous GaN study.¹⁴ By using small angles of incidence, the ordinary dielectric functions of anisotropic AlN can be determined from the diagonal Jones matrix element without losing the accuracy. Thus standard ellipsometry will be suffice to determine the ordinary dielectric functions and other structural parameters.

Fig. 3 shows the nominal sample structures and the corresponding VASE analysis models. Fig 3 (a) is the structure for the two 130 nm AlN/c-sapphire structures on one-side and double-side polished substrates grown by MOVPE. The nominal thickness of the HT AlN and LT GaN nucleation layers are 130 nm and 20 nm, respectively. Fig. 3 (b) is the VASE model representing the structure in Fig. 3 (a). At the small incident angle condition, all the layers in the structure are simulated as

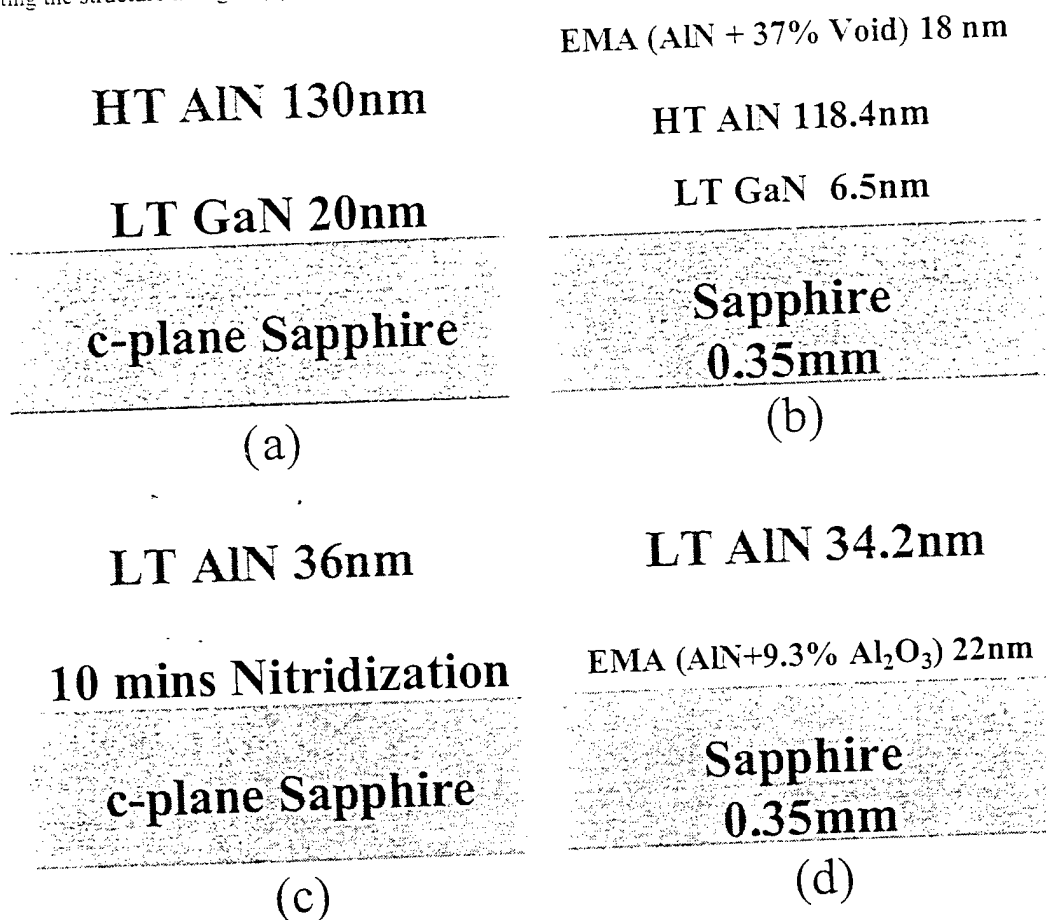


Fig. 3. AlN sample nominal structures and their corresponding VASE model. (a) Sample structure of 130 nm thick HT AlN/c-sapphire grown by MOVPE. (b) VASE model of the HT AlN/c-sapphire. (c) Sample structure of 36 nm thick LT AlN/c-sapphire grown by MBE. (d) VASE model of the LT AlN/c-sapphire.

isotropic material. The surface overlayer was modeled by an EMA layer to account for the surface oxide and roughness. The optical constants of LT GaN and sapphire used in the analysis are from our previous study. Fig. 3 (c) is the nominal structure for 36 nm LT AlN grown by MBE. Notice that there is a 10 minutes nitrogenation process before grow the LT AlN, and it represents by a EMA layer as shown in Fig. 3 (d). The optical constants of HT and LT AlN in the model were represented by two parametric semiconductor models, which are constructed based on their critical point structures. The details about the parametric model is described in reference. 15. The thickness and EMA composition listed in the model are the best values from VASE data fitting.

The VASE data and best fit of HT AlN/c-sapphire are shown in Fig. 4. Fig. 4 (a) and (b) are ψ and Δ of TVASE at four angles of incidence (0° , 10° , 20° , and 30°). Fig. 4 (c) and (d) are the ψ and Δ of RVASE at three small angles of incidence (20° , 30° , and 40°). The two sets of ellipsometric data were coupled together during the data fitting to further reduce the correlation between the fitting parameters. The resulted AlN layer thickness is 118.4 nm with 18 nm surface overlayer. The thickness of overlayer is consistent with previous thermal stability study.¹⁶ Fig. 5 (a) and (b) show the RVASE data and

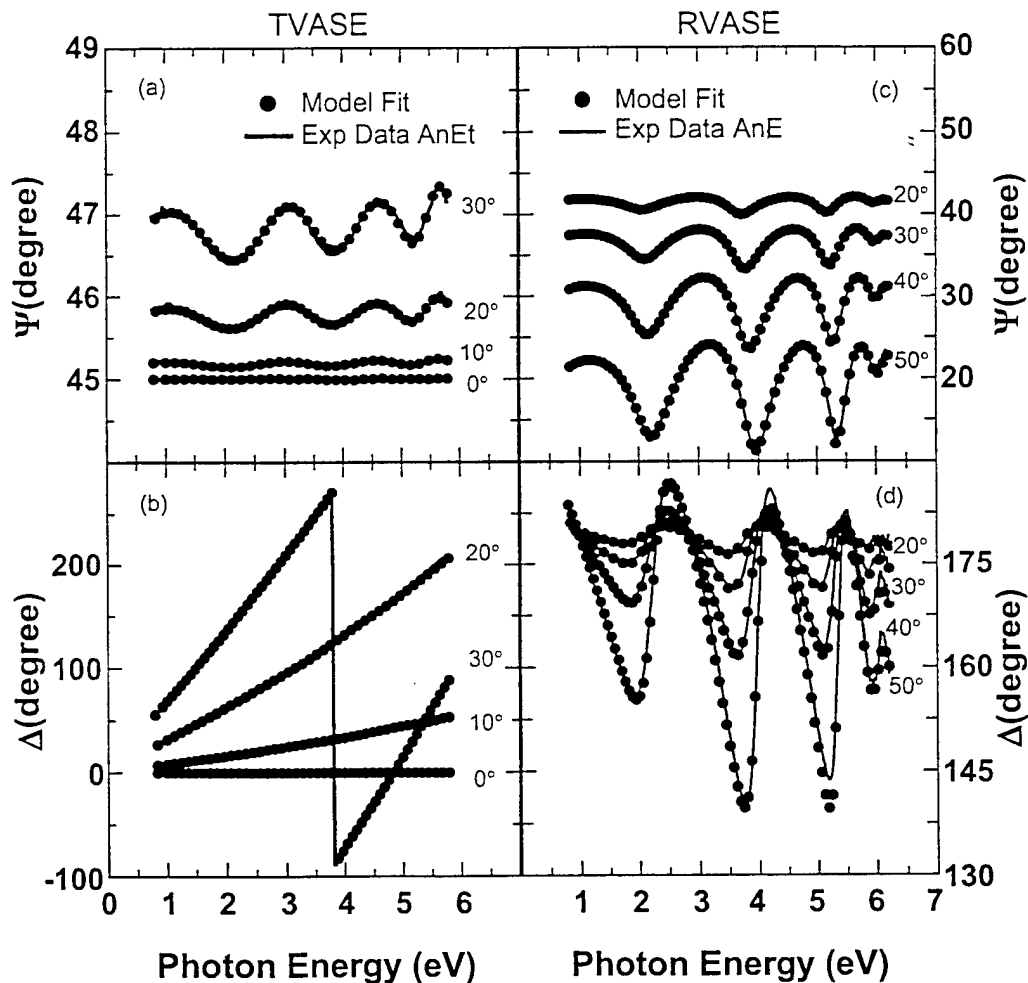


Fig. 4. VASE data and best fit of two HT AlN/c-sapphire samples. (a) ψ data and best fit of TVASE; (b) Δ data and best fit of TVASE; (c) ψ data and best fit of RVASE; (d) Δ data and best fit of RVASE. Solid lines represent experimental data. Dash lines represent the best model fit.

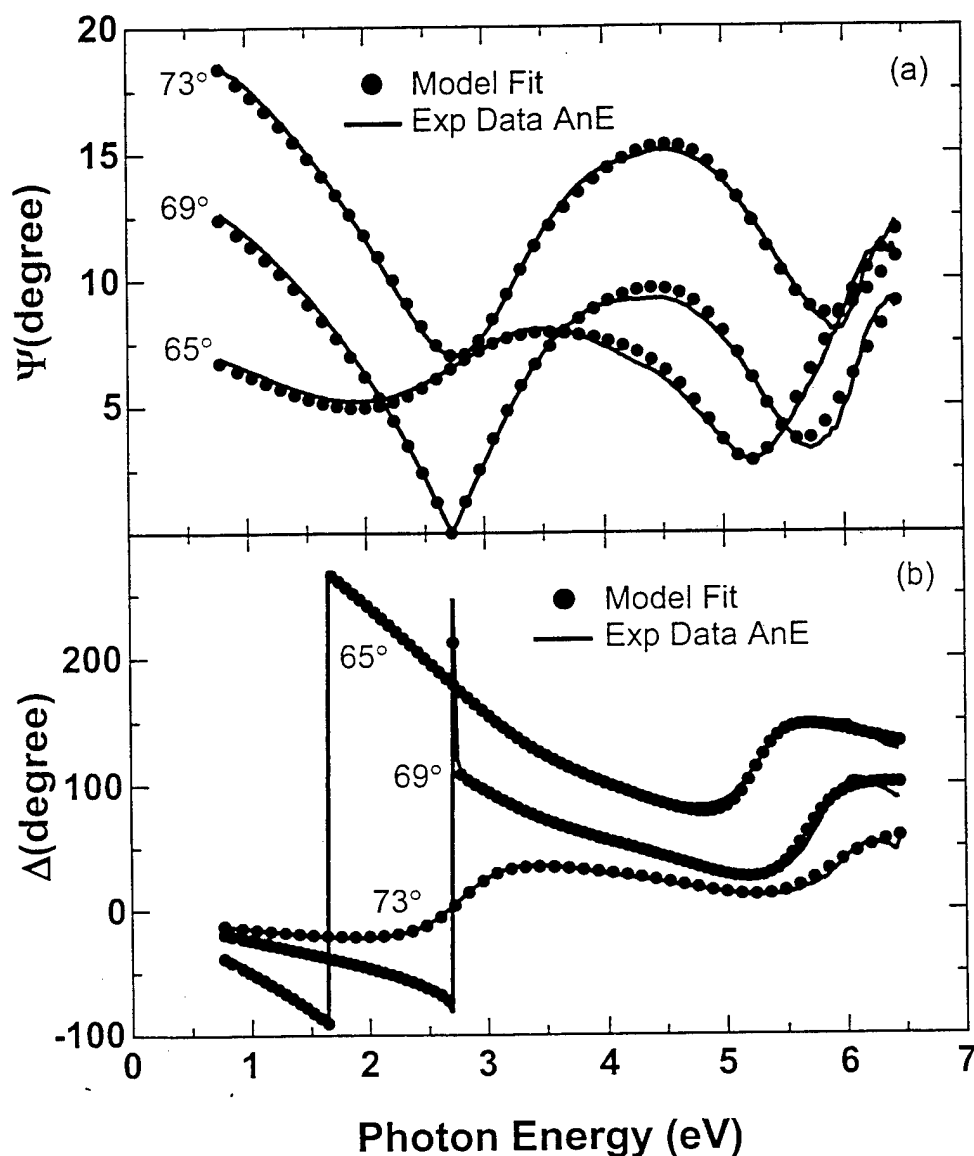


Fig. 5. RVASE data and best fit of LT AlN/c-sapphire. (a) ψ data and best fit; (b) Δ data and best fit. Solid lines represent experimental data. Dash lines represent best model fit.

best fit of the LT AlN/c-sapphire. The resulted film thickness of LT AlN is 34.2 nm which is very close to the nominal value 36 nm. A 22 nm interfacial layer was formed due to the 10 minutes nitrogenation. No surface overlayer is needed in the LT AlN VASE data analysis. High incident angles used for the LT AlN sample is because the anisotropy of such a LT material is not an issue in the material quality study.

The optical constants HT and LT AlN films obtained from VASE data analysis are shown in Fig. 6. The HT AlN is fully transparent below 5 eV, but the absorption of LT AlN starts from below 3 eV. This long absorption tail below the fundamental band gap (~6.2 eV) of AlN may be due to the high-density structure defects caused by both low temperature growth and large lattice-mismatch between AlN and sapphire substrate, the same reason caused the E_2 phonon broadening.

The parametric semiconductor model is Kramer-Kronig (K-K) consistent, the K-K fitting is shown in Fig. 7. The solid lines are the best ϵ_1 result from the VASE data analysis, and the dots represent the calculated ϵ_1 from the known ϵ_2 values using the K-K relation. Fig. 7 (a) and (b) are for HT and LT AlN, respectively. The final results of all fitting parameters are given in Table 2. The K-K relation used in the calculation is¹⁷

$$\epsilon_1^{kk}(E) = \epsilon_1^{offset} + \sum_{i=1}^2 \frac{A_i}{E_i^2 - (E)^2} + \frac{2}{\pi} P \int_{0.75\text{eV}}^{6.5\text{eV}} \frac{E' \epsilon_2^{meas}(E')}{E'^2 - (E)^2} dE' \quad (8)$$

For a specified material, the K-K integral is numerically evaluated to calculate ϵ_1 values from ϵ_2 . The model then adds the contribution from two non-broadening oscillators and a fixed offset to account for contribution outside the experimental measuring range. E_i is the energy location of a non-broadening oscillator that is added to simulate contribution outside the integration range; A_i is the magnitude of the oscillator located at E_i position. In our calculation one oscillators were used outside the measured region.

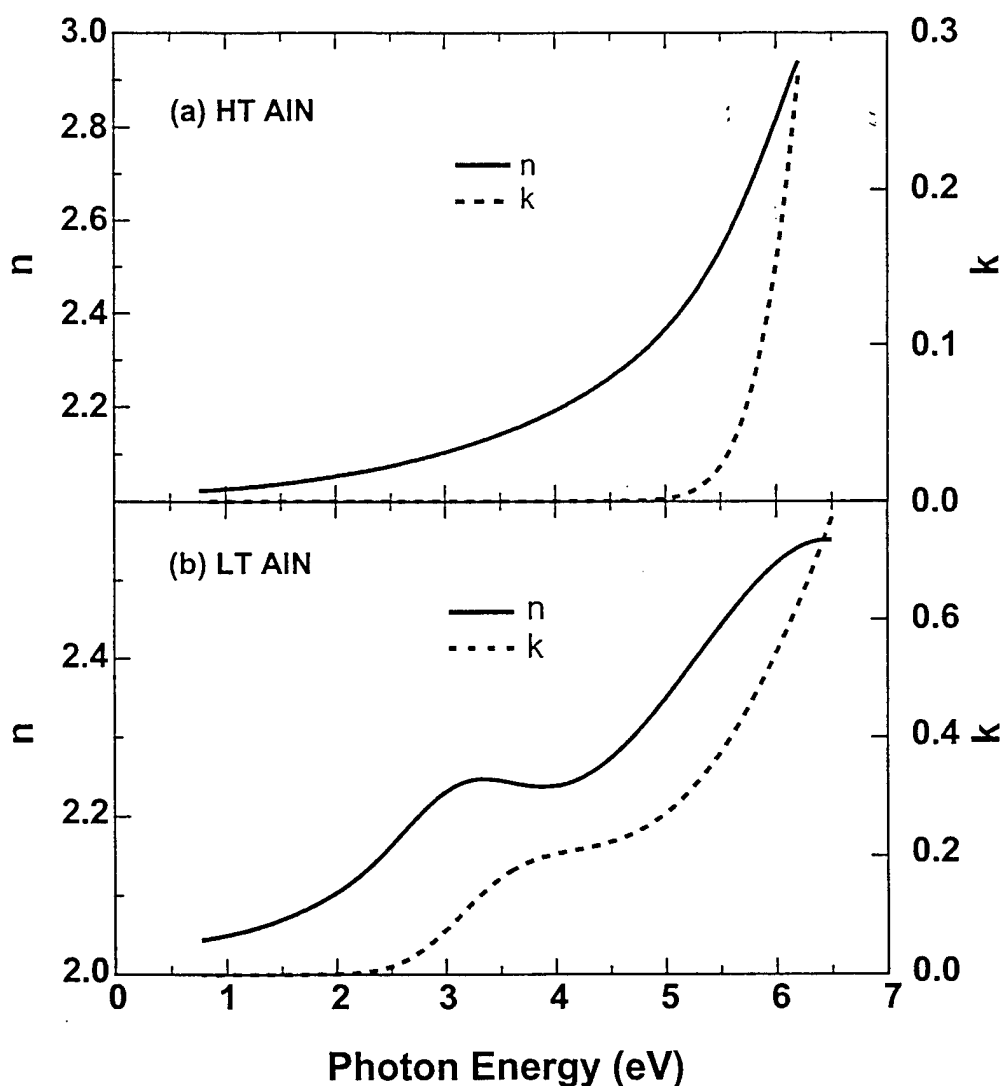


Fig. 6. Optical constants of (a) HT AlN, and (b) LT AlN.

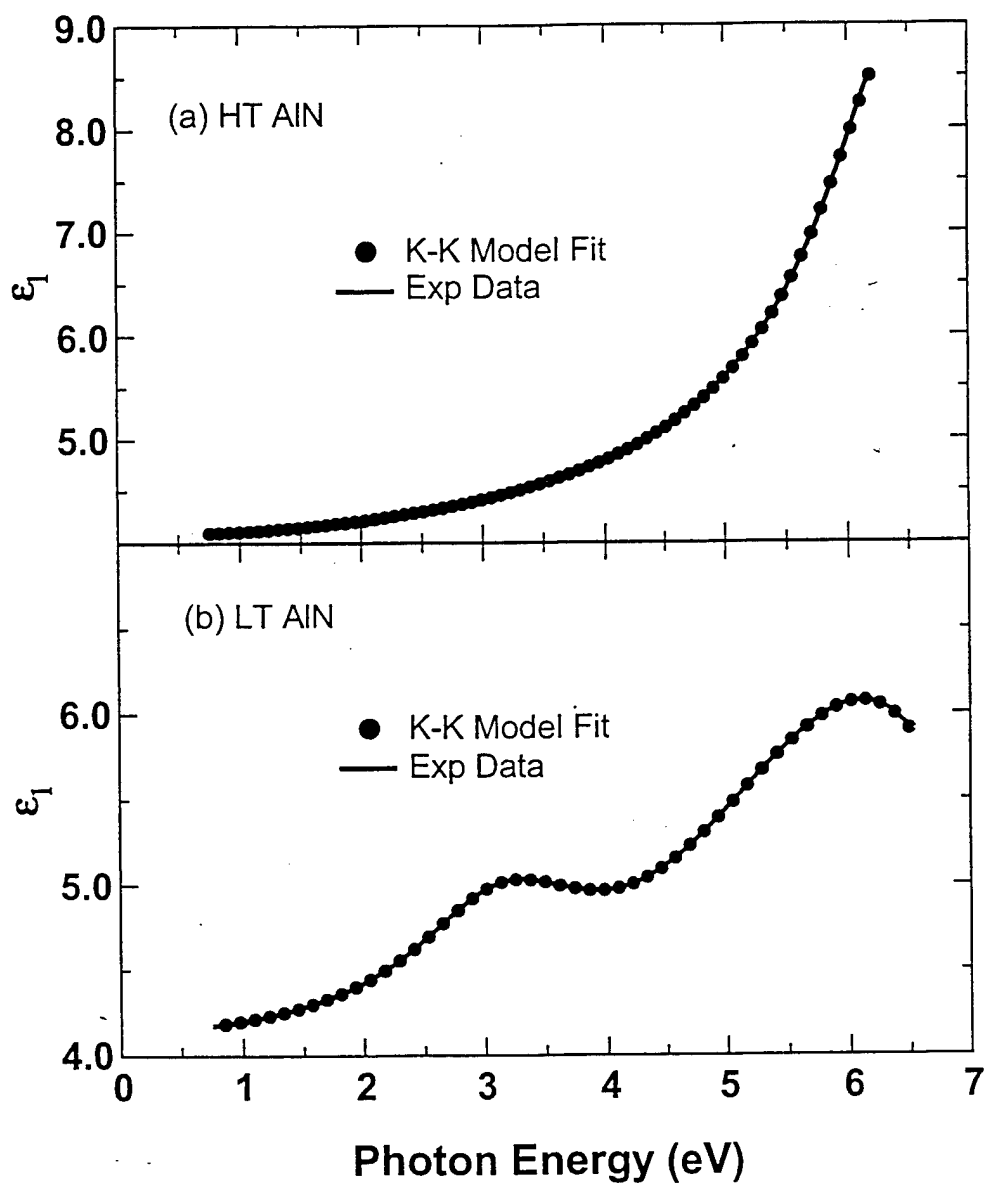


Fig. 7. Kramers-Kronig consistency check AlN dielectric functions. (a) HT AlN; (b) LT AlN.

Table 2. K-K fitting parameters for HT and LT AlN dielectric functions.

Fitting Parameters	E_i	A_i	$\epsilon_1^{\text{offset}}$
Pole (HT AlN)	7.87 eV	17.27	2.29
Pole (LT AlN)	7.76 eV	13.23	2.17

5. Summary

The optical anisotropy nature of AlN films grown on c-plane sapphire substrates was revealed by Raman scattering and generalized variable angle spectroscopic ellipsometry. Optical phonons measured from a 1 μm thick HT AlN agrees very well with the theoretical prediction. Optical constants of HT and LT AlN are determined by TVASE and RVASE along with the structure parameters. The broadening in E_2 phonon and long absorption tail indicate that LT AlN has very high defect density due to low temperature growth and large lattice-mismatch.

Acknowledgments

This work was supported by US Army Research Office under contract No. DAAG55-98-1-0462.

References

1. H. Morkoc, S. Strite, G. B. Gao, M. E. Lin, B. Sverdlov, and M. Burns, "Large-band-gap SiC, III-V nitride, and II-VI ZnSe-based semiconductor device technologies," *J. Appl. Phys.* **76**, pp. 1363-1398, 1994.
2. S. Nakamura, T. Mukai, and M. Senoh, "Candela-class high-brightness InGaN/AlGaIn double-heterostructure blue-light-emitting diodes," *Appl. Phys. Lett.* **64**, pp. 1687-1679, 1994.
3. E. Dogheche, D. Remiens, A. Boudrioua, and J. C. Loulergue, "Growth and optical characterization of aluminum nitride thin films deposited on silicon by radio-frequency sputtering," *Appl. Phys. Lett.* **74**, pp. 1209-1211, 1999.
4. X. Tang, Y. Yuan, K. Wongchotigul, and M. G. Spencer, "Dispersion properties of aluminum nitride as measured by an optical waveguide technique," *Appl. Phys. Lett.* **70**, pp. 3206-3208, 1997..
5. J. F. Muth, J. D. Brown, M. A. L. Johnson, Z. Yu, R. M. Kolbas, J. W. Cook Jr., and, J. F. Schetzina, "Absorption coefficient and reflective index of GaN, AlN, and AlGaIn alloys," *MRS Internet J. Nitride Semicond. Res.*, **4S1**, G5.2 1999.
6. D. E. Aspnes, J. B. Theeten, and F. Hottier, "Investigation of effective-medium models of microscopic surface roughness by spectroscopic ellipsometry", *Phys. Rev. B* **20**, 3292, 1979.
7. T. Azuhata, T. Sota, K. Suzuki and S. Nakamura, "Polarized Raman spectra in GaN," *J. Phys.: Condens. Matter* **7**, pp. L129-L133, 1995.
8. R. M. A. Azzam and N. M. Bashara, *Ellipsometry and Polarized Light*, North-Holland, Amsterdam, 1977.
9. R. M. A. Azzam, and N. M. Bashara, "Generalized ellipsometry for surface with directional preference: application to diffraction gratings," *J. Opt. Soc. Am.* **62**, pp. 1521-1523, 1972.
10. D. W. Berreman, "Optics in stratified and anisotropic media: 4x4 matrix formulation," *J. Opt. Soc. Am.* **62**, pp. 502-510, 1972.
11. M. Schubert, "Polarization dependent parameters of arbitrarily anisotropic homogeneous layered systems," *Phys. Rev. B*, **53**, pp. 4265-4274, 1996.
12. M. Schubert, B. Rheinlander, J. A. Woollam, B. Johs, and C. M. Herzinger, "Extension of rotating analyzer ellipsometry to generalized ellipsometry: determination of the dielectric function tensor from uniaxial TiO_2 ," *J. Opt. Soc. Am. A* **13**, pp. 875-883, 1996.
13. G. H. Wei, J. Zi, K. M. Zhang, X. D. Xie, "Zone-center optical phonons in wurtzite GaN and AlN," *J. Appl. Phys.* **82**, pp. 4693-4695, 1997.
14. C. H. Yan, H. Yao, J. M. Van Hove, A. M. Wowchak, P. P. Chow, and J. M. Zavada, "Ordinary Optical Dielectric Functions of Anisotropic Hexagonal GaN Film Determined by Variable Angle Spectroscopic Ellipsometry," to be published.
15. C. M. Herzinger, B. Johs, U.S. Patent 5,796,983, issued Aug 18, 1998.
16. G. A. Slack and T. F. McNELLY, "Growth of high purity AlN crystals", *J. Cryst. Growth*, **34**, pp. 263-279, 1976.
17. H. Yao, B. Johs, and R. B. James, "Optical anisotropic-dielectric response of mercuric iodide", *Phys. Rev. B*, **56**, 9414 9421, 1997.

Ordinary optical dielectric functions of anisotropic hexagonal GaN film determined by variable angle spectroscopic ellipsometry

C. H. Yan and H. Yao^{a)}

Center for Microelectronic and Optical Material Research, and Department of Electrical Engineering, University of Nebraska, Lincoln, Nebraska 68588-0511

J. M. Van Hove, A. M. Wowchak, and P. P. Chow

SVT Associates, Inc., Eden Prairie, Minnesota 55344

J. M. Zavada

U.S. Army European Research Office, London, United Kingdom

(Received 7 October 1999; accepted for publication 22 June 2000)

Standard variable angle spectroscopic ellipsometry (VASE) has been employed to study the ordinary optical dielectric response of hexagonal gallium nitride (GaN) thin films—an important material for blue and ultraviolet light emitting device applications. The GaN films were grown by molecular beam epitaxy on *c*-plane sapphire substrates (α -Al₂O₃). Room temperature isotropic and anisotropic mode VASE measurements were made at angles of incidence between of 20° and 80°. Evidence of anisotropy was observed from the anisotropic mode measurements, reflecting the nature of wurtzite crystal structure of GaN. The sizable off-diagonal elements (A_{ps} and A_{sp}) of the Jones matrix indicate that the optical axis ($\langle c \rangle$) of the *c*-plane sample are slightly off from the surface normal due to a small miscut of substrates. VASE data simulations by isotropic and anisotropic models indicate that the anisotropic effect on both diagonal and off-diagonal elements of the Jones matrix can be minimized to a negligible level at small angle of incidence. Thus the ordinary optical dielectric functions ($E \perp \langle c \rangle$) are precisely determined by the isotropic mode VASE measurements at angles of incidence between 20° and 40° in the range of 0.75–6.5 eV. The VASE data were analyzed by a model dielectric function based on the GaN critical point structure, which allows for a nonzero extinction coefficient k below the band gap. The thicknesses of these GaN films are accurately determined via the analysis as well. © 2000 American Institute of Physics. [S0021-8979(00)03319-3]

I. INTRODUCTION

The wide band-gap semiconductor GaN and related materials, with their excellent thermal conductivity, large breakdown field, and resistance to chemical attack, have a very promising application potential for both high temperature electronic devices and short wavelength optical emitters.^{1,2} The recent development of high-brightness, blue and green light emitting diodes (LEDs),³ room temperature pulsed,⁴ and continuous-wave quantum well lasers⁵ has greatly encouraged researchers to continue the work on these materials. It is essential to study the optical properties of these optoelectronic materials, such as the optical dielectric functions (or the optical constants) of GaN, for the further improvement of device performance. The optical constants of GaN have been studied intensively since the mid- to late-1960's. Typically, the ordinary refractive indices (n) were measured in the visible and IR spectral range (370–2000 nm), and the extinction coefficients (k) within this region were either ignored or assumed as zero,^{6–9} which is true in theory for the region below band gap. In fact, there is an absorption tail below band gap for most GaN films due to the existence of defect states and impurities. Therefore, it would

be more accurate if a nonzero k model can be employed for the data analysis. The recent works by two different groups have extended the index of refraction data to the region above band gap using spectroscopic ellipsometry.^{8,9} The nonzero absorption below band gap was also observed by other groups.^{10,11}

Most of the high quality GaN films were grown on *c*-plane (0001) sapphire substrates either by molecular beam epitaxy (MBE) or metalorganic vapor phase epitaxy (MOVPE) techniques. Usually GaN grown on sapphire substrates has a wurtzite structure (α -GaN). Nominally the optical axis ($\langle c \rangle$) of the GaN film is perpendicular to the sample surface, and parallel to the $\langle c \rangle$ of sapphire. The fundamental band gap of wurtzite GaN is about 3.4 eV.⁷ As the growth techniques are being improved, higher quality GaN films are being produced with lower defect densities, lower background electron concentration, and higher carrier mobilities. More precise measurements of optical properties thus are needed for future research and fabrication activities. Moreover, GaN is an anisotropic crystal (uniaxial), and this anisotropy cannot be simply neglected during the optical data acquisition even for a nominal *c*-plane sample. The existence of optical anisotropy will affect both the diagonal and off-diagonal elements of the Jones matrix. If the optical axis is strictly perpendicular to the sample surface (perfect *c*-plane

^{a)}Electronic mail: hyao@unl.edu

situation), the Jones matrix is diagonal. This may not be true for most GaN films grown on *c*-plane sapphire substrates, since the crystal is usually cut with an error of several tenths of degree so that the off-diagonal elements of the Jones matrix will not vanish completely. In this situation, the standard reflection variable spectroscopic ellipsometry (RVASE) is not reliable because a portion of light scattering (*p*-*s* or *s*-*p*) has been neglected. Here “*p*” and “*s*” represent the light polarized parallel (*p*) and perpendicular (*s*) to the plane of incidence, respectively. This means that it is necessary to use the generalized ellipsometry technique to detect the off-diagonal elements or to find a condition at which the standard ellipsometry is still effective with negligible off-diagonal elements A_{ps} and A_{sp} .

It would be ideal and straightforward to use generalized ellipsometry (GE) to determine both ordinary and extraordinary dielectric functions of GaN simultaneously. The problem of using GE on a slightly misoriented *c*-plane GaN is the uncertainty of the miscut angle of the sapphire substrate that makes it impossible to set a uniaxial model for VASE data analysis.

Furthermore, even if an ideal *c*-plane GaN is available, the standard way (such as near-Brewster angle of incidence) to perform an ellipsometric measurement for an isotropic sample may be not adequate for the anisotropic structure because both ellipsometric parameters Ψ and Δ (related to the diagonal elements of Jones matrix) are also affected greatly by the optical anisotropy (due to the extraordinary response for *p* polarization). This may cause a few percent error in the resulted optical constants. In order to precisely measure the ordinary optical constants, one has to use special incident angles, other than the standard approach used for isotropic samples, to minimize the extraordinary response (the electric field $E_{\parallel(c)}$) related with the *p* polarization of the incoming light. It is especially important to obtain highly accurate ordinary dielectric functions for the determination of the extraordinary dielectric functions of GaN, since the difference between them is just a few percent in *n* ratio.¹²

The ordinary dielectric functions of GaN can be determined either by *s*-polarized reflectance¹² or by VASE measurements. In theory the *s*-polarized reflectance would be ideal for the determination of the ordinary dielectric functions of a uniaxial anisotropic sample, since the polarization is always perpendicular to the optical axis of a *c*-plane sample regardless of the angle of incidence. The *s*-polarized reflection coefficient is only dependent upon the ordinary dielectric functions.¹² But in practice, *s*-polarized reflectance measurements may not be the best choice since they do not measure the phase change. For most of the samples, the phase information is necessary and critical for the surface layer analysis. Without the phase information, the optical properties determined by the reflectance data will not be accurate. It is especially true for a sample with some native oxide or surface roughness on top. Another major drawback of the reflectance technique is that the measured data are strongly dependent on the light source stability. Any temporal fluctuation and spatial variation may cause a large error in the reflectance data. On the other hand, ellipsometry is a two parameter (Ψ and Δ) measurement technique. The parameter

Δ contains the phase information needed for the surface layer uncertainty determination. Moreover ellipsometric data will not be affected by the light source instability. One problem for using VASE to determine the ordinary dielectric functions is the extraordinary response caused by the *p*-polarized light at nonzero angles of incidence. An alternative way to reduce this extraordinary response is to use a small angle of incidence in the VASE measurement to keep the *p*-polarized part nearly perpendicular to the optical axis (*c*).

In this article, the optical anisotropy of the GaN films grown on *c*-plane sapphire substrates was characterized by generalized variable angle spectroscopic ellipsometry. The impact of optical anisotropy on the determination of ordinary dielectric functions is discussed through generated reflectivity and measured VASE data by isotropic and anisotropic models. Using a small angle of incidence in the VASE data acquisition, the ordinary dielectric functions of GaN are precisely determined via a parametric semiconductor model (with nonzero *k*) in a wide energy range between 0.75 and 6.5 eV. Furthermore, consistency with Kramers–Kronig conditions is maintained.

II. THEORY

A. Standard ellipsometry

Spectroscopic ellipsometry is an experimental method that can be used to measure the change of the polarization state after light is reflected from or transmitted through an optical medium. This medium can be a bulk substrate or a multiple layer structure. By analyzing the measured ellipsometry parameters ψ and Δ with an appropriate physical model, the thickness and optical dielectric functions of each layer can be determined. The parameters ψ and Δ are related to the complex ratio of reflection (or transmission) coefficients for light polarized parallel (*p*) and perpendicular (*s*) to the plane of incidence.¹³ For isotropic material systems,

$$\rho = \frac{R_p}{R_s} = \tan(\psi) e^{i\Delta}. \quad (1)$$

The electric-field reflection coefficient at an incident angle of ϕ is defined as $R_p(R_s)$ for *p*- (*s*)-polarized light. They are the diagonal elements of the Jones matrix in a nondepolarized system:

$$[J]_{\text{sample}} = \begin{bmatrix} R_p & 0 \\ 0 & R_s \end{bmatrix}. \quad (2)$$

The parameters ψ and Δ are not only dependent on dielectric functions, but also on the surface condition, sample structure, and other properties such as the optical anisotropy.

The pseudodielectric function $\langle \epsilon \rangle$ can be obtained directly from the measured ψ and Δ values:

$$\langle \epsilon \rangle = \langle \epsilon_1 \rangle + i \langle \epsilon_2 \rangle = \sin^2 \phi \left[1 + \tan^2 \phi \left(\frac{1 - \rho}{1 + \rho} \right)^2 \right]. \quad (3)$$

For the case of air over a bare bulk material with a perfectly smooth surface, the pseudodielectric and intrinsic dielectric

function are identical. To determine the optical constants of a thin film on a substrate, VASE data must be analyzed using a parametric model that is adjusted to fit the measured data. A regression analysis is usually used to vary the model pa-

rameters (e.g., the optical constants or layer thickness, etc.) until the calculated and measured values match as closely as possible. This is done by minimizing the mean square error (MSE) function, defined as:

$$\text{MSE} = \sqrt{\frac{1}{N-M} \sum_{i,j} \left\{ \left[\frac{\psi(h\nu_i, \phi_j) - \psi^c(h\nu_i, \phi_j)}{\sigma_{i,j\psi}} \right]^2 + \left[\frac{\Delta(h\nu_i, \phi_j) - \Delta^c(h\nu_i, \phi_j)}{\sigma_{i,j\Delta}} \right]^2 \right\}}, \quad (4)$$

where N is the total number of experimental observations (for ellipsometry measurements, there are two observations Ψ and Δ , for each data point), M is the number of fit parameters, σ is the measured standard deviation of the measurement, ϕ is the external angle of incidence, $h\nu$ is the photon energy, and i and j are used to sum over all the photon energies and external angles of incidence, respectively.

B. Generalized ellipsometry

Generalized ellipsometry was first introduced by Azzam and Bashara.¹⁴ The recent developments make this technique more capable and powerful.^{15,16} For an anisotropic material system, the off-diagonal elements of the Jones matrix are not necessary to be zero. In the reflection (RVASE) configuration,

$$[J]_{\text{sample}} = \begin{bmatrix} R_{pp} & R_{sp} \\ R_{ps} & R_{ss} \end{bmatrix}. \quad (5)$$

By using the same approach with considerably more computation, ψ and Δ values can still be determined, but the Fourier coefficients related to ψ and Δ become more complicated.¹⁷ The generalized ellipsometric parameters are defined as below:

$$A_{nE} = \frac{R_{pp}}{R_{ss}} = \tan \psi_{nE} e^{i\Delta_{nE}}, \quad (6)$$

$$A_{ps} = \frac{R_{ps}}{R_{pp}} = \tan \psi_{ps} e^{i\Delta_{ps}}, \quad (7)$$

$$A_{sp} = \frac{R_{sp}}{R_{ss}} = \tan \psi_{sp} e^{i\Delta_{sp}}, \quad (8)$$

where the A_{ps} and A_{sp} describe how much amount p - or s -polarized light becomes s - or p -polarized light after the reflection, respectively. The A_{nE} is the diagonal matrix element.

In summary, the generalized ellipsometry is a technique, which can be used to determine all the elements of the Jones matrix for arbitrarily anisotropic and homogeneous layered systems with nonscalar dielectric susceptibilities. Unlike the isotropic mode VASE measurements, the anisotropic mode measurements, i.e., generalized ellipsometry are made with a fixed pattern for the polarizer position (e.g., $p = -60^\circ$, -30° , 0° , $+30^\circ$, $+60^\circ$, and 90°) at each wavelength. Since

the Fourier coefficients¹⁴ are the functions of A_{ps} and A_{sp} , they are dependent upon the incident polarization in anisotropic materials.

III. EXPERIMENT

The GaN film (about 1 μm thick) used in this work was grown by MBE on c -plane sapphire substrate. The cutting error of crystal orientation is within 1° . The backside of the substrate was unpolished which is sufficiently rough for the reflection VASE and polarized reflectivity measurements. The RVASE optical measurements of both isotropic (standard ellipsometry) and anisotropic modes (generalized ellipsometry) were performed in the energy range 0.75–6.5 eV with a 0.02 eV increment at room temperature. In order to reveal the angular dependence of the optical anisotropy of a c -plane sample, the generalized ellipsometry measurements were performed at 1.4 eV with the angle of incidence ranging from 20° to 80° with 1° increments. Silicon and InGaAs photodiodes are employed in the VASE system. They are polarization state insensitive, and linear over a broad range of beam intensity. The monochromator was placed right after the light source for wavelength scanning.

IV. RESULTS AND DISCUSSION

In order to reveal the optical anisotropy of GaN on c -plane sapphire, a series of anisotropic mode VASE measurements have been made. Two of them are shown in Fig. 1. The RVASE data in Fig. 1(a) were taken at an angle of incidence of 60° , which is near the pseudo-Brewster angle. It can be seen clearly that the off-diagonal elements A_{ps} and A_{sp} are not negligible, especially for A_{ps} below band gap. The strong A_{ps} fringes appeared below 3.4 eV are due to the thin film interference. Notice that they have the same period as the A_{nE} does. For photon energies larger than band-gap value, there are no interference fringes since the GaN film is no longer transparent in this region (the extinction coefficient k is very large). Nonzero A_{ps} and A_{sp} indicate that: (1) GaN film has strong optical anisotropy; (2) the $\langle c \rangle$ axis of GaN is off the surface normal. For such a sample, the A_{ps} and A_{sp} have to be taken into account in the data analysis unless special measurement conditions are employed under which the anisotropic effect can be greatly minimized. The nonzero A_{ps} and A_{sp} means that there is cross-conversion between p - and s -polarized light. We cannot set up an anisotropic model to do the generalized-VASE data analysis and solve both ordinary and extraordinary dielectric functions simulta-

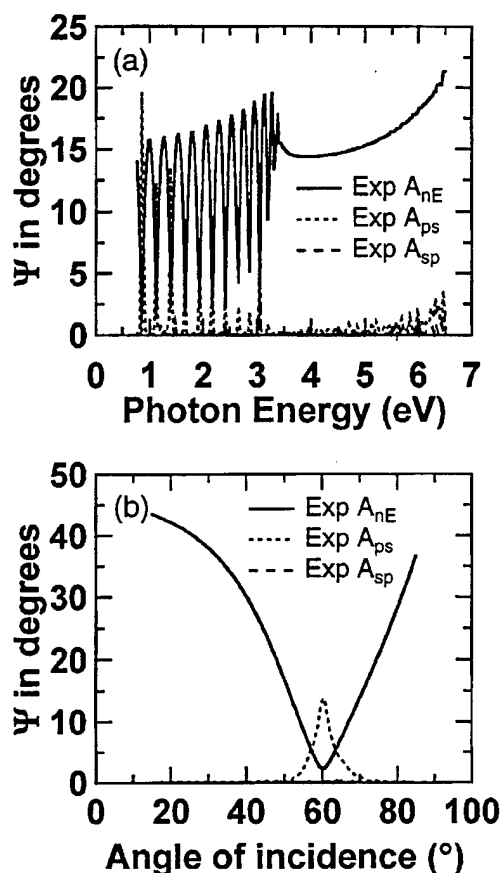


FIG. 1. Anisotropic mode RVASE data of *c*-plane GaN/sapphire. (a) Ψ as a function of photon energy at 60° angle of incidence; (b) Ψ as a function of incident angle at 1.4 eV.

neously, since the offset angle of $\langle c \rangle$ axis from surface normal is unknown. An easier way to determine the dielectric functions of GaN is to solve them separately, and to construct an isotropic model instead of an anisotropic model to solve for the ordinary dielectric functions. Therefore, special measurement conditions must be used to suppress the A_{ps} and A_{sp} values, and to allow us to treat the anisotropic film as a pseudoisotropic material without losing accuracy. To find such measurement conditions, an angular dependent measurement was made at certain wavelength (1.4 eV), as shown in Fig. 1(b). The angular increment is 1°. The off-diagonal elements are detectable in the angle range of 50°–70°, and it has a peak value at about 60°, which is near the pseudo-Brewster angle at 1.4 eV. We have measured curves similar to that in Fig. 1(b) at other photon energies with the peak positions slightly varied due to different Brewster angles at the different wavelengths. In the photon energy range of 0.75–6.5 eV, the A_{ps} peak position can change from about 59° to 67°, i.e., A_{ps} may be detectable from approximately 49° to 77° angle of incidence. In other words, the A_{ps} and A_{sp} are negligible at the angle of incidence below 40° or above 80° for an anisotropic sample with slightly $\langle c \rangle$ axis offset. The above measurement conditions are only useful to minimize the off-diagonal elements (A_{ps} and A_{sp}) related to the misoriented *c*-plane GaN film. To determine ordinary

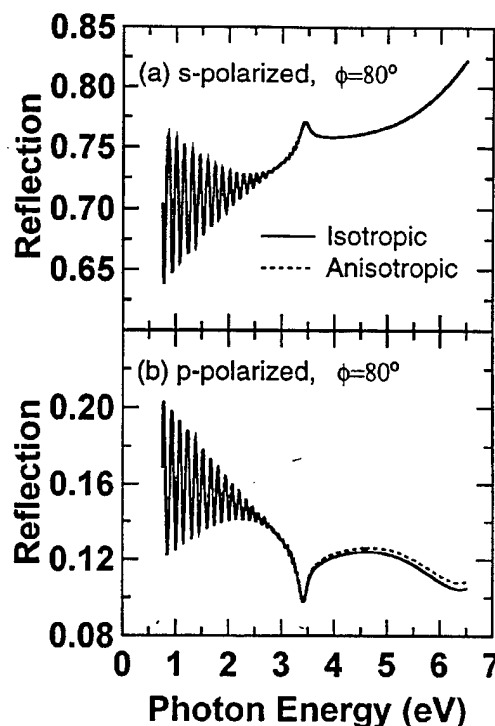


FIG. 2. Simulated *p*-polarized reflectivity data of a GaN (2 μm)/*c*-sapphire structure by isotropic (solid line) and anisotropic (dash line) models at 80° angle of incidence.

dielectric functions of GaN more precisely, the anisotropic effect included in the diagonal elements has to be taken into account in the VASE data analysis.

Usually the ordinary dielectric functions of anisotropic GaN are measured by standard ellipsometry at large angle of incidence such as 60° (Ref. 9) and 70°,¹⁸ and modeled as an isotropic material. In general, results from these studies are suitable as provisional data. However, they lack accuracy because the sample misorientation has been neglected and because the anisotropic nature is overlooked in the data analysis. This may become a problem when precise determination of the extraordinary dielectric functions is required.

To illustrate anisotropic impact on the diagonal elements, the difference of isotropic and anisotropic optical response generated from ideal *c*-plane models (no misorientation) are shown in Figs. 2 and 3. Two simulated GaN/*c*-sapphire models with exactly the same multilayered-structures (2- μm GaN film with 4% thickness nonuniformity) were constructed for the data simulation. In the isotropic model, GaN is assumed to be an isotropic material, with ordinary dielectric functions only. In the anisotropic model, GaN is assumed to be an anisotropic material, with both ordinary and extraordinary dielectric functions. The ordinary and extraordinary functions used in the two models are from a study on GaN/*m*-sapphire.¹⁹ The average difference between extraordinary and ordinary in n values is about +4% in the range of 0.75–6.5 eV. Dielectric functions of sapphire used for the simulations and VASE analysis are from our previous work.²⁰ Data generated by the isotropic and anisotropic models are identical everywhere because the

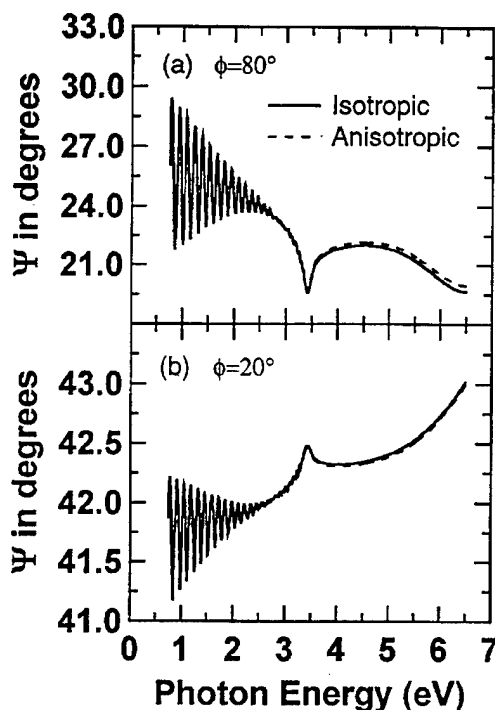


FIG. 3. Simulated RVASE data of GaN (2 μm)/c-sapphire structure by isotropic (solid line) and anisotropic (dash line) models. (a) Large angle of incidence ($\phi = 80^\circ$); (b) small angle of incidence ($\phi = 20^\circ$).

s -polarized light can only cause the ordinary dielectric response that is independent of the angle of incidence. But for nonzero degree angle of incidence, the p -polarized incident light can cause both ordinary and extraordinary responses in an anisotropic material, which will be different from the pure ordinary response in an isotropic material, as shown in Fig. 2. The reflectivity difference between isotropic and anisotropic model is about 3% at 6 eV, and this difference is strongly dependent on the angle of incidence. The difference decreases as the angle of incidence decreases.

Generated VASE data with different angle of incidence for the two models are shown in Fig. 3. The angle of incidence is 80° for Fig. 3(a), and 20° for Fig. 3(b). Notice that the Ψ difference in ratio between two models ($[\Psi_{\text{aniso}} - \Psi_{\text{iso}}]/\Psi_{\text{iso}}$) in Fig. 3(a) is about 20 times larger than in Fig. 3(b). The absolute difference between Ψ values generated by two models in Fig. 3(b) is close to the measurement error bar ± 0.007 , which is within the sensitivity limitation of the instrument. Therefore, the anisotropic effect on the diagonal elements can be greatly minimized by using a small angle of incidence. In addition, the small angle of incidence is also good for suppressing the s - p or p - s cross conversion. Comparing with the measurement error bar, we can conclude that the anisotropic GaN film can be treated as isotropic material at small angles of incidence ($\phi \leq 40^\circ$).

According to the above analysis, VASE data at a small angle of incidence (20° , 40°) were taken from a GaN/c-sapphire sample for the determination of ordinary dielectric functions of GaN. The sample structure was described by a three-layer model, including sapphire substrate, an isotropic GaN film and a surface layer counting for the

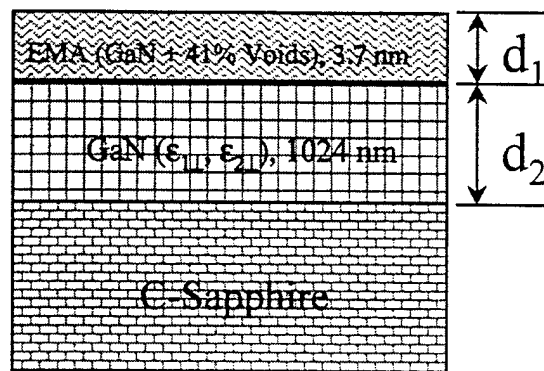


FIG. 4. Structural model sketch of GaN/sapphire with a surface rough layer.

surface roughness of GaN film, as shown in Fig. 4. The VASE data and model fittings are shown in Fig. 5. The top surface layer is described by a Bruggeman effective media approximation (EMA)^{21,22} for a layer consisting of GaN and voids. The model dielectric function (MDF) of GaN, was represented by a simplified Adachi model,¹⁸ which consisted of two critical points (CP) describing the interband transitions (E_0 and E_1 gaps), and two exciton contributions at E_0 and E_1 edges. With the assumption of parabolic band shape for both valence and conduction bands, the contribution of E_0 to $\epsilon(E)$ is^{18,23}

$$\epsilon^{(0)}(E) = A_0 E_0^{-1.5} \{ \chi_0^{-2} [2 - (1 + \chi_0)^{0.5} - (1 - \chi_0)^{0.5}] \}. \quad (9)$$

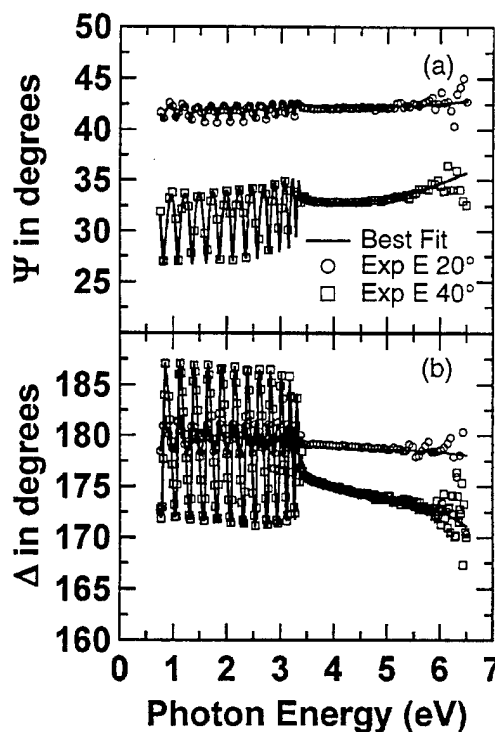


FIG. 5. RVASE data and model fittings of a GaN/c-sapphire sample. (a) Ψ data and the best model fit at 20° and 40° angles of incidence; (b) Δ data and the best model fit at 20° and 40° angles of incidence. The solid line represents the best model fit. The circle and square represent the data taken at 20° and 40° angles of incidence, respectively.

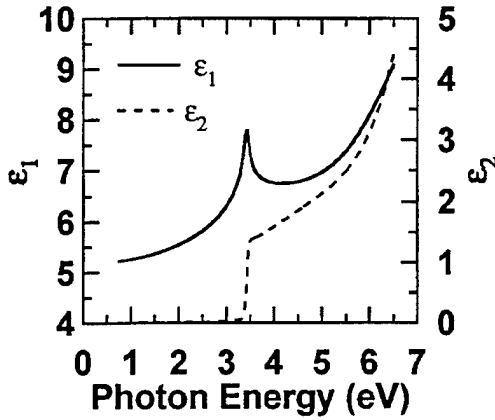


FIG. 6. Ordinary dielectric functions of GaN obtained from the small angle of incidence RVASE data analysis of a GaN/c-sapphire sample.

The E_1 contribution to $\epsilon(E)$ can be expressed as

$$\epsilon^{(1)}(E) = A_1 \chi_1^{-2} \ln(1 - \chi_1^2), \quad (10)$$

and

$$\chi_j = (E + i\Gamma_j)/E_j, \quad (11)$$

where j can be 0 or 1 for Eqs. (9) and (10), respectively. A_j , E_j , and Γ_j are amplitude, transition energy, and broadening parameter of the E_0 and E_1 CP structures, respectively. The contributions to $\epsilon(E)$ from excitons at E_0 and E_1 edges are approximated by two discrete damped Lorentzian line shapes with complex amplitudes:

$$\epsilon^{(jx)}(E) = \frac{A_{jx} \exp(ip_{jx})}{E_{jx} - E - i\Gamma_{jx}}, \quad (12)$$

where $j=0, 1$ for E_0 and E_1 , respectively. E_{jx} , Γ_{jx} , and A_{jx} are center energy, broadening, and amplitude of each exciton, respectively, and p_{jx} is the phase factor of the complex amplitude. The total dielectric response due to interband transitions and excitonic contributions, in the energy range of 0.75–6.5 eV, is then given by

$$\epsilon(E) = \epsilon_\infty + \epsilon^{(0)}(E) + \epsilon^{(0x)}(E) + \epsilon^{(1)}(E) + \epsilon^{(1x)}(E). \quad (13)$$

The dielectric constant ϵ_∞ accommodates contributions from CP structures at energies higher than E_1 , which are not directly included in the model. The upper CPs are not considered in this model is due to the limit of experimental data at 6.5 eV. This parametric dispersion model can, without compromise to the quality of data fitting, replace the usual tabulated optical constants lists by using a reasonable small set of adjustable parameters (15 parameters total in this model ex-

TABLE I. Best fitting parameters for GaN ordinary dielectric functions.

CP contribution	$A_j(A_{jx})$	$E_j(E_{jx})$	$\Gamma_j(\Gamma_{jx})$	p_{jx}
$\epsilon^{(0)}$	30.15 (eV) ^{1.5}	3.44 (eV)	0.22 (eV)	...
$\epsilon^{(0x)}$	1.07 (eV)	3.42 (eV)	0.19 (eV)	-1.52
$\epsilon^{(1)}$	2.90	6.94 (eV)	0.047 (eV)	...
$\epsilon^{(1x)}$	3.34 (eV)	6.92 (eV)	1.86 (eV)	-0.025
ϵ_∞	0.23			

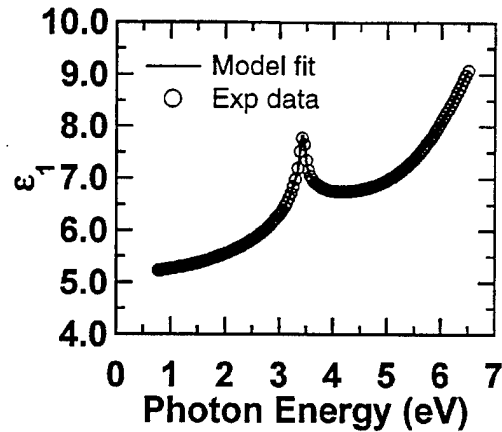


FIG. 7. Kramers-Kronig consistency check of the ordinary dielectric functions of GaN.

cept film thickness and surface parameters). It reduces parameter correlation in data fittings, and enforces continuity on the optical constants.

With a small amount of surface roughness (about 3.7 nm thick EMA layer with 41% voids resulted from the best fit), the VASE data at both angles of incidence were fitted extremely well. The GaN film thickness resulting from VASE data analysis is about 1024 nm, which is close to the nominal value of 1 μm .

The ordinary dielectric functions of GaN film grown on c-plane sapphire substrate determined in this work are shown in Fig. 6. The fitting parameters of GaN ordinary dielectric functions are listed in Table I. The starting values of the fitting parameters are set based on the critical point structure of GaN.¹⁸ Notice that the E_0 and E_1 values are slightly different from those given in Ref. 18. This may be due to the simplification of the present model and the limited spectral range of the experimental data. The sharp turn of ϵ_2 near the band edge and the very weak absorption tail indicate that this film has high crystal quality. In order to check the Kramers-Kronig (KK) consistency of the resulting GaN ordinary dielectric functions, a KK fitting is shown in Fig. 7. The circles are the best ϵ_1 result, and the solid line is the calculated ϵ_1 from the known ϵ_2 values using the KK relation. The final results of all fitting parameters are given in Table II. The KK relation used in the calculation is^{24,25}

$$\epsilon_1^{\text{kk}}(E) = \epsilon_1^{\text{offset}} + \sum_{i=1}^2 \frac{A_i}{E_i^2 - (E)^2} + \frac{2}{\pi} P \int_{0.75 \text{ eV}}^{6.5 \text{ eV}} \frac{E' \epsilon_2^{\text{meas}}(E')}{E'^2 - (E)^2} dE'. \quad (14)$$

TABLE II. Kramers-Kronig fitting parameters for GaN ordinary dielectric functions.

Pole No.	E_i	Fitting parameters	
		A_i	$\epsilon_1^{\text{offset}}$
1	7.491	2.001	1.04
2	14.092	24.6	

For a specified material, the KK integral is numerically evaluated to calculate ϵ_1 values from ϵ_2 . The model then adds the contribution from two nonbroadening oscillators and a fixed offset to account for absorption outside the experimental measurement range. E_i is the energy location of a nonbroadening oscillator that is added to simulate absorption outside the integration range, A_i is the magnitude of the oscillator located at E_i position. In our calculation two oscillators were used outside the measured region.

V. SUMMARY

The optical anisotropy of GaN films grown on *c*-plane sapphire substrates was revealed by the generalized variable angle spectroscopic ellipsometry. This anisotropy can be observed via the nonzero off-diagonal Jones matrix. These off-diagonal elements are nonnegligible in a range of incident angles for slightly miscut samples. However, these elements may become undetectable beyond this range of angles. At a small angle of incidence ($\phi < 40^\circ$), the optical anisotropic effect on both off-diagonal and diagonal elements of the Jones matrix can be greatly reduced. Thus the ordinary dielectric functions of GaN are accurately determined in the range of 0.75–6.5 eV by fitting the RVASE data with an isotropic CP model dielectric function. The comparison of the calculated ϵ_1 and the experimental ϵ_1 indicates that the dielectric functions obtained in this study are KK consistent.

ACKNOWLEDGMENT

This work was supported by U.S. Army Research Office under Contract No. DAAG55-98-1-0462.

¹H. Morkoç, S. Strite, G. B. Gao, M. E. Lin, B. Sverdlov, and M. Burns, J. Appl. Phys. **76**, 1363 (1994).

- ²S. Nakamura, T. Mukai, and M. Senoh, Appl. Phys. Lett. **64**, 1687 (1994).
- ³S. Nakamura, M. Senoh, N. Iwasa, and S. Nagahama, Jpn. J. Appl. Phys., Part 2 **34**, L797 (1995).
- ⁴S. Nakamura, M. Senoh, S. Nagahama, N. Iwasa, T. Yamada, T. Matsushita, H. Kiyoku, and Y. Sugimoto, Jpn. J. Appl. Phys., Part 2 **35**, L74 (1996).
- ⁵S. Nakamura, M. Senoh, S. Nagahama, N. Iwasa, T. Yamada, T. Matsushita, H. Kiyoku, Y. Sugimoto, T. Kozaki, H. Umemoto, M. Sano, and K. Chocho, Appl. Phys. Lett. **72**, 2014 (1998).
- ⁶E. Ejder, Phys. Status Solidi A **6**, 445 (1971).
- ⁷S. Logothetidis, J. Petalas, M. Cardona, and T. D. Moustakas, Phys. Rev. B **50**, 18017 (1994).
- ⁸H. Amano, N. Watanabe, N. Koide, and I. Akasaki, Jpn. J. Appl. Phys., Part 2 **32**, L1000 (1993).
- ⁹G. Yu, G. Wang, H. Ishikawa, M. Umeno, T. Soga, T. Egawa, J. Watanabe, and T. Jimbo, Appl. Phys. Lett. **70**, 3209 (1997).
- ¹⁰W. R. L. Lambrecht, B. Segall, J. Rife, W. R. Hunter, and D. K. Wickenden, Phys. Rev. B **51**, 13516 (1995).
- ¹¹J. Petalas, S. Logothetidis, S. Bouladakis, M. Alouani, and J. M. Wills, Phys. Rev. B **52**, 8082 (1995).
- ¹²G. Yu, H. Ishikawa, T. Egawa, T. Soga, J. Watanabe, T. Jimbo, and M. Umeno, Jpn. J. Appl. Phys., Part 2 **36**, L1029 (1997).
- ¹³R. M. A. Azzam and N. M. Bashara, *Ellipsometry and Polarized Light* (North-Holland, Amsterdam, 1977).
- ¹⁴R. M. A. Azzam and N. M. Bashara, J. Opt. Soc. Am. **62**, 1521 (1972).
- ¹⁵D. W. Berreman, J. Opt. Soc. Am. **62**, 502 (1972).
- ¹⁶M. Schubert, Phys. Rev. B **53**, 4265 (1996).
- ¹⁷M. Schubert, B. Rheinlander, J. A. Wollam, B. Johs, and C. M. Herzinger, J. Opt. Soc. Am. A **13**, 875 (1996).
- ¹⁸T. Kawashima, H. Yoshikawa, S. Adachi, S. Fuke, and K. Ohtsuka, J. Appl. Phys. **82**, 3528 (1997).
- ¹⁹C. H. Yan and H. Yao (unpublished).
- ²⁰H. Yao and C. H. Yan, J. Appl. Phys. **85**, 6717 (1999).
- ²¹D. E. Aspnes, J. B. Theeten, and F. Hottier, Phys. Rev. B **20**, 3292 (1979).
- ²²H. Yao, B. Johs, and R. B. James, Phys. Rev. B **56**, 9414 (1997).
- ²³M. Schubert, J. A. Woollam, G. Leibiger, B. Rheinländer, I. Pietzonka, T. Sass, and V. Gottschalch, J. Appl. Phys. **86**, 2025 (1999).
- ²⁴H. Yao, B. Johs, and R. B. James, Phys. Rev. B **56**, 9414 (1997).
- ²⁵H. W. Yao, J. C. Erickson, H. B. Barber, and R. B. James, J. Electron. Mater. **28**, 760 (1999).

Extraordinary optical dielectric functions of anisotropic hexagonal GaN film determined by variable angle spectroscopic ellipsometry

C. H. Yan, H. Yao^{a)},

Center for Microelectronic and Optical Material Research, and Department of Electrical Engineering, University of Nebraska, Lincoln, NE 68588-0511

J. M. Van Hove, A. M. Wowchak, and P. P. Chow

SVT Associates, Inc

J. M. Zavada

US Army European Research Office, London, UK

Abstract

Variable angle spectroscopic ellipsometry (VASE) has been employed to study the extraordinary optical dielectric response of hexagonal gallium nitride (GaN) thin film grown on c-plane sapphire substrates (α -Al₂O₃) by molecular beam epitaxy (MBE). Room temperature VASE measurements were made, in the range of 0.75 to 6.5 eV, at the angle of incidence in between of 60 and 80 degree. VASE data simulations by isotropic and anisotropic models indicate that the anisotropic effect can be detected most-sensitively at large angles of incidence (near the pseudo-Brewster angle). Thus the extraordinary optical dielectric functions ($\mathbf{E} \parallel \langle \mathbf{c} \rangle$) are precisely determined by standard VASE measurements at 60°, 70°, and 80° angles of incidence in the range of 0.75 to 6.5 eV. The surface roughness was also considered in the VASE data analysis in order to separate it from the anisotropic effect. The VASE data is analyzed by a model dielectric function based on the GaN critical point structure, which allows for a non-zero extinction

^{a)} Electronic mail: hyao@unl.edu

coefficient k below the band gap. The thicknesses of these GaN films are accurately determined via the analysis as well.

1. Introduction

The wide band gap semiconductor GaN is an important material for light emitting device applications in the green, blue and UV regions^{1, 2, 3}. GaN films grown on sapphire substrates usually have hexagonal structure, which is optically anisotropic. The ordinary optical dielectric functions of GaN have been studied intensively since 1960's^{4, 5, 6}. The most recent data of ordinary dielectric functions were determined by variable angle spectroscopic ellipsometry (VASE) with⁷ or without⁸ the consideration of surface roughness and the optical anisotropy. But the extraordinary dielectric functions of GaN, on the other hand, are not well documented. Yu⁹ reported the extraordinary functions below the fundamental band gap measured by polarized reflectance without the consideration of the surface roughness. Polarized reflectance spectroscopy is a straightforward technique to measure the extraordinary response of GaN. However it may be lack of accuracy because not only reflectance is an intensity sensitive method, but also it is lack of sensitivity on surface roughness. The later is because of the phase information cannot be obtained in a reflectance spectrum. But this does not mean that the reflectance spectrum will not be affected by the surface roughness.

In principle, the best way to determine the extraordinary dielectric functions is using the generalized ellipsometry (GE), which can accurately distinguish the difference between the ordinary and extraordinary dielectric response by measuring the off-diagonal elements of Jones matrix (A_{ps} and A_{sp})⁷. But the GE measurements for the determination of the extraordinary functions require non c-plane samples, or say the optical axis of a GaN film has to be certain degree away from the surface normal, and this angle has to be

well determined before the GE measurements. In fact, Most of high quality GaN films were grown on c-plane (0001) sapphire substrates either by molecular beam epitaxy (MBE) or metalorganic vapor phase epitaxy (MOVPE) techniques. The optical axis $\langle c \rangle$ of the GaN film grown on c-plane sapphire is perpendicular to the sample surface nominally, and parallel to the $\langle c \rangle$ of sapphire. In this case the off-diagonal elements of Jones matrix are zero. Therefore, Measuring a GaN film grown on c-plane sapphire by GE will not bring any information about the off-diagonal elements. An alternative way to determine the extraordinary dielectric functions of GaN films grown on c-plane sapphire substrates is to employ the standard ellipsometry under some special conditions.

For an anisotropic material, both Ψ and Δ will be affected greatly by the optical anisotropy. This effect is also incident-angle dependent. At certain angle of incidence (near pseudo-Brewster angle), extraordinary optical response ($E \parallel \langle c \rangle$) has the maximum sensitivity. At small angle of incidence, the extraordinary response has almost no sensitivity in the Ψ and Δ . This is how the ordinary dielectric functions were determined in our previous study⁷. In this paper, the extraordinary dielectric functions of a GaN film grown on c-plane sapphire substrates were determined by standard variable angle spectroscopic ellipsometry at large angles of incidence, via a parametric semiconductor model (allow nonzero-k) in a wide energy range of 0.75eV to 6.5 eV, and they are Kramers-Kronig consistent. The impact of surface roughness on the VASE data analysis is also discussed through model-generated reflectivity and VASE data.

2. Theory

2.1. Ellipsometry for isotropic films

For an isotropic material system, the ellipsometric parameters Ψ and Δ are defined as below.

$$\rho = \frac{R_p}{R_s} = \tan(\psi)e^{i\Delta} \quad (1)$$

R_s and R_p are the total reflection coefficients of a multiple-layer structure for s and p polarized light, respectively. They are the diagonal elements of Jones matrix in a no depolarized system. In the case of a substrate with one surface overlayer, light can see two interfaces (air-film, and film-substrate) for both reflection and transmission. The total reflection coefficients (R_s and R_p) are expressed as¹⁰:

$$R_s = \frac{r_{12}^s + r_{23}^s \exp(-j2\beta)}{1 + r_{12}^s r_{23}^s \exp(-j2\beta)} \quad (2)$$

$$R_p = \frac{r_{12}^p + r_{23}^p \exp(-j2\beta)}{1 + r_{12}^p r_{23}^p \exp(-j2\beta)} \quad (3)$$

Where

$$\beta = 2\pi \left(\frac{d}{\lambda} \right) \tilde{N}_2 \cos \phi_2 \quad (4)$$

r_{12}^s , r_{23}^s , r_{12}^p , and r_{23}^p are the Fresnel reflection coefficients of a single interface. The general formats of p- and s-polarized reflection coefficients are

$$r_{12}^s = \frac{N_1 \cos \phi_1 - N_2 \cos \phi_2}{\tilde{N}_1 \cos \phi_1 + \tilde{N}_2 \cos \phi_2} \quad (5)$$

$$r_{12}^p = \frac{\tilde{N}_2 \cos \phi_1 - \tilde{N}_1 \cos \phi_2}{\tilde{N}_2 \cos \phi_1 + \tilde{N}_1 \cos \phi_2} \quad (6)$$

\tilde{N}_1 and \tilde{N}_2 are the complex indices of reflection of the upper and lower medium. ϕ_1 is the angle of incidence, and ϕ_2 is the refraction angle (they are related by Snell's law).

The ψ and Δ are not only dependent on dielectric functions, but also on the angle of incidence, surface condition, sample structure, and other properties such as the optical anisotropy for anisotropic materials.

2.2. Ellipsometry of anisotropic films

For a uniaxial anisotropic film, when the optical axis $\langle c \rangle$ is perpendicular to the film surface, i.e., the c-plane case, the three-phase total reflection coefficients for s- and p-polarized light are¹¹

$$R_s = \frac{r_{12}^s + r_{23}^s \exp(-j2\beta_s)}{1 + r_{12}^s r_{23}^s \exp(-j2\beta_s)} \quad (7)$$

$$R_p = \frac{r_{12}^p + r_{23}^p \exp(-j2\beta_p)}{1 + r_{12}^p r_{23}^p \exp(-j2\beta_p)} \quad (8)$$

Where r_{12}^s, r_{23}^s are the *Fresnel* reflection coefficients at the first and second interfaces for s-polarization. r_{12}^p and r_{23}^p are the Fresnel reflection coefficients at the first and second interfaces for p-polarization. They are

$$r_{12}^s = \frac{N_1 \cos \phi_1 - N_{2\perp} \cos \phi_2}{N_1 \cos \phi_1 + N_{2\perp} \cos \phi_2} \quad (9)$$

$$r_{23}^s = \frac{N_{2\perp} \cos \phi_1 - N_{3\perp} \cos \phi_3}{N_{2\perp} \cos \phi_1 + N_{3\perp} \cos \phi_2} \quad (10)$$

$$r_{12}^p = \frac{\tilde{N}_{2\parallel}\tilde{N}_{2\perp}\cos\phi_1 - \tilde{N}_1[(\tilde{N}_{2\parallel})^2 - (\tilde{N}_1)^2\sin^2\phi_1]^{\frac{1}{2}}}{\tilde{N}_{2\parallel}\tilde{N}_{2\perp}\cos\phi_1 + \tilde{N}_1[(\tilde{N}_{2\parallel})^2 - (\tilde{N}_1)^2\sin^2\phi_1]^{\frac{1}{2}}} \quad (11)$$

$$r_{23}^p = \frac{\tilde{N}_3[(\tilde{N}_{2\parallel})^2 - \tilde{N}_1\sin^2\phi_1]^{\frac{1}{2}} - \tilde{N}_{2\parallel}\tilde{N}_{2\perp}\cos\phi_3}{\tilde{N}_3[(\tilde{N}_{2\parallel})^2 - \tilde{N}_1\sin^2\phi_1]^{\frac{1}{2}} + \tilde{N}_{2\parallel}\tilde{N}_{2\perp}\cos\phi_3} \quad (12)$$

β_s and β_p represent the phase difference for the s-polarized wave and p-polarized wave.

$$\beta_s = \frac{2\pi d[(\tilde{N}_{2\perp})^2 - (\tilde{N}_1)^2\sin^2\phi_1]^{\frac{1}{2}}}{\lambda} \quad (13)$$

$$\beta_p = \frac{2\pi d\tilde{N}_{2\perp}[(\tilde{N}_{2\parallel})^2 - (\tilde{N}_1)^2\sin^2\phi_1]^{\frac{1}{2}}}{\lambda\tilde{N}_{2\parallel}} \quad (14)$$

Where λ is the wavelength of the monochromatic light in vacuum and d is the thickness of the anisotropic film.

Look into the definition of Ψ and Δ , it is obvious that these two parameters depend on $\tilde{N}_{2\perp}$ and $\tilde{N}_{2\parallel}$, and the angle of incidence.

3. Experiments

The GaN film (about 1 μm thick) studied in this work was grown by MBE on c-plane sapphire substrate. The cutting error of crystal orientation is within about 1°. The backside of the substrate was unpolished which is rough enough for making good reflection VASE and polarized reflectivity measurements from the front surface. The RVASE optical measurements of both isotropic and anisotropic modes were performed in the energy range of 0.75 eV to 6.5 eV with a 0.02 eV increment at room temperature.

Multiple angles of incidence ranging from 60° to 80° were employed in order to resolve the optical anisotropy of GaN film and its surface roughness.

4. Results and discussion

In order to explore the extraordinary response of GaN on c-plane sapphire, a optimum measurement condition has to be determined before the data taking. Generated Ψ values at an arbitrary photon energy (2 eV) as a function of incident angle are shown in Fig 1. Data in Fig. 1 (a) is obtained from a simulated sample structure consisted of a 2 μm sapphire film and a silicon substrate. Fig. 1 (b) is a similar simulation from a GaN (2 μm)/c-sapphire structure. Isotropic and anisotropic model mean that the sapphire and GaN films are assumed isotropic or anisotropic in data generation. The ordinary and extraordinary dielectric functions of sapphire and GaN used in the calculation are from our previous study^{7, 12}. It is obvious that Ψ values are strongly dependent on the angle of incidence for both isotropic and anisotropic models. The difference between isotropic and anisotropic model is significant at large angles near the pseudo-Brewster angle in both cases. At low incident angles ($<50^\circ$), the difference is negligible. Therefore, 60° , 70° and 80° are the good angles for resolving the extraordinary response of the GaN film.

For a real sample, surface over-layer is always an important issue in an ellipsometric study, since the native oxide or/and surface roughness are existed on many materials. Surface over-layer can alter both Ψ and Δ significantly and will affect the values of the extracted dielectric functions from the VASE data. In order to see the over-

layer effect on a GaN/sapphire sample, a simulated sample is constructed which consists of an EMA (effective media approximation) layer¹³ (50% voids, and different thickness), an isotropic GaN film (1 μm thick), and a c-plane sapphire substrate, as shown in Fig. 2. The generated VASE data as a function of incident angle is shown in Fig. 3. The photon energy in Fig. 3(a) and (b) is 5 eV (above the GaN band gap), and 2 eV (below the band gap) in Fig. 3 (c) and (d). It is obvious that both Ψ and Δ are very sensitive to the thickness of surface over-layer, and the most sensitive region happens near the Brewster angle, for both 5 eV and 2 eV cases. Notice that Δ is much more sensitive to surface-roughness than Ψ , and the sensitivity could be in one monolayer scale. Therefore the surface roughness can be accurately determined by VASE. This is one of the main reasons that VASE is a more sensitive measurement than reflectance spectroscopy. The surface effect can also be observed in the full range Ψ and Δ spectra, as shown in Fig. 4. With only 4 nm difference in over-layer thickness, Δ alters significantly at both angles in the above band gap region. It is also shown that the surface effect for the below band gap region is much weaker.

Generated reflectance data with and without surface roughness is shown in Fig. 5. As mentioned above, the surface effect is more sensitive in the above band gap region in the reflectance spectra. It is also sensitive to rough surface at large incident angles ($65^\circ < \phi < 85^\circ$ in this GaN/sapphire case). Therefore using 75° as the angle of incidence⁹ without considering the surface roughness may result a large error bar in the resulted

dielectric functions. In stead, 60° may be a better choice as the angle of incidence if using polarized reflectance spectroscopy for GaN study.

Based on the above discussions we know that both anisotropy and surface roughness affect Ψ and Δ spectra. In general, surface roughness affects Δ more than Ψ , especially at the near Brewster angle region and above band gap region. While optical anisotropy affects Ψ more than Δ , and this happens in the whole spectral range, and high angles of incidence. There are some conditions at which these two effects may be separated, such as at 60° angle of incidence for the GaN/c-sapphire case. It can be found in Fig. 4 and Fig. 5 that there is a very weak surface roughness effect at 60° angle of incidence while the anisotropy effect is still manageable as shown in Fig. 1 (b). In order to resolve both the extraordinary response and the surface roughness, a series of VASE measurements were performed at large angles of incidence, *i.e.*, 60° , 70° , and 80° . The VASE data is analyzed with a three-phase model as shown in Fig. 6. The fitting parameters are the surface over-layer thickness d_1 , its void percentage, GaN film thickness d_2 and the MDF parameters for GaN dielectric functions^{14,15} of the extraordinary part. The GaN ordinary dielectric functions⁷ and sapphire dielectric functions¹² are from our previous study. Some of the final fitting results are shown in the Fig. 6. The GaN film is 1024 nm thick, which is closed to the nominal value (1 μm). The surface over-layer is about 3.7 nm thick with 41% voids. The VASE data and the best fit are shown in Fig. 7. The fitting parameters of GaN extraordinary dielectric functions are listed in Table 4.1. The details of this parametric model description and the method of

use are same as the ordinary part. The resulting ordinary and extraordinary dielectric functions are plotted in Fig. 8. $\epsilon_{1\parallel}$ is larger than $\epsilon_{1\perp}$ everywhere in the whole measured range, and the average difference between them is about 3.5%. The abrupt step around band gap in ϵ_2 curves indicates the high quality of this film, which indicates low defect density and low impurity concentration.

Kramer-Kronig consistency check was performed on both ordinary and extraordinary dielectric functions. The k-k results are shown in Fig. 9, and Table 2 and 3. The solid dots circles are the best ϵ_1 results for ordinary and extraordinary, respectively. The solid line is the calculated ϵ_1 from the known ϵ_2 values using the K-K relation. The K-K relation used in the calculation is^{16, 17}

$$\epsilon_1^{kk}(E) = \epsilon_1^{offset} + \sum_{i=1}^2 \frac{Ai}{E_i^2 - (E)^2} + \frac{2}{\pi} P \int_{0.75\text{eV}}^{6.5\text{eV}} \frac{E' \epsilon_2^{meas}(E')}{E'^2 - (E)^2} dE' \quad (15)$$

For a set of known dielectric functions, ϵ_1 can be calculated from ϵ_2 using the above K-K integral in the measured energy region (0.75 eV to 6.5 eV). The model then adds the contribution from two non-broadening oscillators and a fixed offset to account for absorption outside the experimental measuring range. E_i is the energy location of a non-broadening oscillator that is added to simulate the absorption outside the integration range. A_i is the magnitude of the oscillator located at E_i position. In our calculation two oscillators were used outside the measured region.

Summary

Extraordinary dielectric functions of a GaN film grown on c-plane sapphire substrates were revealed by the standard variable angle spectroscopic ellipsometry in the range of 0.75 to 6.5 eV. Model simulations indicate that large incident angles (near the pseudo-Brewster angle) have the best sensitivity on resolving the extraordinary response and the surface roughness simultaneously. It also shows that VASE is a better choice than the reflectance spectroscopy when surface over-layer exists. The real part of the extraordinary function is larger than that of the ordinary by an average value of 3.5%. The comparison of the calculated ϵ_1 and the experimental ϵ_1 indicates that the dielectric functions obtained in this study are K-K consistent.

Acknowledgments

This work was supported by US Army Research Office under contract No. DAAG55-98-1-0462. Dr. Sam Alterovity at NASA Lewis Research Center for providing GaN/sapphire samples in the early stage of this study.

References

- ¹ H. Morkoc, S. Strite, G. B. Gao, M. E. Lin, B. Sverdlov, and M. Burns,
J. Appl. Phys. **76**, 1363 (1994).
- ² S. Nakamura, M. Senoh, S. Nagahama, N. Iwasa, T. Yamada, T. Matsushita,
H. Kiyoku and Y. Sugimoto, Jpn. J. Appl. Phys. **35**, L74 (1996).
- ³ S. Nakamura, M. Senoh, S. Nagahama, N. Iwasa, T. Yamada, T. Matsushita,
H. Kiyoku, Y. Sugimoto, T. Kozaki, H. Umemoto, M. Sano, and K. Chocho,
Appl. Phys. Lett. **72**, 2014 (1998).
- ⁴ E. Ejder, Phys. Status Solidi A **6**, 445 (1971).
- ⁵ S. Logothetidis, J. Petalas, M. Cardona, and T. D. Moustakas, Physical Review B,
50, 18017 (1994).
- ⁶ H. Amano, N. Watanabe, N. Koide, and I. Akasaki, Jpn. J. Appl. Phys.
32, L1000 (1993).
- ⁷ C. H. Yan, H. Yao, J. M. Van Hove, A. M. Wowchak, P. P. Chow, and J. M. Zavada,
J. Appl. Phys. **88**, 3463 (2000)..
- ⁸ G. Yu, G. Wang, H. Ishikawa, M. Umeno, T. Soga, T. Egawa, J. Watanabe,
and T. Jimbo, Appl. Phys. Lett. **70**, 3209 (1997).
- ⁹ G. Yu, H. Ishikawa, T. Egawa, T. Soga, , J. Watanabe, T. Jimbo, and M. Umeno
Jpn. J. Appl. Phys. **36**, L 1029 (1997).
- ¹⁰ R. M. A. Azzam and N. M. Bashara, *Ellipsometry and Polarized Light*,
(North-Holland, Amsterdam, 1977).
- ¹¹ D. den Engelsen, J. Opt. Soc. Am. **61**, 1460 (1971).

- ¹² H. Yao, C. H. Yan, J. Appl. Phys. **85**, 6717 (1999).
- ¹³ D. E. Aspnes, J. B. Theeten, and F. Hottier, Phys. Rev. B **20**, 3292 (1979).
- ¹⁴ T. Kawashima, H. Yoshikawa, S. Adachi, S. Fuke, and K. Ohtsuka, J. Appl. Phys. **82**, 3528 (1997).
- ¹⁵ M. Schubert, J. A. Woollam, G. Leibiger, B. Rheinländer, I. Pietzonka, T. Saß, and V. Gottschalch, J. Appl. Phys. **86**, 2025 (1999).
- ¹⁶ H. Yao, B. Johs, and R. B. James, Phys. Rev. B, **56**, 9414 (1997).
- ¹⁷ H. W. Yao, J. C. Erickson, H. B. Barber, and R. B. James, J. Electronic Materials **28**, 760 (1999).

Figure captions

Fig. 1. Generated VASE data as a function of angle of incidence at 2 eV. (a) Sapphire (2 μm thick) on silicon substrate. (b) GaN (2 μm thick) on a c-plane sapphire substrate. Solid line represents the isotropic sapphire or GaN layer; dash line represents the anisotropic layers.

Fig. 2. A simulation sample structure with the surface over-layer for VASE data generation the surface roughness is described by a EMA layer with 50% voids.

Fig. 3. Surface roughness effect observation through VASE data simulations (angle dependence). Generated VASE data of Fig. 2 structure at 2 eV and 5 eV by isotropic model with different over-layer thickness. (a) Ψ as a function of angle of incidence at 5 eV; (b) Δ as a function of angle of incidence at 5 eV; (c) Ψ as a function of angle of incidence at 2 eV; (d) Δ as a function of angle of incidence at 2 eV.

Fig 4. Surface roughness effect observation through VASE data simulations (energy dependence). Generated VASE data as a function of photon energy at 60° and 80° angles

of incidence by isotropic model with different over-layer thickness. (a) Ψ spectra with 0 and 4 nm thick over-layer; (b) Δ spectra with 0 and 4 nm thick over-layer.

Fig. 5. Surface roughness effect observation through reflectance data simulations (both angle and energy dependence). (a) Generated reflectance data as a function of energy at 60° and 80° angles of incidence; (b) Generated reflectance data as a function of angles of incidence at 2 eV photon energy (below band gap); (c) Generated reflectance data as a function of angles of incidence at 5 eV photon energy (above band gap).

Fig.6. The three-phase model of the MBE grown GaN on c-plane sapphire sample.

Fig. 7. Experimental VASE data and the best model fit of a GaN/c-sapphire sample at three angles of incidence. The circles and solid line represent the experimental data and the best fit, respectively.

Fig. 8 Ordinary and extraordinary dielectric functions determined from the VASE data analysis. The solid line represents the ordinary dielectric functions (ϵ_{\perp}). The dash line represents the extraordinary dielectric functions (ϵ_{\parallel}).

Fig. 9. Comparison of the experiment results and the calculated ϵ_1 value for both the ordinary and extraordinary dielectric functions of GaN. The solid dots and circles represent experiment results, while the lines represent calculated values by K-K fit.

Table 1. The best fitting parameters for GaN extraordinary dielectric functions.

CP contribution	$A_j (A_{jx})$	$E_j (E_{jx})$	$\Gamma_j (\Gamma_{jx})$	p_{jx}
$\epsilon^{(0)}$	$38.5 \text{ (eV)}^{1.5}$	3.44 (eV)	0.27 (eV)
$\epsilon^{(0x)}$	1.32 (eV)	3.42 (eV)	0.18 (eV)	-1.55
$\epsilon^{(1)}$	2.67	6.96 (eV)	0.003 (eV)
$\epsilon^{(1x)}$	4.77 (eV)	6.94 (eV)	1.38 (eV)	-0.01
ϵ_∞	0.24			

Table 2. Kramers-Kronig fitting parameters for GaN ordinary dielectric functions.

Fitting Parameters	E_i	A_i	$\epsilon_1^{\text{offset}}$
Pole #1	7.491	2.001	1.04
Pole #2	14.092	24.6	

Table 3. Kramers-Kronig fitting parameters for GaN extraordinary dielectric functions.

Fitting Parameters	E_i	A_i	$\epsilon_i^{\text{offset}}$
Pole #1	7.4883	3.805	1.05
Pole #2	13.534	21.123	

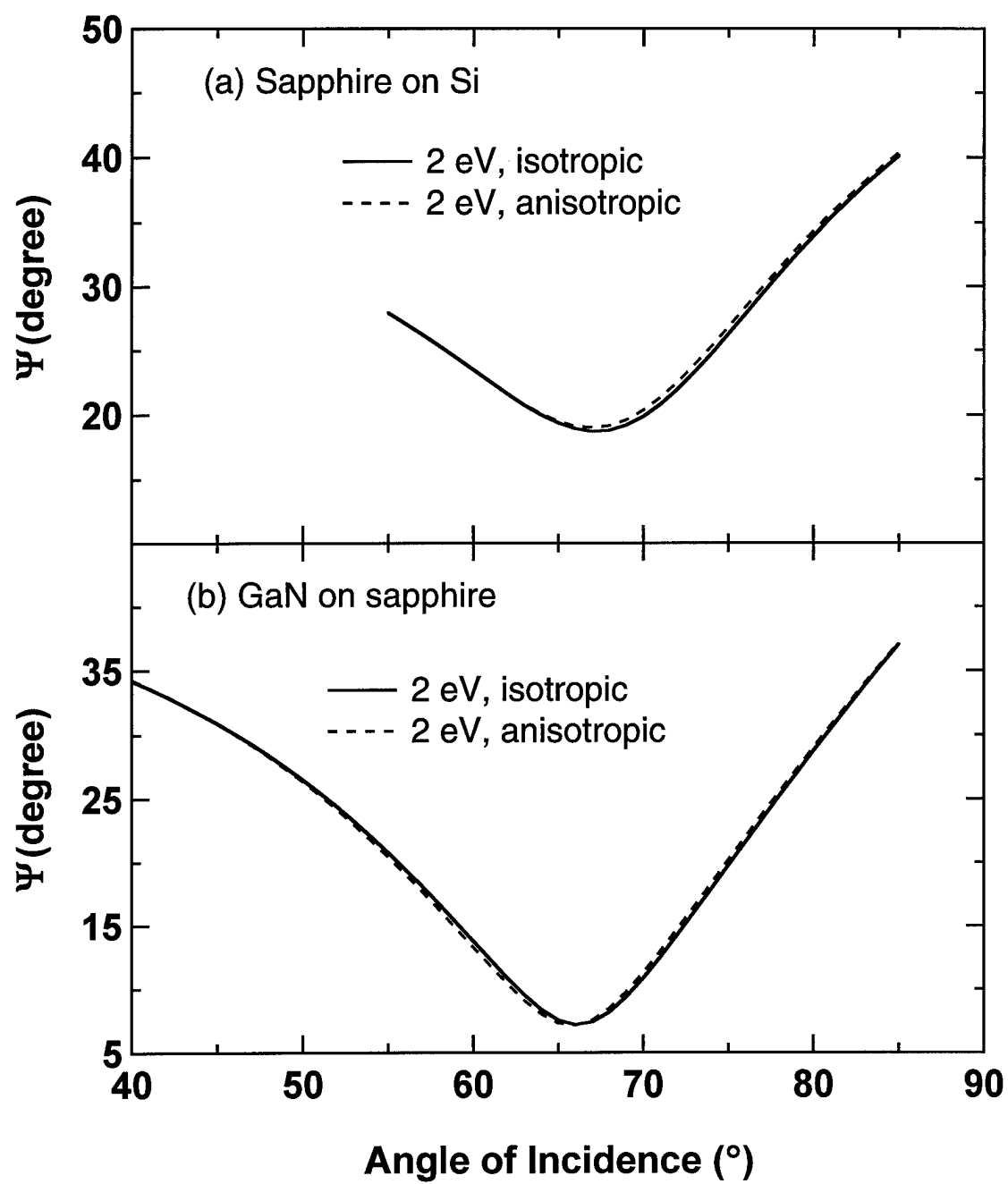


Fig. 1

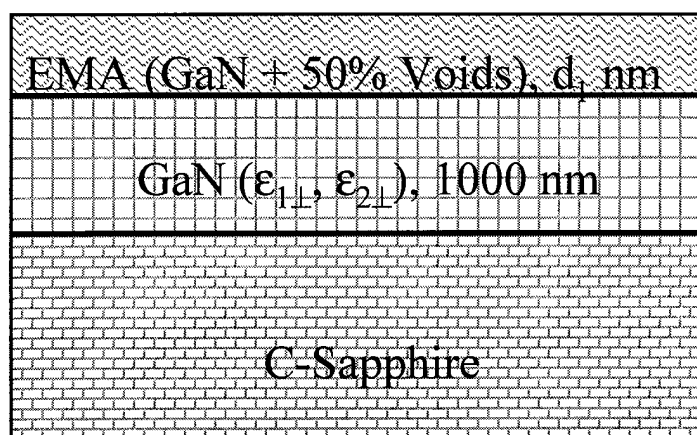


Fig. 2

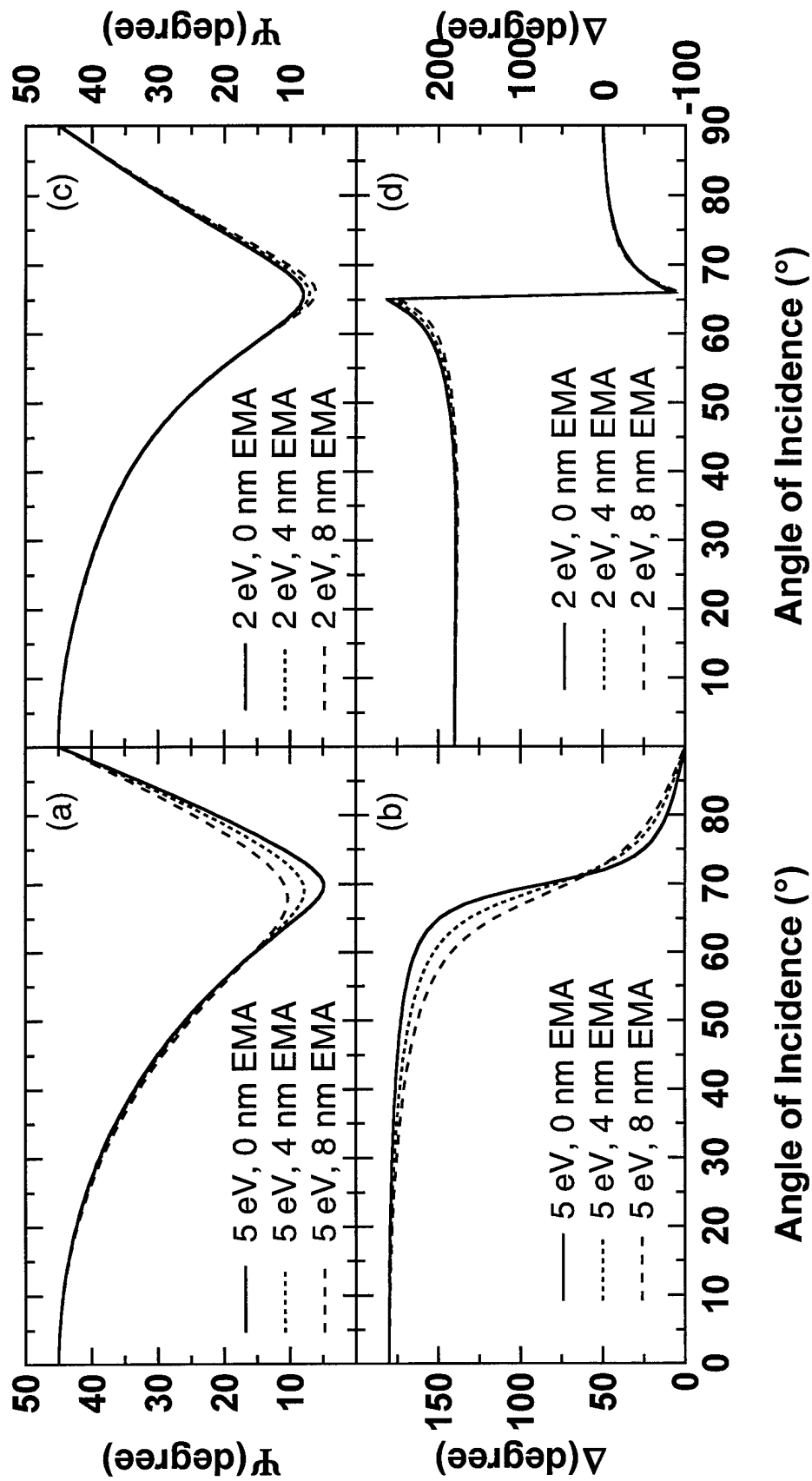


Fig. 3

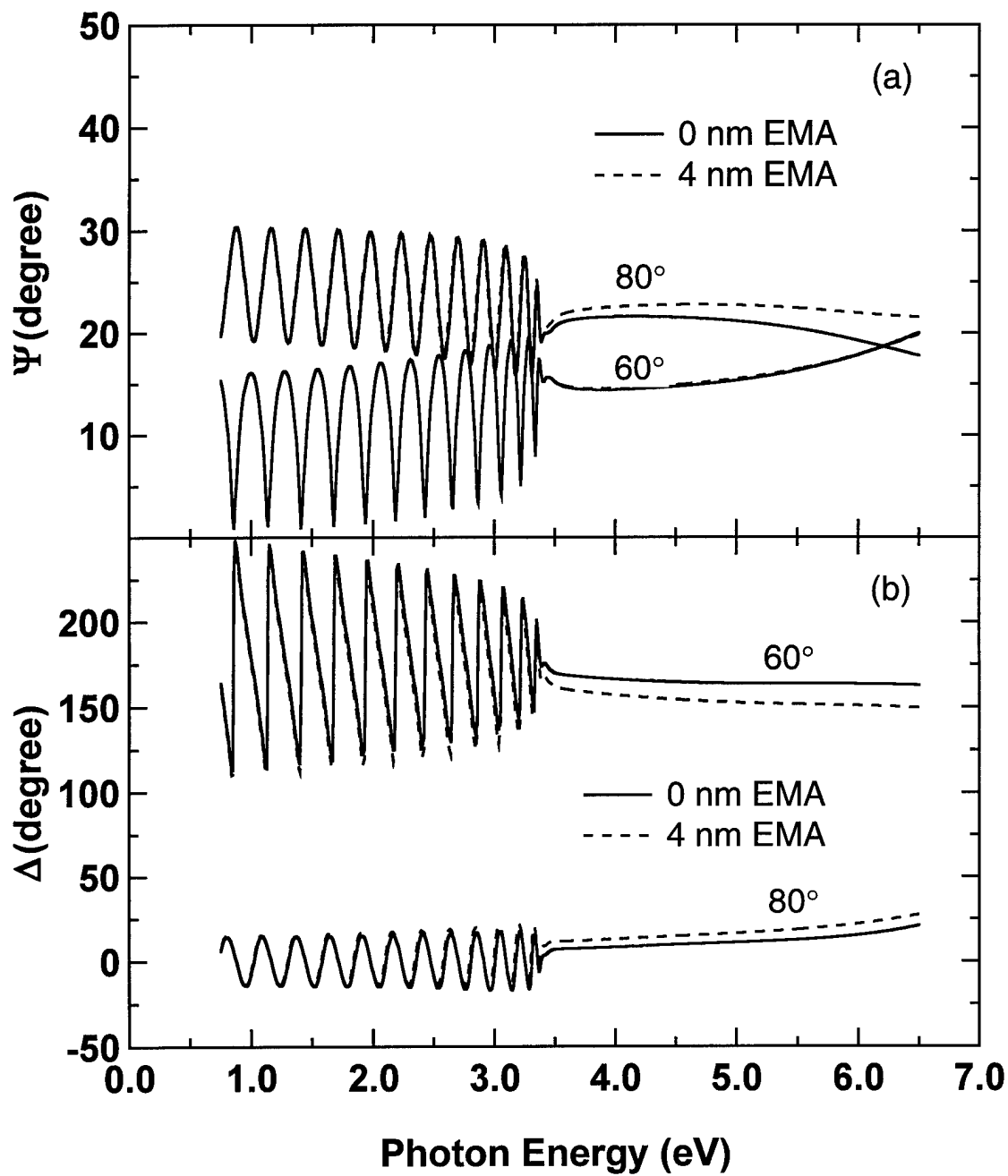


Fig. 4

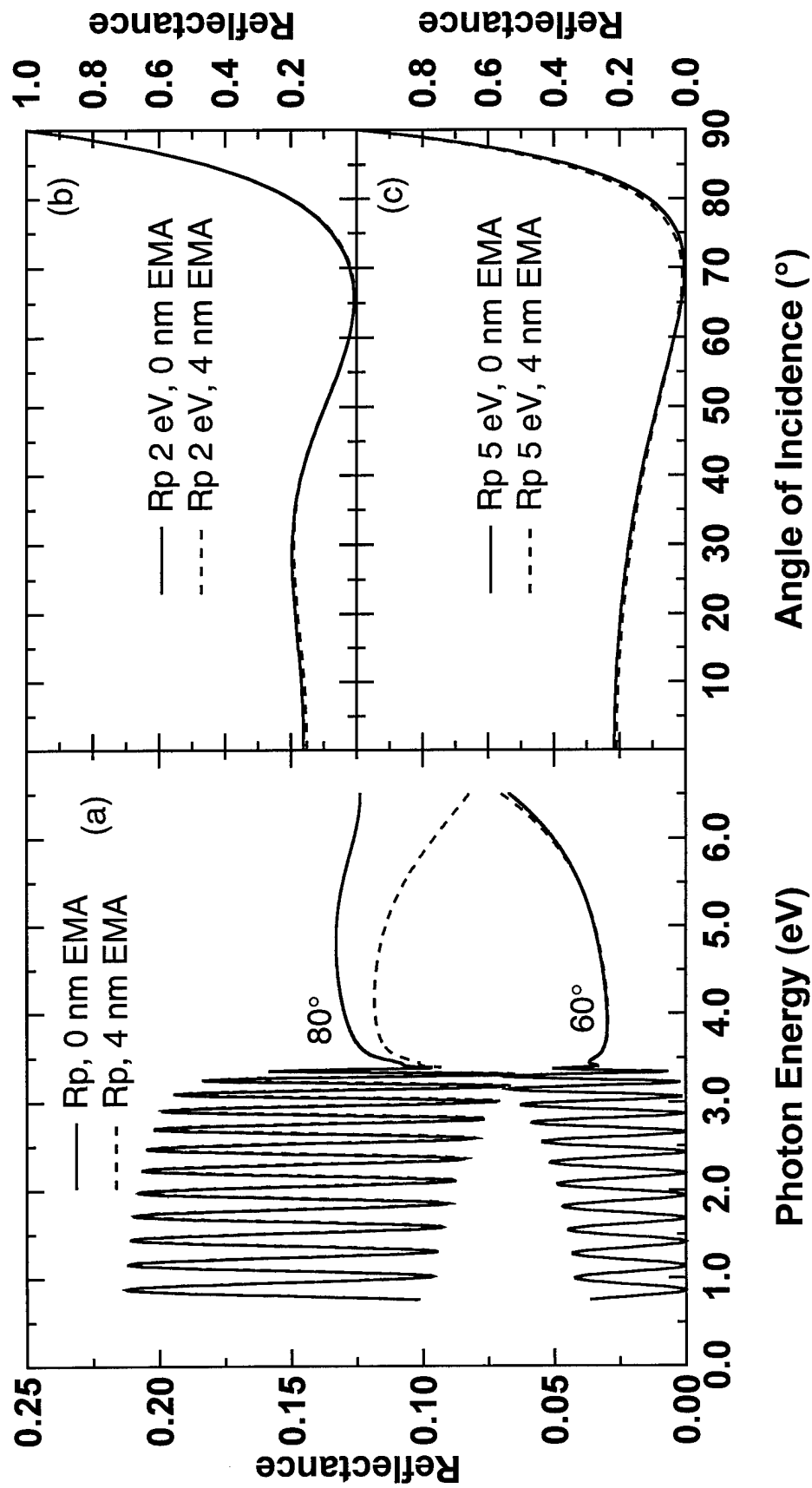


Fig. 5

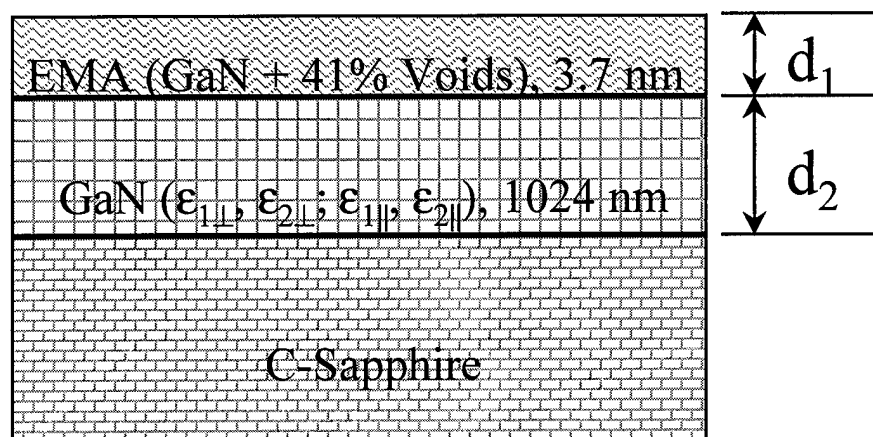


Fig. 6

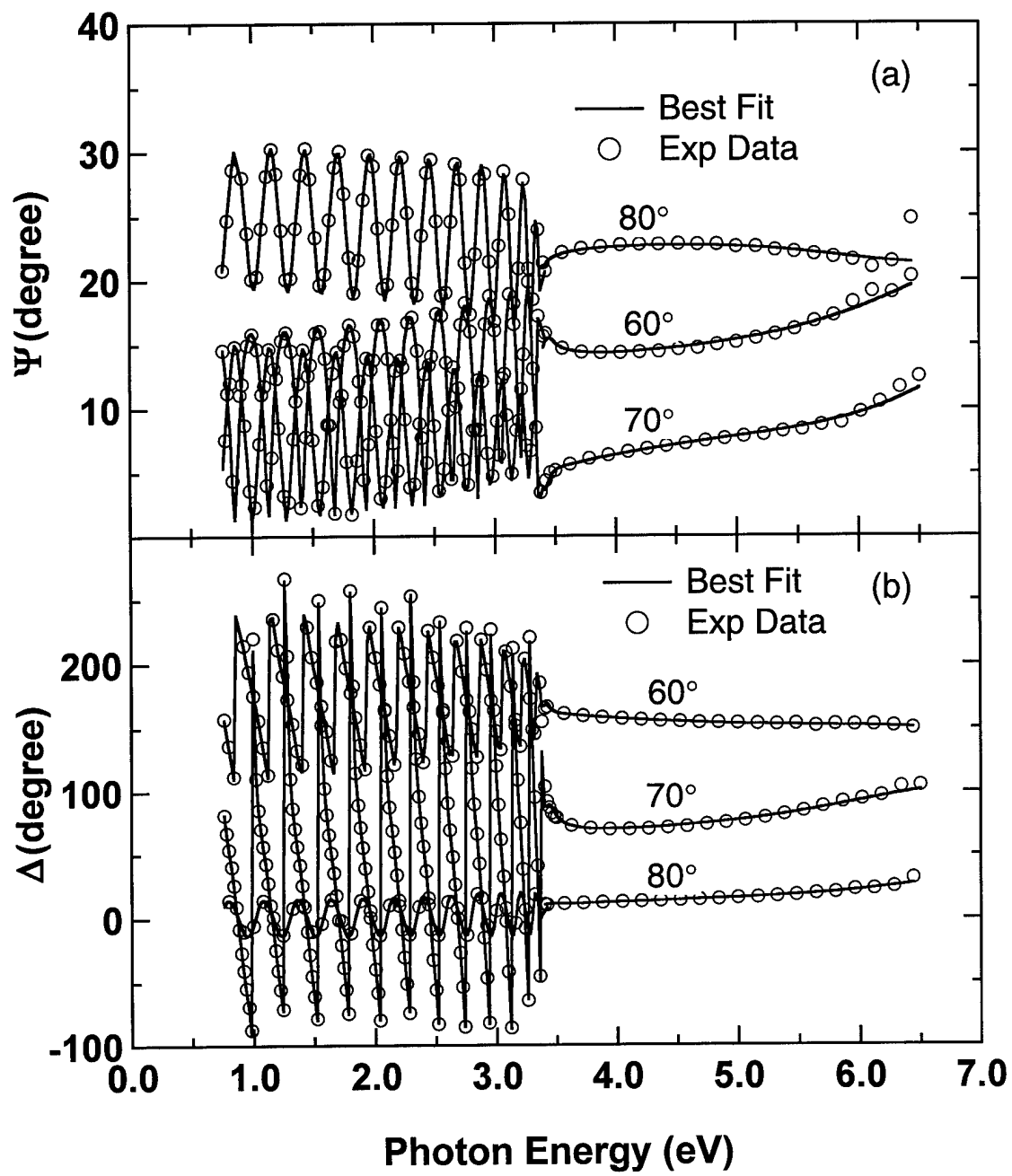


Fig. 7

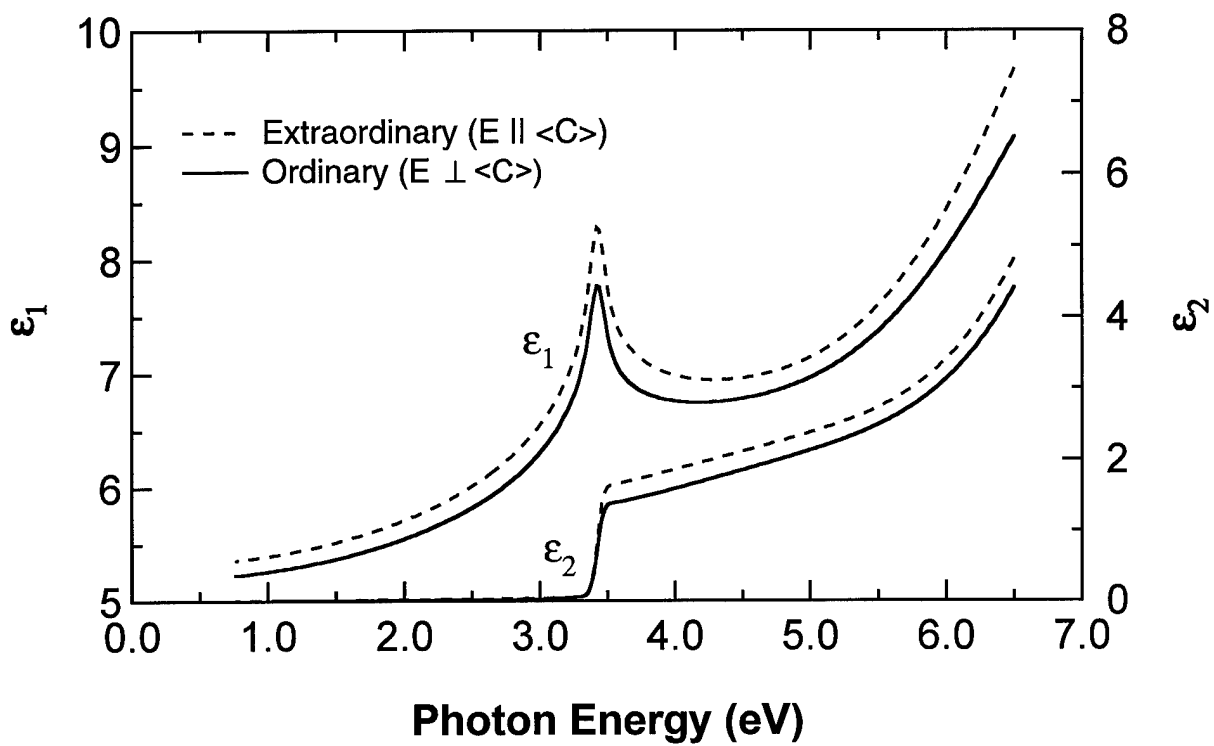


Fig. 8

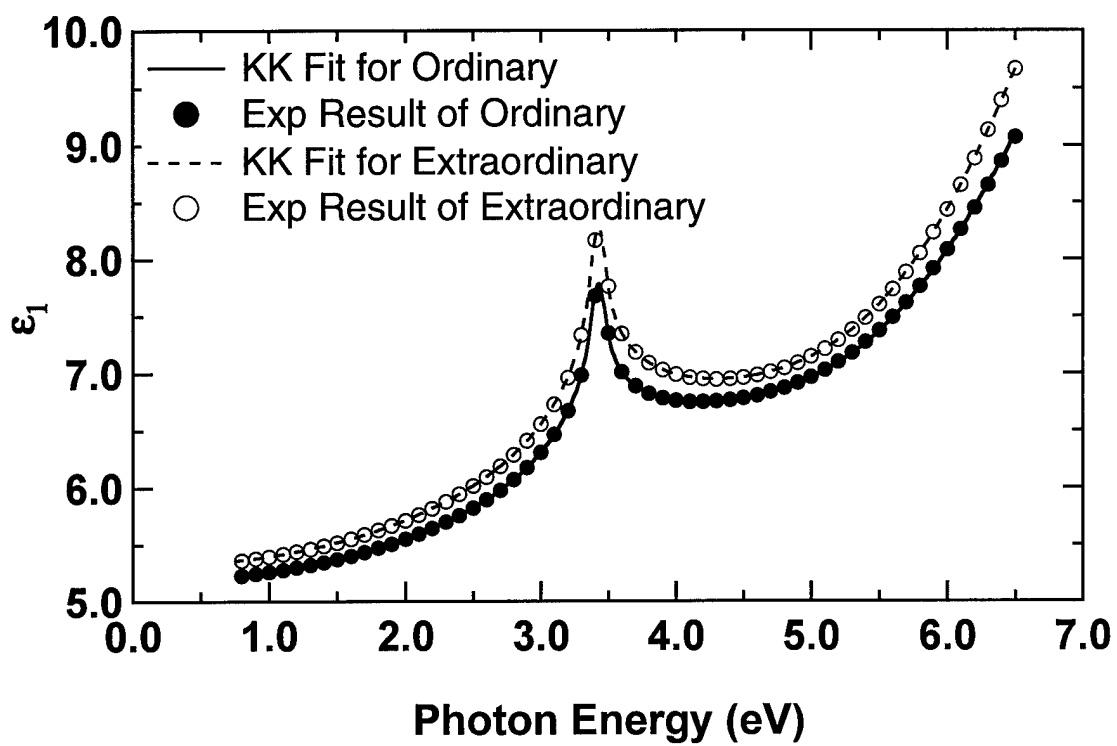


Fig. 9

7

**Optical Characterization of Anisotropic III-Nitride
Wide Band-Gap Semiconductors and Related Materials**

by

Chunhui Yan

A DISSERTATION

Presented to the Faculty of
The Graduate College in the University of Nebraska
In Partial Fulfillment of Requirements
For the Degree of Doctor of Philosophy

Major: Interdepartmental Area of Engineering
(Electrical Engineering)

Under the Supervision of Professor Huade Walter Yao
Lincoln, Nebraska

May, 2000